UiT The Arctic University of Norway

Faculty of Biosciences, Fisheries & Economics
Department of Arctic & Marine Biology

Characterization of the circadian clock in Hooded Seals (*Cystophora Cristata*) and its interaction with mitochondrial metabolism

A multi-tissue comparison and cell culture approach

Fayiri Kante

BIO-3950 Master's Thesis in Biology, June 2021

Acknowledgment

I sincerely thank my supervisors Shona Wood and Alexander Christopher West for giving me the opportunity to explore the subject of this master thesis. It has been a pleasure to learn various laboratory techniques and progress in my scientific abilities this year under your supervision. I am grateful for your patience and kindness; it has been very exciting to obtain new results and satisfaction to put them in perspective and reflect on their meaning.

Thank you, Alex, for your time in the Lab and your explanations of the protocols.

Thank you, Shona, for your precious feedbacks on my writing and my results.

I would like to thank Professor Arnoldus Schytte Blix, Professor Lars Folkow, the technical personnel Renate Thorvaldsen, Hans Arne Solvang, and Hans Lian for their help and demonstration during the tissue sampling, and Chandra Sekhar Ravuri for the help in cloning and sequencing the genes.

Thank you, Chiara Ciccone, for introducing me to the oroboros, for the good times in the lab, and for your enthusiasm about seal research and your encouragements.

To my master student companion Anna and Linn, thank you for the laughs in the lab and at the office.

Mom, Dad, Inari, thank you for your lessons and your support over the year.

Abstract

Circadian rhythms regulate the behavior, physiology, and metabolism of living organisms over a 24h period. From daily activity to cellular function, they are present across all taxa and help predict and anticipate the changes in the environment. The polar regions are subject to different photoperiods across the year, which impact the environmental conditions on a seasonal and daily basis. Studies have shown different circadian responses to this environment from several arctic species. Moreover, there is an increasing interest in the circadian implications on diverse cellular mechanisms. Evidence of crosstalk between circadian core clock genes and hypoxia with genes involved the mitochondrial dynamics, as well as oxygen sensing, provide a basis to study those mechanisms in a model which faces those 2 challenges in its natural environment. The hooded seal (*Cystophora Cristata*) is an expert diver, with excellent hypoxia tolerance, and an arctic mammal exposed to the special light environment. The primary aim of this study was to characterize the circadian clockwork in the hooded seal using *in-vivo* sampling and hooded seal skin fibroblasts. The secondary aim was to explore the clockwork and the variation mitochondrial metabolism in a circadian context with the culture of hooded seal skin fibroblasts.

We show that the clock genes are expressed in different seal tissues, with a higher expression in the brain than in peripheral tissues. There was no difference in the expression of those genes between the middle of the day and the middle of the night. Nevertheless, seal skin fibroblasts respond to treatments designed to entrain the circadian clockwork and showed a significant circadian oscillation in the key clock genes; PER-2, ARNTL, NR1D1. Finally, we showed that there is a time-of-day variation in the respiratory capacity of mitochondria in seal skin fibroblasts and in MFN1, a gene involved in mitochondrial dynamics.

These results suggest that despite living in the arctic, hooded seals have a functional circadian clock. It also suggests that the respiration capacity and therefore, the capacity of the animal to utilize oxygen varies throughout the day, which could influence its diving ability.

Overall, this thesis provides new knowledge on the circadian rhythm in seals and how mitochondrial metabolism may be influenced. These data encourage further research to depict mitochondrial dynamics and metabolism in a circadian and hypoxic conditions, as well as animal circadian behavior for an integrative perspective.

Table of Contents

List of Tables

List of Figures

1 INTRODUCTION

1.1 Chronobiology in living organisms

Chronobiology is the study of living organisms under cyclic time frames. Those time frames can be years for circannual rhythms, days for circadian rhythms, under a day for ultradian rhythms. “Circadian” is composed of Circa, the Latin word for “approximately” and “Diem” which means day. Circadian rhythms are the study of daily rhythms in organisms. Those rhythms help an organism predict daily environmental changes and prepare its physiology and metabolism accordingly. “circa” implies that biological rhythms have a degree of flexibility, unlike the earth rotation day which is strongly consistent. Most environments are affected by the day/ night cycle, temperature changes, and other environmental cues derived from it. These cues which entrain rhythms are called Zeitgebers. Because Zeitgebers have been consistent throughout evolution, it is not surprising that most of the organisms have a systemic response to these changes.

Life adapted to aerobic respiration 2.5 billion years ago during the Great Oxidation Event and while this change allowed the use of oxygen, it induced the production of reactive oxygen species (H2O2 for example) as a by-product, from which cells had to elaborate a defense mechanism. The peroxiredoxin that protects the cells from H2O2 is estimated to have emerged during this period, coinciding with the KAI proteins, responsible for circadian rhythm in cyanobacteria. Both metabolic and circadian systems could have evolved simultaneously under the influence of the sun and oxygen. The response of the cells to cyclic exposure to oxidation could have driven the evolution of the circadian rhythms and be an original connection between metabolism and chronobiology (Edgar et al. 2012).

The relation between Chronobiology and metabolism appears important. Many metabolic diseases are paired with misalignment of the clock rhythms. The presence of circadian rhythms in the different tissues and their intercommunication has an influence on energy homeostasis, hormone production, xenobiotic metabolism that implies communication between chronobiology and metabolism (Koronowski and Sassone-Corsi 2021).

Cyanobacteria are a primitive prokaryote which exhibits circadian adaptation in its molecular biology. These photosynthetic organisms are responsible for most of the 21% oxygen in the atmosphere and life as we know it. Because photosynthesis and nitrogen fixation occurs at the same place, the organism (*Synechococcus Elongatus PCC 7942)* has a temporal differentiation between photosynthesis in daylight and nitrogen fixation at night. This differentiation continues even under constant light (Bhadra, Thakkar et al. 2017). It has however been demonstrated that even if the internal clock keeps ticking in a constant environment, it is only an advantage when an environment is matching the rhythmicity of the organism (Woelfle et al. 2004). The fungus *Neurospora Crassa* also displays a circadian regulation of their conidia formation (Bell-Pedersen 2002), which demonstrates the widespread of circadian principles across kingdoms.

In the apparent silent and still *Plantae* kingdom, circadian regulation of biochemical processes directly related to sun activity could be a great advantage. In *Arabidopsis thaliana,* matched circadian clock of plants with their environments double their productivity, probably by synchronization of the light-harvesting complex with the light environment (Dodd 2005).

All those mechanisms have a similar function, to measure time. However, they are quite different in their mechanisms. Against such a strong environmental cue that is the day/night cycle, clock mechanisms could have appeared several times during evolution, and the different clockworks could be convergent. The observation that the proteins involved in the timekeeping mechanism are not related between animals and cyanobacteria, as well as in the plants, supports this hypothesis (Rosbash 2009).

1.2 The Arctic environment

The Arctic has different definitions depending on which prism it is studied. The name comes from the Greek Arktos, bear, and refers to the constellation Ursa Major and Ursa Minor, visible only in the northern hemisphere. The Arctic circle is defined by the latitude 66.5° North from which the sun does not rise for more than 24h in winter (Figure 1). This is due to the tilt of the Earth's rotational axis of 23.5°. It exposes the North and South poles region to high light seasonality, with the phenomena of polar night and midnight sun.

Figure 1 **Map of the Arctic**. reprinted from CIA World Fact Book. The arctic circle (blue) is defined by the latitude 66.5° North while the arctic region (red) is defined by the 10°C isotherm. They have different geographical limitations, the Arctic circle is defining the special light regime interesting in the field of chronobiology.

Because of the tilt of the earth, and its elliptical rotation around the sun, the regions above the Arctic circle are more exposed to the sun's rays light, with constant daylight around the summer solstice (Figure 2). On the other hand in the winter times, the sun rays do not reach the arctic circle, exposing the region to constant darkness around the winter solstice (Figure 2). The Arctic is also defined by a climatic definition. It is the isotherm at which the temperature for the warmest month of the year is not above 10°C (Figure 1). This limit does not depend on latitude and can variate greatly due to regional climate. The region is cold in general because it does not receive direct light for part of the year has cold winters and cool summers. The Arctic tree line is closely related to the 10°C isotherm line. It is the line above which the trees do not grow anymore because of the temperature. Temperature is a stress indicator, the isotherm and treeline limits are used in many disciplines as a good ecological indicator. The water temperature remains cold in the summer, even if great variations depend on the inflow of currents and sea ice movements. More than the cold, it is the very singular light-dark cycle with a high seasonality (Figure 2) defined by the Arctic circle that is of interest to study chronobiology in the Arctic. Most, if not all, daily variations in the environment are derived from the sun. In an environment where the light environment is constant, is the circadian clock still an advantage or can it handicap the organism?

The evolutionary advantage of chronobiology is to anticipate daily and seasonal changes. It allows the organisms to prepare their physiology, activity, and metabolism for expected conditions. There is a distinction between behavioral and physiological rhythms versus the circadian oscillation of the molecular clock. Activity patterns or physiological patterns like variation in body temperature or hormone level can be used as a proxy to measure circadian oscillation. However, the proxy might not reflect the circadian clockwork and the animal could benefit in adapting to the environmental conditions rather than its own clock.

The measure of the molecular clockwork implies the measure of the gene expression of the model. It requires constant conditions to measure its free-running period, like an artificial DD cycle and a great time definition between sampling timepoints.

Studies done on several models show different responses to the arctic environment.

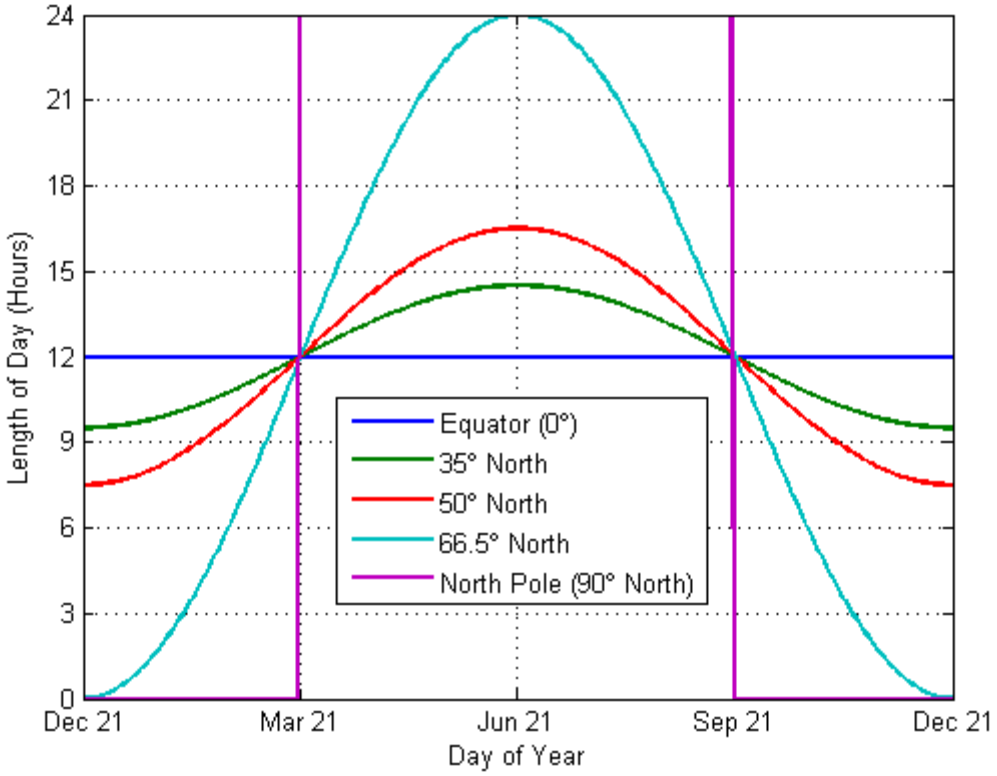

Figure 2 **Graph of the annual variation in photoperiod at different latitudes.** reprinted from http://www.atmo.arizona.edu/students/courselinks/fall16/atmo336/lectures/sec4/seasons.html. The higher the latitude, the more the photoperiod varies throughout the year with a difference between day and night-time. At the equator, there is no difference in photoperiod between summer and winter, while in the north pole, the polar night (21 September-21 Mars) and midnight sun (21 Mars-21september) divide the year into 2 very distinct light conditions.

A study on scallops *C. islandica* used a genetic and behavioral approach to identify the clock genes in scallops and record circadian activity. The clock genes were identified and their expression during the polar night was rhythmic with a circadian and tidal rhythm, as well as behavioral rhythmicity (Perrigault et al. 2020). This study shows how the behavior can be linked with the molecular clockwork to provide evidence of persistent circadian rhythm in the arctic environment.

Similarly, the Svalbard Ptarmigan maintains its circadian clock machinery during the polar night and the midnight sun. The bird behavior is however decoupled from the clock and it

shows no rhythmic behavior (Appenroth et al. 2021). The principal role of the circadian clock would be to maintain seasonal timekeeping, essential for those birds with important seasonal phenotypes. This study shows that the output of the clock can be decoupled from the clock and cannot determine whether or not the molecular clockwork is ongoing.

It was thought that Svalbard reindeers do not have a functional circadian clock (Lu et al. 2010). They show no rhythm in their behavior (Van Oort et al. 2005) and their melatonin production is not regulated (Stokkan et al. 2007). However, a recent study shows that they maintain rhythmicity throughout the year (Arnold et al. 2018). The environmental cues are however greatly affecting their physiology. During the polar night, the reindeers maintain rhythms in different organs. The rumen temperature, as well as the heart rate and the behavior of the animal, were rhythmic with a different period than 24h. the rhythms between the different measurements were asynchronous. The intense feeding period during the summer makes the reindeer ignore their rhythms. They become arrhythmic and they are more influenced by the feeding behavior than by their circadian rhythm (Arnold et al. 2018). The Svalbard reindeer like the Svalbard ptarmigan adapts its circadian output according to the environment rather than to its own clock. It is however not sure if the molecular clock is normally oscillating.

Some other mammals are less affected by the environment and rely on their internal timekeeper. The Arctic ground squirrel shows persistent rhythmicity throughout the arctic summer and is even capable to entrain its clock during this period (Williams et al. 2017). Their clock is resistant to experimental abrupt changes in light regime and remains entrained, probably an adaptation to the life in the burrow where light changes are abrupt, but where the animal must keep track of the external time, without entraining to the darkness of its habitat.

The polar bears are sharing the sea ice with hooded seals and even if one prey on the other, they both belong to the same clade of Arctoidea. The polar bears exhibit circadian activity rhythms with great interindividual variations. The light exposure affects the length of those rhythms (Ware, Rode et al. 2020). This study measured the activity of female polar bears with GPS and accelerometer and did not measure physiological parameters. During the months of seal pupping, the activity of bears was greatly variable. Some individuals were diurnal and some animals were nocturnal, which suggests that feeding behavior can interact with

circadian activity. Moreover, the females were more likely to become arrhythmic in April-June, possibly because they are pursued by males. The breeding behavior could thus also interfere with their rhythms which are not predominant. This result highlight that the circadian output is not only different between species but that there are also differences between individuals.

Those different examples illustrate that the output of the clock can be weakened by the special light regime of the Arctic, and its advantage competes with opportunities given by the light environment. Some animals have maintained their clock output, from birds to bears, and it can be crucial for seasonal rhythmicity, to prepare physiological changes as well as breeding activities. Seals share the same environment as the polar bears during months of the year and like the Svalbard reindeer, have a restricted period during which they are giving birth and breeding, which has to be synchronized, and new knowledge of the seal's rhythm is of interest.

Little is known about hooded seals chronobiology. Studies of tagged hooded seals (Folkow, Mårtensson, and Blix 1996) showed that the Greenland population does not follow a clear migratory pattern. Individuals are foraging sometimes for more than 3 months they come back to the pack ice in March to breed and moult, but spend most of the year foraging at sea. The diving behavior is the best proxy of their activity. They have different types of dives. Shallow dives are rarely longer than 20 minutes and 200m deep. The shallow dives are believed to be for active hunting of prey, which is costly in energy and depletes the oxygen stores. The other type of diver longer and between 300m and 600m, and probably include ambush tactics that are less oxygen demanding. An interesting difference in diving depth between day and night has been observed. The seals dive deeper during the day. It could be a response to the movement of their prey in the water column or an implication of their physiology and hunting tactics at a certain time of day. There is also a seasonal variation in the length of the dives. They are longer during winter than during summer. These observations give an idea of the behavior of the seal. It is however impossible to draw physiological and circadian conclusions. The tagging only recorded dive depth, where other data like core body temperature could have helped determine intrinsic rhythmicity. Because the tagged animals are foraging in their natural habitat, environmental factors cannot be controlled, and the reason for the difference in dive depth cannot be determined. Recent

tagging campaigns confirmed those results but did not provide further information on the circadian behavior of hooded seals (Andersen et al. 2013; Vacquie-Garcia et al. 2017).

Circadian variations in levels of melatonin have been observed in hooded seal pups, at the very start of their life. This oscillation in plasma level was not dependent on the day/ night cycles as the pup kept in constant light remain rhythmic. Furthermore, the pineal gland atrophy's in the adult seal. In other mammals, melatonin levels are rhythmic throughout life and light suppresses the production from the pineal gland. This result in Hooded seals suggests the existence of a clock-inducing circadian expression in the pup but not the adult (Aarseth, Van'T Hof, and Stokkan 2003). This unusual finding might be related to the diving condition of hooded seals and melatonin is likely to be involved in vasoconstriction and dilatation, which would be essential for the fetus survival when the mother dives. The hooded seal fetus could thus be able to interfere with the oxygen management of the mother with a circadian-regulated hormone.

1.3 Hooded seals

1.3.1 General biology

Hooded seals are arctic Phocidae belonging to the pinnipeds. They get their Latin *name Cystophora Cristata* from the inflatable nasal septum males display during the breeding season. They also have an inflatable nasal sac that serves the same purpose (Figure 3). Males weigh from 200kg to 350kg and females from 200 kg to 250kg (Schytte Blix 2007).

Although they spend most of the time in the water, they start their life on the pack ice in march when they come to give birth and breed (Folkow, Mårtensson, and Blix 1996). Once the pups are born, the mothers lactate them for only 2 to 4 days, the shortest parental care in the mammalian class. Their milk is 61% fat (Oftedal, Boness, and Bowen 2011)and over this limited nursing period, the pups gain up to 24kg, from 10-12kg at birth to 34kg, an increase of 7kg per day. Hooded seals are precocial animals and after the nursing period, they are left alone on the ice for a month during which they fast and are vulnerable. The pack-ice offers almost no protection from predation by a polar bear and from the climate. The only defense mechanism for the pups is to adopt a freezing behavior (Schytte Blix 2007).

Their fur and blubber layer protect them from wet surfaces and cold temperatures. Hooded seal pups shed their lanugo fur in utero and are born with a fur steel blue on the back and white on their belly. They are thus called blueback and after successive moults, the immature have colored patches varying from black to brown on a silver-grey fur (Schytte Blix 2007).

1.3.2 Diving response

Hooded seals are expert divers and hold the record for the longest and deepest dives amongst pinnipeds. Dives that lasted for 57,25 minutes at depth of 1652,3m have been recorded (Andersen, et al. 2013). The limiting factor during dives is the oxygen stores. An increase in oxygen storage capacity and control over its depletion is essential to managing such dives.

In response to diving, mammals enter apnea, they stop breathing. Hooded seals have watertight nostrils to avoid water entering their airways, particularly at great depth.

Peripheral vasoconstriction isolates non-vital organs from the blood flow used for vital organs, especially the brain. It happens where the vessels perfuse the organs with new blood rather than from the capillaries of the organs (Bron et al. 1966). In this fashion, the blood is still irrigating the organs, and exchanges between the hemoglobin and myoglobin in muscles, for example, are still occurring, delaying the hypoxic state.

The shunt in peripheral organs results in a dramatic increase in blood pressure. To compensate for that effect, seals enter bradycardia (Thornton and Hochachka 2004). Their heart rate drops from a hundred beats per minute to ten per minute (Irving, Scholander, and Grinnell 1941). Seals have control over their heart rate and vasoconstriction state and it can be adapted to their time underwater in voluntary dives.

Figure 3 **Male and Female hooded seal**. The male (right of the picture) display its nasal septum and is bigger than the female (left of the picture) (Seal's photo, front page and above, are courtesy of Shona Wood)

1.3.3 Oxygen stores

Seals store oxygen mostly in their muscles and in their blood using the same protein as other mammals, hemoglobin and myoglobin. In the brain, a specialized neuroglobin stores oxygen, and its unusual distribution in both neurons and astrocytes suggest that it plays a role in the brain physiology under hypoxia (Mitz, Reuss et al. 2009).

Seals have proportionally more blood volume than terrestrial mammals and the hemoglobin concentration, hematocrit, is higher, thus carrying more oxygen per blood volume. The myoglobin in the skeletal muscles is also higher in hooded seals than in other mammals. This can be observed by the dark red colour of the muscles. It provides them with greater oxygen storage per mass of muscle. The muscles' capacity to store oxygen is gained throughout the dive and maturation of the pups (Lestyk et al. 2009). Seals do not rely on their lungs for

oxygen storage. They empty their lungs before diving and they collapse at depth to reduce buoyancy and limit decompression sickness troubles (Falke et al. 1985).

1.3.4 Metabolism in diving

Aerobic metabolism occurs in the presence of oxygen. The cell through respiration uses oxygen to produce ATP, the energy trade of cellular metabolism. The by-product of cellular respiration is water and carbon dioxide. They are easily taken out of the body, transported in the blood, and expelled in the lungs gas exchanges for carbon dioxide, as well as in the urine and feces for water. Aerobic metabolism produces a large amount of ATP and is the preferred metabolic pathway due to its nontoxic by-products.

Anaerobic respiration on the other hand does not use oxygen as the last electron acceptor but a substrate with less oxidizing power, it results in less energy taken out from this pathway and thus less ATP produced. Anaerobic respiration is used when the oxygen levels are not high enough to sustain aerobic respiration. The by-product of anaerobic metabolism is lactate. It is a toxic compound for the cell and requires oxygen to be transformed back into glucose in the liver through NADH.

Hooded seals are using both aerobic and anaerobic pathways during their dives. While the aerobic pathway is dependent on limited oxygen stores, the anaerobic pathway produces lactate that will require more post-dive resting time between dives to be eliminated, limiting the feeding time of the seal (Kooyman et al. 1980).

The aerobic dive limit (ADL) was defined as the time a seal could use aerobic metabolism while diving. It was experimentally measured as the time underwater without a post-dive increase in arterial lactate concentration (Kooyman et al. 1983).

This aerobic dive limit depends on the diving response of the animal. If he decides not to induce bradycardia and vasoconstriction for short dives, the oxygen stores in the blood will be depleted at the same rate as in the muscles, resulting in a much shorter aerobic dive limit. Seals often modulate their response, isolating their most demanding muscles from the circulatory system to only deplete local blood oxygen and use anaerobic metabolism to preserve oxygen blood stores (Arnoldus Schytte Blix 2018).

1.3.5 Metabolical depression

The use of anaerobic metabolism is not the only answer to oxygen restriction. A lower metabolic rate during dives is essential to reduce oxygen consumption.

Heart bradycardia does not induce an increase in the workload but has an adverse effect because of peripheral vasoconstriction. The blood flow during dives is reduced to 10% of the basal volume (Arnoldus Schytte Blix et al. 1976). Such a low workload at a frequency down to 4-6 beats/min enables the heart to function under anaerobic metabolism, relying on local glycogen (Kerem, Hammond, and Elsner 1973).

Seals can cool down their brain by 2.5°C during dives, reducing their brain's oxygen consumption by 25% (A. S. Blix et al. 2010) as a lower temperature reduces metabolism. Not only they can cool their brain, but it is also a lot more tolerant to hypoxia, functioning at oxygen levels that are far lower from the limit at which terrestrial mammals show impairments (Erecińska and Silver 2001). The distribution of neuroglobin in the brain is not limited to neurons. It is distributed in glial cells, which might play an important role in removing the lactate from neurons that could rely mostly on anaerobic metabolism (Mitz et al. 2009).

The hooded seals, as an expert diver, have been a historic model in diving and hypoxia research. As an arctic species, it is an excellent model to study its rhythms to gain knowledge in the circadian organization of arctic animals in general. The growing link between the circadian clock, metabolism, and hypoxia place it at the crossroad of the 3 disciplines and makes it a perfect model.

1.4 The mammalian circadian clock

The mammalian circadian clock is hierarchical, with a master clock and peripheral clocks which are subsequently synchronised. The master clock is a brain structure: the suprachiasmatic nucleus, SCN. This region, in the hypothalamus, of 10,000 neurons sitting on top of the optic chiasm is necessary for circadian behavior (Ralph et al. 1990). When isolated, the SCN maintains its rhythm *in-vivo* and *in-vitro*. (Weaver 1998). It plays an essential role in maintaining internal clocks synchronized within the body and with the environment. The SCN

is synchronized to the environment from the light perception in the retina by the melanopsin of the intrinsically photosensitive retinal ganglion cells (ipRGCs). The cells, via the retinohypothalamic tract, innervate directly in the SCN, which can entrain to the photoperiod (Legates, Fernandez, and Hattar 2014)(Figure 4). The SCN synchronises metabolism and behavior via different innervation routes and hormonal signaling. The SCN is divided into 2 regions, a dorsal "shell" and a ventral "core". Both regions innervate different hypothalamic axis involved in viscera innervation, hormonal regulation (Buijs and Kalsbeek 2001), activity, and wakefulness cycles (Abrahamson, Leak, and Moore 2001)(Figure 4). The master clock is the major synchronizer but it is the not only one. Other central oscillators in the brain different than the SCN are subordinating the rhythms in organisms, like the activity, appetite, memory formation (Begemann, Neumann, and Oster 2020). Activity patterns can feedback on the SCN and the feeding time is capable of entraining peripheral clocks, independently of the SCN (Schibler and Sassone-Corsi 2002). The SCN remains the major oscillator in the circadian organization of the body. SCN neurons are directly synchronized at the molecular level and regulate the peripheral clocks in organs and physiological parameters by integration of neuronal and hormonal signals (Hastings, Maywood, and Brancaccio 2018)(Figure 4). 5% to 9% of the genes not included in the core loop are rhythmically expressed in different organs like the liver and heart. There is no more than 10% overlap between tissues, which indicates a tissue-specific response to the circadian stimulation (Hastings, Reddy, and Maywood 2003). The neuroendocrine pathway regulates hormone secretion that can synchronize peripheral organ clocks. Angiotensin II is a hormone rhythmically expressed (Kala, Fyhrquist, and Eisalo 1973) capable of entraining clock gene expression in the vascular smooth muscle cells. Those cells are structuring the vessel walls and give it its dynamic properties that govern the blood pressure (Nonaka et al. 2001)(Figure 4). Circadian rhythms also influence glucose tolerance (Morris et al. 2015) and the renal glomerular filtration rate (Voogel et al. 2001) (Figure 4). Mammals are homeotherms and they maintain a set temperature at all times. This regulation happens in the preoptic area of the hypothalamus and is influenced by circadian rhythm (Figure 4) through the SCN which project to the region. The temperature setpoint peaks at the end of the day and is at its lowest at the end of the night (Morf and Schibler 2013). Other parameters like plasma melatonin, cortisol, and alertness are controlled by circadian rhythms (Dijk et al. 2012). One of the most evident rhythms is the sleep/wake cycle, greatly influenced by melatonin. Melatonin is secreted at night in the pineal

gland and released in the circulation (Russel J. Reiter 1991). Its secretion is regulated by the internal clock (Keijzer et al. 2014) and is suppressed by light (Lewy et al. 1980). Receptors to melatonin have been found in many peripheral systems such as the immune system, the cardiovascular, urinary, and reproductive systems as well as in different brain areas (Reppart, Weaver, and Godson 1996). It not only affects the sleep/ wake cycle, but also the temperature cycle (Cagnacci, Elliott, and Yen 1992), the energy metabolism and glucose regulation (McMullan et al. 2013) and participate in reactive oxygen species regulation (R. J. Reiter et al. 2016).

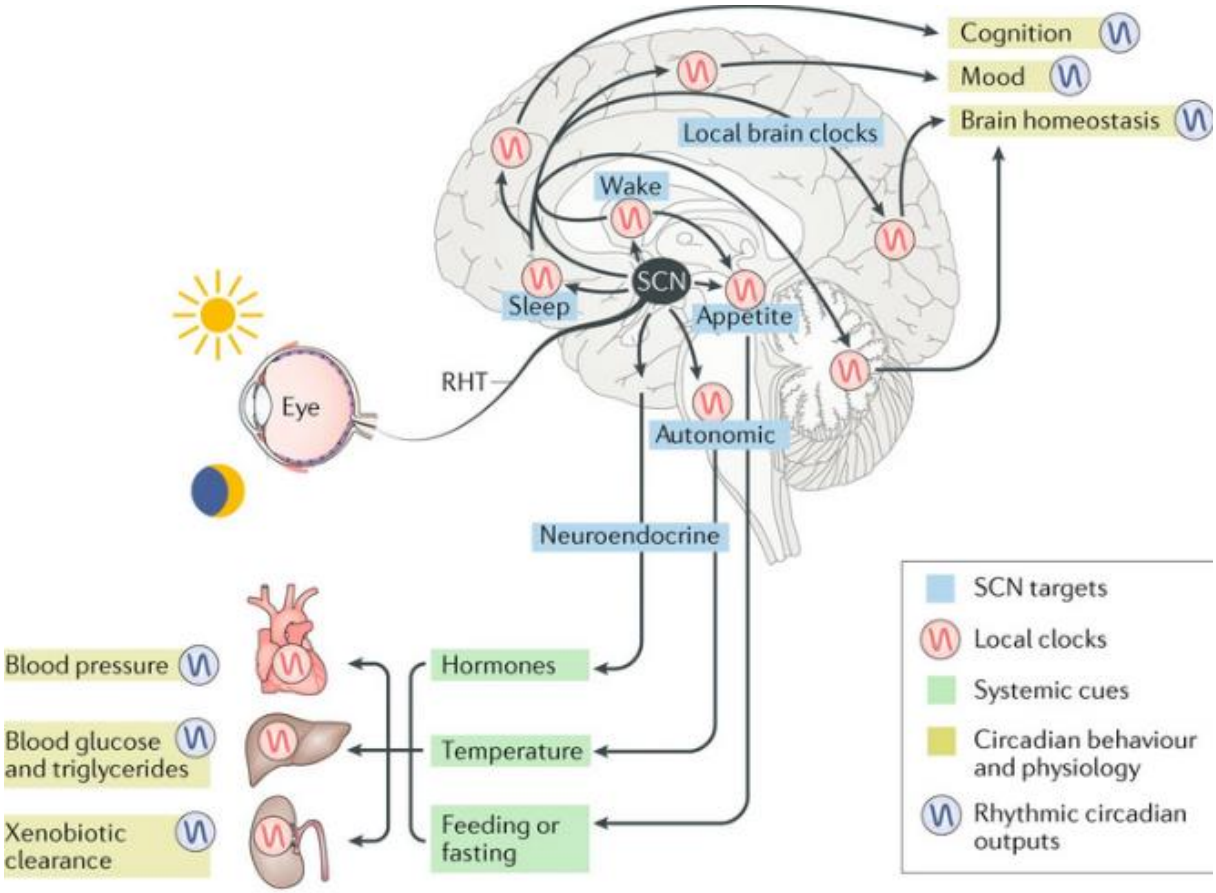

Figure 4 **The different clocks in the body regulates multiple physiological outputs**. Reprinted from (Hastings, Maywood et al. 2018). The light entrains the master clock by photic cues. The SCN then synchronises other local clocks in the brain by direct neuronal pathways. Those clocks will affect the brain's physiology and functions. The peripheral clocks are synchronized by systemic cues (hormones, temperature) and they regulate different physiological parameters of the target organs.

1.5 The molecular clock: a transcriptional translational feedback loop.

The mammalian transcriptional translational feedback loop is composed of 4 major proteins (loop 1 Figure 5). CLOCK for circadian locomotor output cycles kaput and BMAL1 for brain and muscle ARNT-like 1 also called ARNTL are the activators of the clock, while PER for period and CRY1 for Cryptochrome are the repressors. CLOCK and BMAL1 are basic helix-loop-helix transcription factors. They form a heterodimer that binds to E boxes. E boxes are DNA motifs promoting the expression of a downstream gene when they are activated. The E box targeted by CLOCK-BMAL1 recruits factors for the transcription of PER and CRY1 proteins (Figure 5). Those proteins in the cytoplasm bind to each other, and the serine/ threonine kinases casein kinase 1δ (CK1δ) and CK1ε (C. Lee et al. 2001; Gallego and Virshup 2007). The complex PER/CRY1 is phosphorylated and then translocated to the nucleus where it will suppress its own transcription by interacting with its transcription factors per CLOCK and BMAL1 (loop 1 Figure 5). When the concentration in PER/CRY1 is depleted, the inhibition on CLOCK/BMAL1 is no longer active and PER and CRY1 are expressed for another cycle (Gallego and Virshup 2007)(loop 1 Figure 5).

Another feedback loop with Rev-erbα,β, and RORα,β,andγ exist (loop 2 Figure 5). While Rev-erbα is downregulated by CRY1 and PER, it is upregulated by CLOCK and BMAL1. In return, the expression of Rev-erbα diminishes the expression of its activator, inducing a circadian expression of CLOCK and BMAL1 as well as its own expression (Preitner et al. 2002)(loop 2 Figure 5). On the other hand, the ROR element is promoting the expression of BMAL1 (Guillaumond et al. 2005)(loop2 Figure 5). This positive feedback loop is not essential for the clock to cycle properly but it makes the clock more resilient to environmental changes (Partch, Green, and Takahashi 2014).

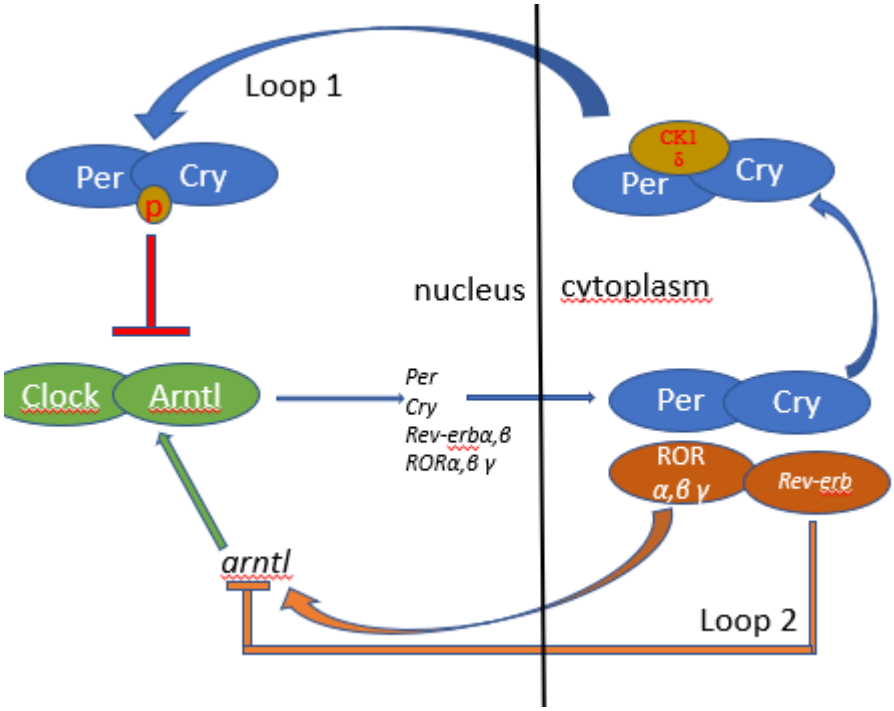

Figure 5 **Transcriptional translational feedback loop controls the circadian clock.** Loop 1 is the main regulatory loop, while loop 2 is stabilizing the molecular clock. On loop 1, Clock and ARNTL induce the expression of Per and CRY1 in the cytoplasm. After phosphorylation by CK1δ, Per, and CRY1 inhibit the expression of Clock and BMAL1 which result in their own suppression. On loop 2, ROR and Rev-erb are upregulated by Clock and ARNTL. ROR element promotes the expression of ARNTL while Rev-erb downregulates it.

A classic transcriptional translational feedback loop would last for a few hours maximum. For the circadian mechanism to last for 24h, phosphorylation is essential. It is a post-translational modification, affecting directly the proteins. The gene expression is not directly representative of the action of the protein and it causes a delay in the interactions. 3 targets of phosphorylation are nuclear entry, formation of protein complexes, and protein degradation (Gallego and Virshup 2007).

This is supported for example by the hamster mutant tau that has a 20h short period and is mutated in the casein kinase CKIε (Lowrey et al. 2000). a mutation in the kinase and not the core clock gene can entrain a change in period.

The glycogen synthase kinase-3 (GSK-3) is also susceptible to affect the clock genes with the regulation of nuclear entry of PER (Iitaka et al. 2005). It also stabilises Rev-erbα (Yin et al. 2006) and thus reduces BMAL1 expression. The casein kinase I CKI is phosphorylating PER. This results in nuclear translocation in some cell types and cytoplasmic accumulation in others (Vielhaber et al. 2000). There is different phosphorylation activity through the cycle (Gallego and Virshup 2007).

Another example of the importance of the post-translational regulation is the binding of casein Kinase1 with PER and with CRY1 with the F-box and leucine-rich repeat protein 3 (FBXL3), while CK1-PER mediates an accumulation in the cytoplasm, and FBXL3-CRY1 is stabilising CRY1 in the nucleus and lengthening the period (St. John et al. 2014)

1.6 Mitochondrial metabolism

The metabolism can be summarized at the cellular level as the reactions that are occurring to maintain its functions and meet its energy needs. Different metabolic pathways exist to use the potential energy available at its maximum or to reduce its use at the minimum (Judge and Dodd 2020). The organization of metabolism in pathways is a great way to keep the energy derived from the degradation of high-energy molecules like glucose under control. While the acquisition of energy by the cell is called catabolism and transfer energy to ATP, GDP, and NADH, anabolic reactions use the energy from those molecules to maintain cell functions, like mRNA transcription or protein translation for example. (Judge and Dodd 2020). Mitochondria are the center of energy production in the cell. In the mitochondrial matrix, energy from glucose is degraded in NADH and FADH2, and ATP in the citric acid cycle. One cycle results in 1 molecule of ATP (TCA cycle Figure 6), which is the high energy molecule used for metabolism, as well as 2 NADH molecules and 1 FADH2. Those high-energy molecules will be used in the respiratory system, in complex I and II (I and II Figure 6). The NADH gives its high-energy electrons to complex I that will be donated to the coenzyme Q. In the meantime, protons are transferred in the mitochondrial intermembrane space, using the electron force. FADH2 gives its high-energy electrons to complex II that are transferred to the coenzyme Q, without pumping protons in the intermembrane space. The coenzyme Q transports electrons to the complex III (III Figure 6) that transfer protons in the

intermembrane space and the electrons to the cytochrome C. The cytochrome C then transfers the electrons to the final acceptor of the electron transport system, the complex IV, which uses the electron to bind protons and oxygen molecules in a final product that is H2O, water. The proton gradient built up by the different complexes is used by the ATP synthase to phosphorylate low-energy ADP molecules in high-energy ATP molecules (Figure 6) that will be used for cell metabolism (Martínez-Reyes and Chandel 2020).

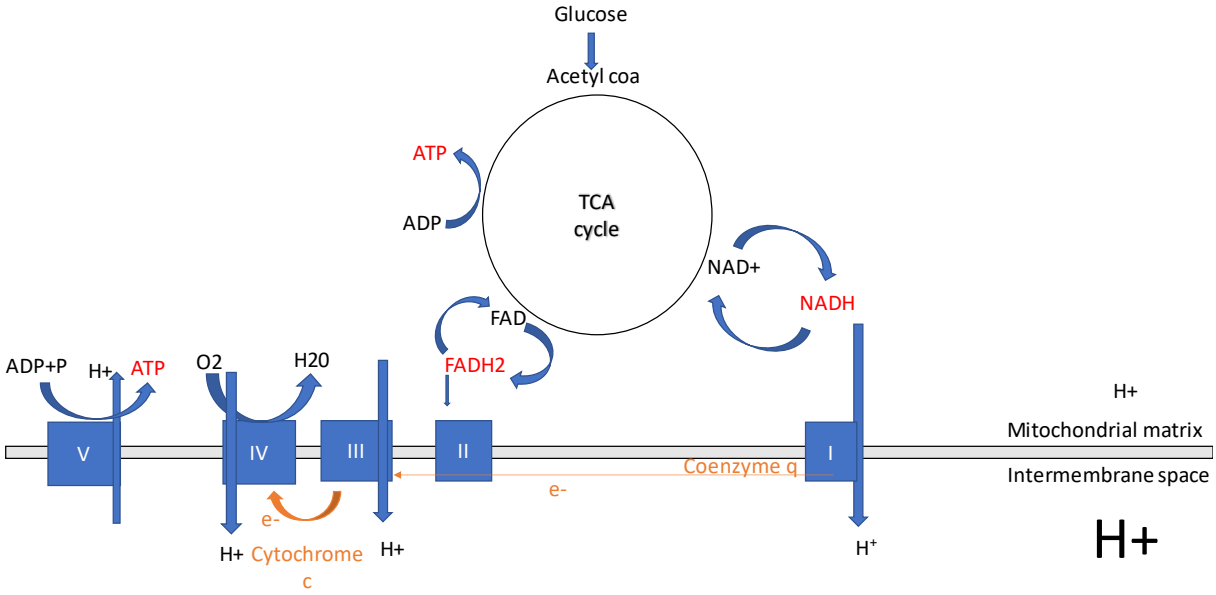

Figure 6 **The TCA cycle in the mitochondrial matrix and the respiratory system.** Tricarboxylic acid cycle (TCA Cycle): From glucose, the TCA cycle produces high energy metabolites (ATP, NADH, and FADH2) from lower energy molecules (ADP, NAD+, FAD). While ATPS can directly be used, NADH and FADH2 are used in the respiratory system to build a proton gradient by direct use in the complex I and II. Electrons are transferred from complex I and II to complex III by the coenzyme q, then to the complex IV by the cytochrome C. this participate in generating the proton gradient in the intermembrane space. This proton gradient is coupled with ATP synthase (V) to produce energy in the form of ATP.

1.7 Crosstalk between clock and metabolism

The different steps of the TCA cycle transfer in an organized manner the energy to molecules in the cells that will be used in other pathways. The energy available in the cells is directly dependent on the energy intake at a higher level, by direct food intake or organ physiology. The daily food intake is regulated by circadian rhythms from the suprachiasmatic nuclei as well as secondary clocks (Challet 2019). It is reasonable to think that the circadian clock also regulates metabolism by food intake. The gene expression in liver mice showed that even if the genes expressed were tissue-specific, the key limiting enzymes were directly regulated by the circadian rhythms (Panda et al. 2002). Evidence of direct interactions between the clockwork and the metabolism. In the pancreas of mice lacking clock functions, there was intolerance to glucose and deficiency in insulin production, despite a normal behaviour (Sadacca et al. 2011). This shows the direct influence of the clock genes on energy metabolism, independently of circadian regulation of the entire animal.

Direct crosstalk between BMAL1 and HIF-1A exists. HIF-1A is like BMAL1 a basic helix loop helix protein that heterodimerizes with HIF1B during hypoxia or mitochondrial stress to induce expression of genes involved in the anaerobic glycolysis and physiological response to hypoxia, like erythropoiesis and angiogenesis. Peek et al. present, in muscle fibers of mice how the circadian clock can mediate the activation of HIF-1A at different times of the day. There is a greater capacity during the active phase when hypoxic conditions are more likely to be encountered (Peek et al. 2017).

Mitochondrial metabolites like succinate and fumarate, as well as ROS produced during respiration, can interact with HIF-1α and induce a pseudohypoxia state (Martínez-Reyes and Chandel 2020). This highlights the relation between mitochondrial metabolism and hypoxia sensing.

1.8 Aim of the thesis

Hooded seals have been used as a great model to study hypoxia and the adaptation of expert diving mammals. Compared to other deep divers like whales, or even other pinnipeds like walruses, their size, behaviour, and needs make it possible to study them not only in their natural habitat but also in the laboratory.

As arctic animals, they are subject to the seasonal variation in the daily light regime, in addition to the variation related to dive depth, but little research has been done under the angle of chronobiology. Recent studies demonstrate a relationship between the circadian clockwork mechanisms and metabolism, especially in the context of hypoxia. Hooded seals are an opportunity to study how the clock of an arctic animal is behaving and how it can interact with the biology of a hypoxia-tolerant diver.

The overarching aim of this thesis was to characterise the hooded seal molecular clockwork. A secondary aim was to explore the link between mitochondrial metabolism and the circadian clock in a diving mammal.

These aims were explored through the 5 following objectives:

-In silico identification of hooded seal clock genes

-Validation of in-silico predicted clock genes by cloning and sequencing

-Validation and quantification of predicted clock genes in multiple tissues from the hooded seal in the mid-light and mid-dark phase

-Development of a hooded seal cell culture model to test the circadian properties of seal clock genes

-Characterisation of mitochondrial metabolism in relation to circadian phase within the seal cell culture model

2 MATERIALS AND METHODS

2.1 Hooded seals

The Hooded seals (*Cystophora cristata*) K1-K6 19 (Table 1) were captured in March 2019 (n = 6 weaned pups) in the pack ice of the Greenland Sea under permits from relevant Norwegian and Greenland authorities. They were brought to UiT – The Arctic University of Norway, where they were maintained in a certified research animal facility in connection with other studies. They were offered freshly thawed, human food grade frozen herring (Clupea harengus) according to each animal's physiological needs, supplemented daily with marine animal dietary vitamins and minerals (Sea Tabs ® MA, Pacific Research Labs Inc., PO Box 675890, Rancho Santa Fe, CA 92067, USA). The photoperiod in the seal facility was accelerated towards 12h of light and 12 hours of darkness for 14 days and the animals were exposed to the 12L;12D for 18 days.

2.2 Euthanasia

The animals were juveniles at 11-12 months of age. Three seals were culled at mid-day, (Zeitgeber time 6, ZT6) at 9h in the morning local time, and the three other seals were culled at mid-night, (ZT18) 21H local time. K2 K4 and K6 were culled during the light phase and K1-K3 and K5 were culled during the night phase (Table 1). The handling of the animals culled during the dark phase was done in the dark. All handlings on animals were done by Professor Lars Folkow, technical personnel Renate Thorvaldsen, Hans Arne Solvang, and Hans Lian.

The tank was drained, in the dark for the ZT18 culled animals. The seal was then caught and injected with the sedation zolazepam/tiletamine (Zoletil Forte Vet., Virbac S.A.,France; 1.8 - 3.0 mg per kg of body mass) intramuscular according to its body mass (Table 1). When sedated, the seal was transported to the autopsy room. The seals culled during the mid-night timepoint had their eyes covered until euthanasia to avoid interaction with light. In the autopsy room, a thermometer was set to monitor the seal's temperature and a catheter was

placed to the extradural intravertebral vein, just in case an injection of additional drug was necessary.

The seals were measured in length while gas anesthesia was performed with an endotracheal tube to ventilate the lungs with a mix of air/Isoflurane at 2-4% (Forene, Abbott, Germany) (Table 1). The mix was pumped periodically with a manual resuscitator to mimic respiration pulses for 5 minutes. A pulse oximeter was installed in the tongue of the animal to monitor its pulse and oxygen level. When fully anesthetized, the seal was euthanized by exsanguination via the carotid arteries

Animal	Sex	Mass	Standard length	Euthanized	Sedation[1]	Anesthesia[2]	Photoperiod[3]
K1-19	F	75	142	03.03.20	150 mg im 40 mg iv	4% ISO 1 min 2% ISO 5 min	DARK
K2-19	M	81.7	139	28.02.20	150 mg im 70 mg iv	4% ISO 1 min 2% ISO 5 min	LIGHT
K3-19	M	68.7	140	04.03.20	180 mg im	2% ISO 5 min	DARK
K4-19	M	73.5	141	02.03.20	150 mg im	2% ISO 5 min	LIGHT
K5-19	M	73	139	05.03.20	150 mg im 50 mg iv	2% ISO 5 min	DARK
K6-19	F	68	137	03.03.20	200 mg im	2% ISO 5 min	LIGHT

Table 1 **Seals' standard information**. The table is recapitulating each animal's sex mass, date of euthanasia, the quantity of sedation and anesthesia, and the light phase during the culling. [1] Zoletile Forte Vet / [2]Isoflurane is mixed with air/ [3] Photoperiod was accelerated towards 12L:12D, starting January 27th and on 12L (03-15 h):12D (15-03 h) rhythm from February 10^{th,} 2020 and until the date of euthanasia.

2.3 Tissue sampling:

The seal's head was cut sagitally from the nose line and put in oxygenated ice-cold ACSF to preserve the brain. The brain was then extracted and tissues from different brain regions were collected (Figure 7). We sampled the visual cortex VC, the bulbus olfactorius BO, the hippocampus H, the cerebellum CE, and the somatosensory cortex SC (Figure 7). The samples were minced using a scalpel for better penetration of the RNA later solution in the tissue, to ensure better preservation (Figure 7).

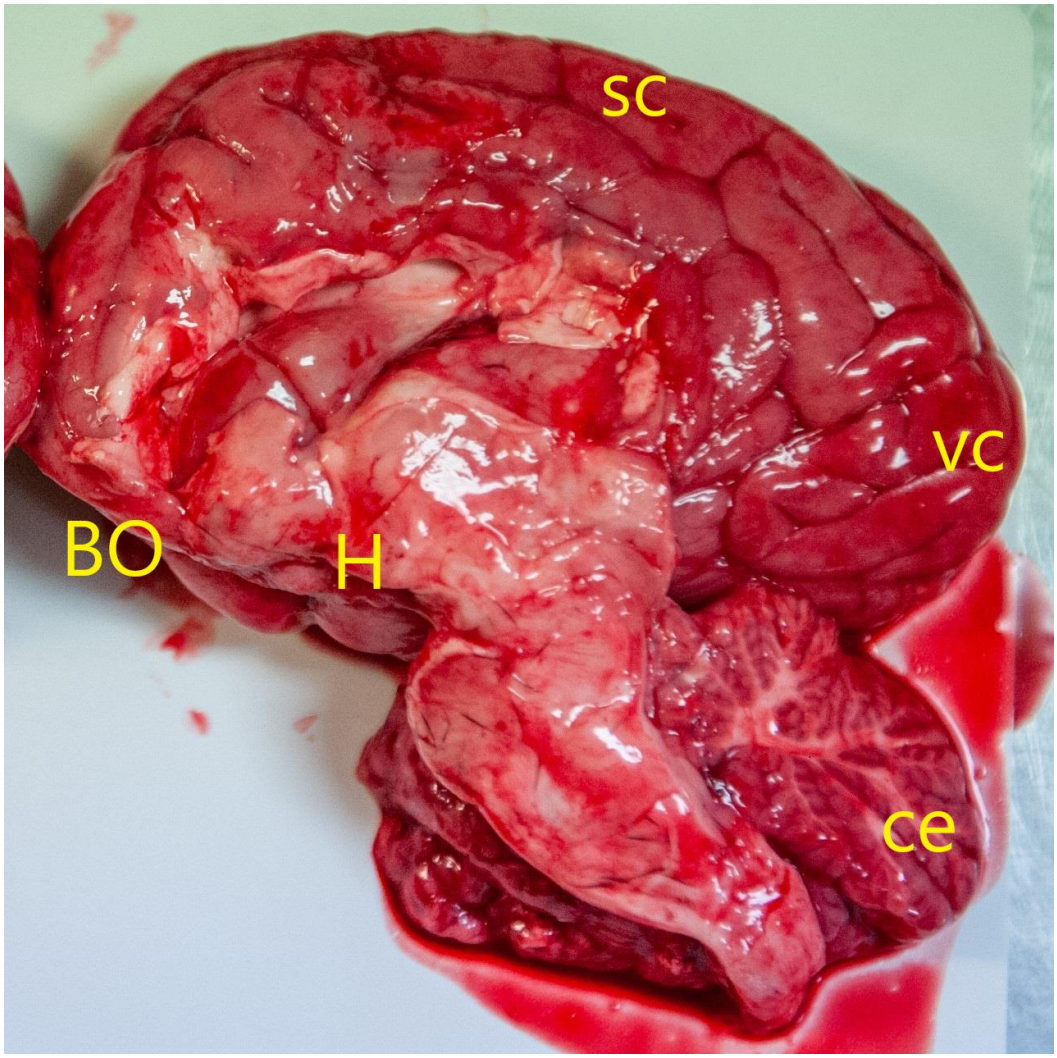

Figure 7 **hooded seal brain regions annotated**. Sagittal section of hooded seal brain with the different regions that were sampled for the experiments on tissue (result section 3.2): VC visual cortex BO bulbus olfactorius, H hippocampus, CE cerebellum, SC somatosensory cortex. Photo courtesy of Frederik Markussen taken from a different brain that the one used during the experiment.

The peripheral tissues were sampled from the posterior part of the left organ of the animal for the kidney, lungs, heart, and liver (Figure 8). The skin fibroblasts were collected from the hind flipper between the digits with a biopsy punch.

All the tissues were cut into small pieces and placed in 4ml of RNA later in Cryovials with a sample size/volume RNA later ratio of 1/10. They were stored 24 hours at 4°C and then stored at -20°C until RNA extraction.

Figure 8 **Hooded seal peripheral organs annotated**. Different organs that were sampled for the experiment a) heart b) lungs c) kidney d) liver. The tissues used in the experiment are from a different animal. Photo courtesy of Rikke Gunnufsen

2.4 mRNA extraction and cDNA conversion

2.4.1 Tissue lysis

To extract the RNA from the frozen tissue in RNA later, the samples were let thaw first. 30mg of tissue was cut with a sterile scalpel and forceps. The tissue was then minced in very thin. Those steps were done on an aluminum foil to avoid contamination of the samples, and the instruments were cleaned with RNase Away after each sample. The foil was used for a single sample and cleaned with RNase Away before use. the minced tissue was then inserted in a low bind tube with 600µl of RLT buffer+ *β-mercaptoethanol* and a metal bid. The tubes were inserted in the Tissue Lyser for 6 minutes at 20 shakes/ second.

If after the first 6 minutes the tissue was not homogenised with the buffer, the tissue lyser step was repeated until the lysate was homogenised. It was then continued by the RNA extraction

2.4.2 Cell lysis

The cell plates were taken out of the -80°C freezer to thaw at room temperature. The cells were collected with 350µl of RLT buffer in a QIA shredder spin column. To make sure to collect the maximum number of cells, the buffer and cells were mixed in the well to detach all the cells by pipetting in and out the mix. The column was centrifugated for 2 minutes at full speed. 350µl of 70% ethanol was mixed with the homogenised lysate and transferred in the RNeasy spin column (2.4.3).

2.4.3 RNA extraction

the RNA extraction was done following the protocol of the RNeasy mini kit from Qiagen, using columns and reaction reagents from the same kit. Sterile filtered tips and tubes were used during the protocol, and good lab practices were followed. On column DNase at the beginning of the extraction was done when possible (reagents availability), following the instructions of the Qiagen DNase kit.

2.4.4 Quantification of RNA

To control that the mRNA extraction was efficient, the concentration of the samples was directly measured after the extraction protocol before freezing to avoid multiple freezing-thawing cycles and degradation of the mRNA. The samples were kept on ice during the

measurement of the batch. The measures were done using a nanodrop, it is an optical reader measuring the wavelength of a droplet sample and from it determines the concentration in DNA or RNA, as well as the purity of the sample from protein and salt contaminants. The nanodrop was set to measure RNA. The blank sample for calibration was the same water that was used to collect the mRNA during the last step of the extraction protocol.

To measure the concentration, 1µl of each sample was deposited in the optical reader and mRNA concentration, as well as the 260/280 and 260/230 ratios for protein and salt purity, were registered. The reader was cleaned after each measure with a tissue.

The usual ranges of mRNA concentrations were from 100ng/µl to 450ng/µl.

2.4.5 Dnase treatment+ cDNA conversion

The samples were then purified from the remaining DNA with a DNase treatment if it did not happen at the beginning of the extraction (2.4.3).

The mRNA concentration values were used to normalise the quantity of cDNA that would be reverse transcribed (Table 2). The lowest concentration of the 6 samples for a specific tissue was used to calculate how much µg of RNA could be in 7.2 µl. The other samples were then normalised to this concentration by calculating how much volume of sample solution was needed to reach the same mRNA content and how much water is needed to have a final volume of 7,2µl.

	Equation
Lowest mRNA quantity R used to normalise the other samples	R=Lowest [mRNA] X 7,2µl
volume of sample for a normalised concentration of the other samples	VNORM = [mRNA]/R
Volume of water to add	= VNORM - 7,2 µl

Table 2 **Normalisation of mRNA**. 3 equations were used to normalise the mRNA concentration of different samples after extraction to base the qPCR results on the same initial mRNA concentration.

The normalisation step ensures that the mRNA concentration is the same in all the samples and that the qPCR will measure the difference in mRNA transcription and not a simple difference in concentration.

0.8µl of buffer and 0.1µl of DNase were added in each sample.

The mix was heated at 37°C for 10 minutes for the enzymatic reaction to happen. The reaction was stopped by adding 0.9µl of EDTA at a concentration of 0.05M in each tube and it was heated at 75°C for 10 minutes

The cDNA conversion uses reverse transcriptase to convert the mRNA in DNA that will be targeted by the primers during the qPCR.

10 µl of cDNA buffer and 1µl of the enzyme reverse transcriptase were added to each tube right after the DNase treatment. It was heated in the thermocycler for an hour at 37°C and cooled down at 4°C.

The cDNA sample was then stored at -20°C until further use. cDNA is more stable and less fragile than mRNA. It is better to proceed until the samples are converted into cDNA than to leave them as mRNA.

2.5 Gene identification

2.5.1 Primer design

The primers for hooded seals were designed based on the dog (*Canis lupus*) version of genes compared to a Weddell seal (*Leptonychotes weddelli*) genome. The seal genome has been published by the broad Institute in pub Med with samples provided by Dr. Daniel P. Costa from the Department of Ecology & Evolutionary Biology, University of California (https://www.ncbi.nlm.nih.gov/assembly/GCF_000349705.1/). It was retrieved as a fna file. The different genes of interest were taken from the dog reference breed and were retrieved from the ensemble database. We used the cDNA sequence.

Several databases of the Weddell seal genome were created. Using BLAST 2.6.0, they were compared with the query from the dog gene. A file with information about the length of the

query and the scaffold that the genome sequence is located on. Then this file will look for the smallest and biggest query values (Figure 9). They represent the first and last nucleotide which aligns between the gene of interest and the genome as well as the exons.

The gene region was then extracted from the database of the seal genome using the scaffold number, the first and last query number. To verify that it was the right region, a few nucleotides from the first and last query values were matched with the first and last nucleotides of the extracted region. They should align at the beginning and the end of the genome if the strand is plus/plus, the end, and the beginning of the strand is plus/minus. In ApE, the seal sequence (exons/introns) all the exons were annotated and pasted in an ApE file. This is the coding sequence that will be used to design the primers (Figure 9).

The seal's gene region was then compared with the query to only annotate the exons and retrieve the coding sequence. The primers were designed from the seal coding sequence using Primer3. The primer size was between 18 and 23 bases, with a melting temperature between 52 and 54. The G-C percentage was between 40% and 60%, and the maximum poly X was set to 3. The product size of a primer pair ranges between 75 and 150 base pairs. The primers were designed in conserved regions of the coding sequence for each gene, preferably across 2 exons. Pairs of primers ending with C and G were preferred due to their stronger hydrogen bond to the target. Primers with matching polynucleotides were avoided because they present a higher risk of primer folding. Coding sequences from the dog and the seal were aligned using clustal omega. This alignment shows where the conserved regions of both sequences are. The primer pairs were selected within the conserved regions and possibly across 2 exons.

2.5.2 Primer efficiency

The primer efficiency was tested by a qPCR run of the same sample at different concentrations. 6 serial dilutions, from the original concentration, using 20 microliters of the n-1 solution and diluting it with 20 microliters of pure water.

Primers efficiency was calculated by plotting a standard curve of the log-transformed concentrations against the CT numbers of the serial dilution. The slope coefficient from the plot is used to calculate the % efficiency in the Thermofisher qPCR efficiency calculator. Only primers with efficiency above 90% were used (Figure 9).

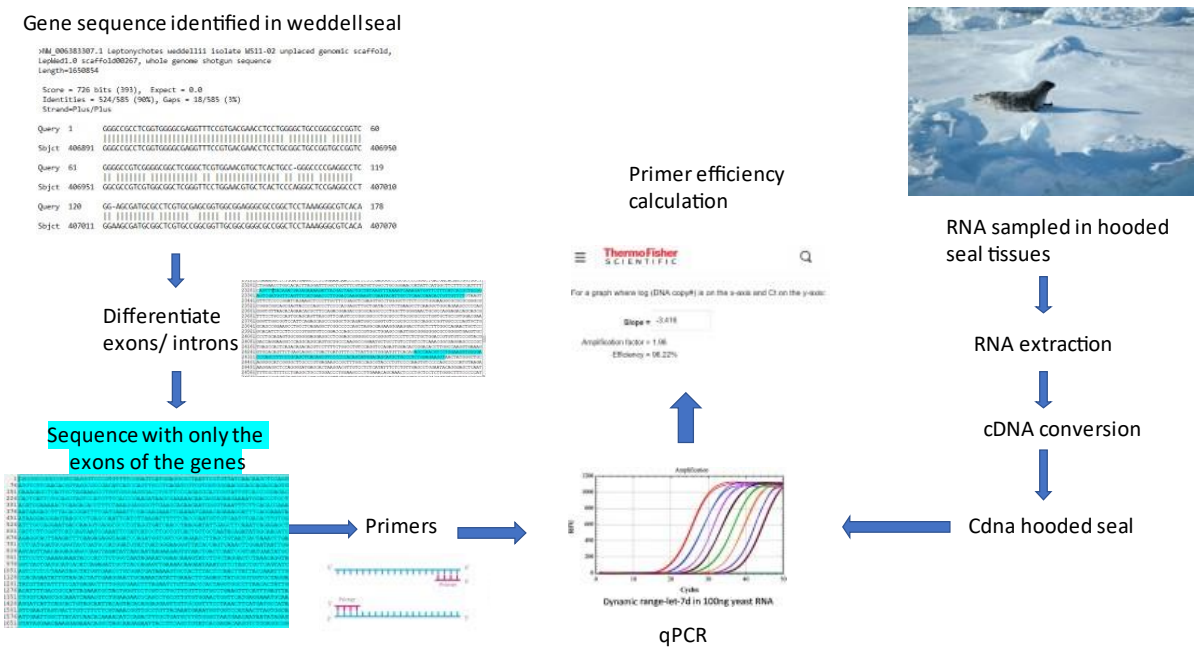

Figure 9 **Flowchart of the steps necessary for the gene identification** (section 2.4; 2.5.1;2.5.2). the gene of interest was identified in the Weddell seal genome when compared to the dog gene. The exons of the genes are then isolated and primers designed from this sequence. mRNA was extracted from the tissue samples and converted in cDNA to be used on qPCR with the primers designed. The primer efficiency was then calculated, primers with an efficiency higher than 90% were used.

2.5.3 Primer validation

2.5.3.1 Sequencing of the product.

A cloning and sequencing experiment was used to confirm that the primer product corresponds to the seal product designed in silico. The cloning kit used was the Zero Blunt PCR Cloning Kit. The PCR product of the gene was ligated to a vector, a kanamycin-resistant plasmid (Appendix Figure 42) for 5 minutes at bench temperature. The vector is then inserted into a bacteria by heat-shock at 42°C for 30 seconds and the transformation mixture is cultured on Lysogeny broth (LB) gel with kanamycin (Figure 10).

Only the positive recombinant bacteria can grow on the media. Several colonies will form on the plates and are then cultured overnight in a shaking incubator at 37°C to grow bacteria.

We then pick four single colonies from the plate 4 replicates for each gene and grow them overnight in LB broth kanamycin resistant (Figure 10).

The plasmids were then extracted from the bacterias using the Qiagen QIAamp DNA Mini Kit and water was added to have a concentration of 100ng/µl. the DNA fragments were then mixed with the primer M13F, Bigdye buffer, and H20 for a big dye PCR. After the PCR, the products were sent to sequencing.

2.5.3.2 Analysis of sequencing

The electropherogram files from the Sanger sequencing were red in ApE. The peaks are indicative of base in the sequence. The further the read in the sequence, the smaller the peaks will get. An overall look at the electropherogram can inform if the sequencing was successful or not (Figure 10).

The entire sequence is then retrieved using the option “new DNA from basecall” in the file menu. This will give us the plasmid sequence that contains the PCR product. The plasmid DNA has to be removed to only have the sequence of interest. The primer used was the M13F and it should be flanked downstream AGAATTCGCCCTT and upstream AAGGGCGAATTCCA. The nucleotides outside those 2 sequences are deleted, including the sequences (Figure 10).

The remaining PCR product is then compared to the target sequence from the seal genome using clustal omega. If both sequences align, it means that the PCR primers targeted the right sequence. The PCR product may have ligated forward or backward and it might be necessary to use the reverse complement. A few mismatches between both sequences can be due to inter-species differences between the Weddell and Hooded seal (Figure 10).

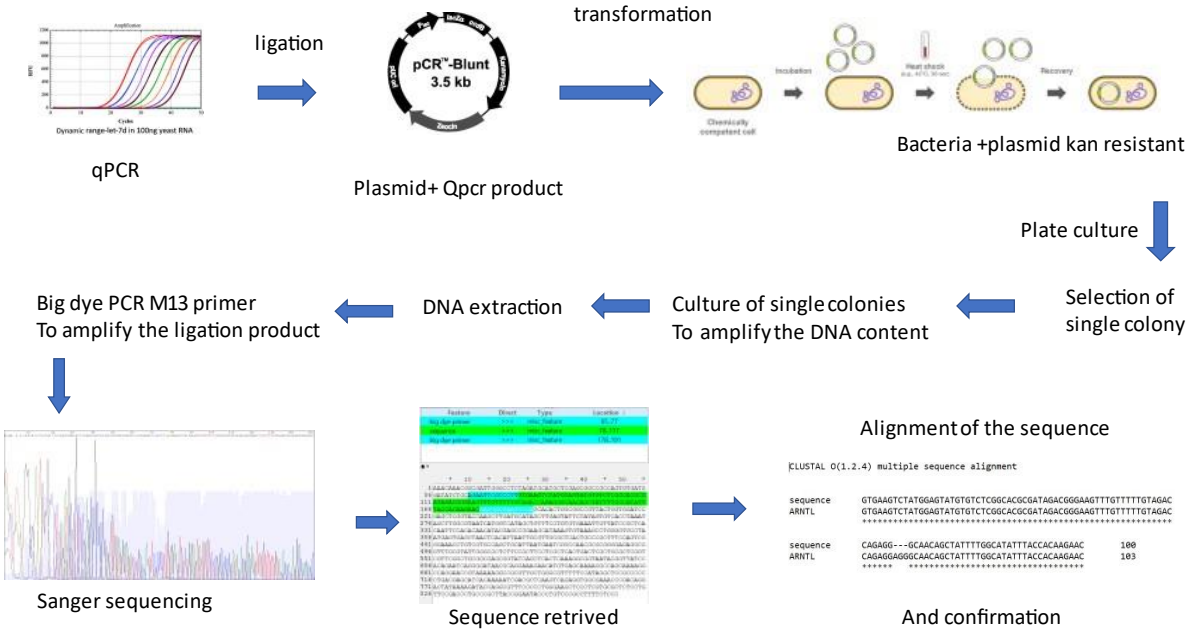

Figure 10 **Flowchart of the steps necessary for the primer validation** (section 2.5.3) qPCR products were ligated to a plasmid and inserted in E-coli bacteria by heat shock and cultured overnight on selective media. Single colonies were picked and cultured in selective media overnight before DNA extraction. The plasmid product was amplified by Big dye PCR and sequenced. The ligation product sequence was retrieved and analysed with the predicted sequence.

2.6 qPCR

The quantitative Polymerase Chain Reaction qPCR is a technique using fluorescence to detect the concentration of a DNA primer product in a sample over temperature cycles. A simple PCR reaction relies on the multiplication of a DNA sequence defined between 2 primers using temperature variations to open the double-stranded DNA, bind the primer to its target, and replicates the target sequence using the DNA polymerase. This process is repeated over cycles and the product targets grow exponentially.

The specificity of qPCR is the use of a fluorescent reporter to report the amplification every cycle. The Taqman reporter is composed of a fluorescent dye and a quencher that inhibits the fluorescence. The DNA polymerase, when it replicates the amplicon, cleaves the reporter and the fluorescent dye emits fluorescence, detected by the machine.

The qPCR reagents used are from the Promega GoTaq qPCR kit. The mix for one well is listed in Table 3. A master mix was prepared to limit the experimental error. The 96 wells plates used were from Bio-Rad and the based on duplication of a DNA primer product from a sample over on temperature cycles

Mix	1 Well	1X Master Mix
Gotaq	10 µl	10X µl
Forward primer	1 µl	1X µl
Reverse primer	1 µl	1X µl
H2O	7 µl	7X µl
sample	1 µl	

Table 3 **qPCR master mix composition**.

The machine used is the Bio-Rad CFX Connect Real_Time PCR system computer control machine. The software used to run the qPCR program is Bio-Rad manager. The program was used to select different qPCR cycles depending on the primer. Some primers were more efficient with an annealing temperature of 55°C while others were more efficient with an annealing temperature of 57°C. The software was used to analyse the melting curve of the product (Figure 11). The presence of a single clear peak means that there is only one product, the product of the qPCR target amplified, while multiple peaks imply the presence of multiple amplified products and a non-selectivity of the primers on the sample.

The amplification curve for each well was informative of wells in which the reaction did not function. It also gives a general idea of the efficiency of the qPCR plate.

The CT values were then extracted in an excel file and further analysis was done using the double delta CT (ddCT) method. the first step of this method is to calculate the CT average of each duplicate for the housekeeping gene and the gene of interest. The difference between the gene of interest and the housekeeping gene dCT is then calculated for each well (dCT). The difference between the dCT of experimental samples and the chosen average control samples

gives the ddCT value. The ddCT value is then transformed by the equation 2^(-ddCT) to have the difference in gene expression expressed in fold change. Because the measure in fold expression depends on the mean values of the control group, it is not possible to compare groups to a different control group without changing the calculations.

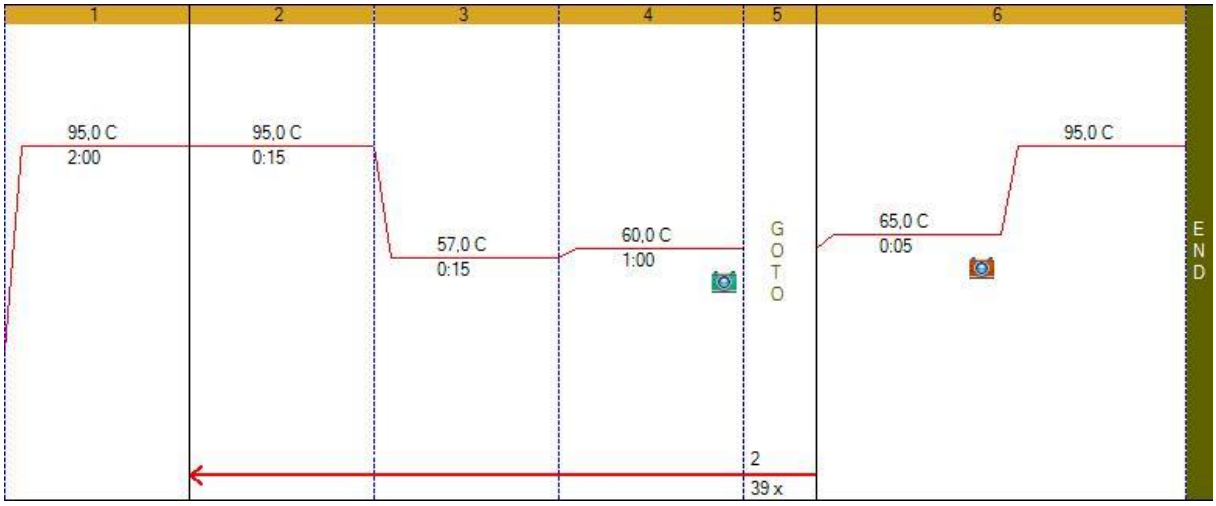

Figure 11 **Temperature cycle for qPCR**. The program used for the qPCR repeats 39 times the temperature cycle. The annealing temperature (step 3) was 57 or 55°C depending on the primer.

2.7 Cell cultures

2.7.1 Culture

The cells cultured were skin fibroblasts of hooded seals from the so-called Greenland's West Ice population collected in 2018.

The cells were cultured at 37°C and 5% CO2. The culture media was the modified Dulbecco's Modified Eagle's Medium-high glucose with 20% FBS and 1% penicillin - Streptomycin. The cells were on their 4th passage when taken from liquid nitrogen and on their 7^{th} passage at the latest during the experiments. They were cultured on T75 plastic flasks and the media was changed every 3 days.

A passage was done when the cells reach 70% to 90% confluency. Using 1µl of trypsin at a concentration of 0.05%. it was left in the incubator for a minute to detach the cells. If the cells

were still attached, the flask was put back in the incubator, no more than 5 minutes. In addition to the trypsin, mechanical taping of the flask helped detach the cells.

Once detached, they were collected in a falcon tube with 12ml of prewarmed media. A volume of media and cells from the falcon tube was re-seeded in a new flask or the old one for up to 3 passages. The volume of re-seeded cells depends on the number of flasks needed and the time available to culture them until they reach confluency. The smaller the volume is divided between each new flask, the more flasks can be seeded after a passage, but the lower the initial cell concentration will be. It will be longer for the cells to be confluent. Media was added to the newly seeded flasks to have a final volume of 12ml.

2.7.2 Cell treatment experiment protocol to reset the clock

The cells of hooded seals were exposed to different treatments and controls for 1 hour. Cells were treated by replicates of 4 in the same 6 wells plate. Each well plate was subject to a specific treatment

The negative control plate stayed in the incubator the entire time of the experiment and was not subject to any treatment or manipulation.

The DMSO control plate was treated with 2µl of 1/1000 diluted DMSO in each well, the Dexamethasone replicates were treated with 2 µl on each well at a concentration of 100nM (diluted in DMSO). The Forskolin plates were treated with 2 microliters on each well at a concentration of 10Um (diluted in DMSO). The melatonin treatment on each well was 2 microliters of melatonin at a concentration of 100ug/ml (diluted in ethanol), which is the physiological concentration in the seal pups (Aarseth, Van'T Hof, and Stokkan 2003). The ethanol control was 2 µl in each well of 0.1% ethanol solution.

Each of the treated plates was taken out separately and put back in the incubator after administration of the treatment to minimize the effect of the temperature while they were under the hood.

After the incubation time of an hour, the cells of each experimental plate were washed with PBS once and directly dry frozen at -80°C for further mRNA extraction.

2.7.3 Cold shock experiment protocol

The cold shock experiment exposed cells to a change in incubation temperature from 37°C to 18°C for 30 minutes. The cells were then put back at 37°C and collected at 30 minutes, 60 minutes, 90 minutes, and 120 minutes after being re-exposed to their normal incubation temperature. The control of this experiment was a plate of cells collected before exposure to 18°C.

The experiment was done with 4 wells replicates on a 6 wells plate at each timepoint. For collection, the cells were washed with PBS and instantly frozen on dry ice before storage at -80°C for further mRNA extraction.

2.7.4 Temperature cycling with collection at a constant temperature.

12 six wells plates with each 4 wells of confluent cells were used for the temperature cycle experiment. All plates were exposed to 3 temperature variation cycles of 12h at 39.5°C and 12h at 36.5°C. The collection of the plates started in the second half of the 4^{th} cycle (36.5°C phase). 3 plates were collected with a 4 hour resolution. The temperature was then maintained at 39.5 for the 9 other collection times, with the same 4 hours resolution between each plate (Figure 12). For collection, the plates were washed with PBS and directly frozen on dry ice before storage at -80°C

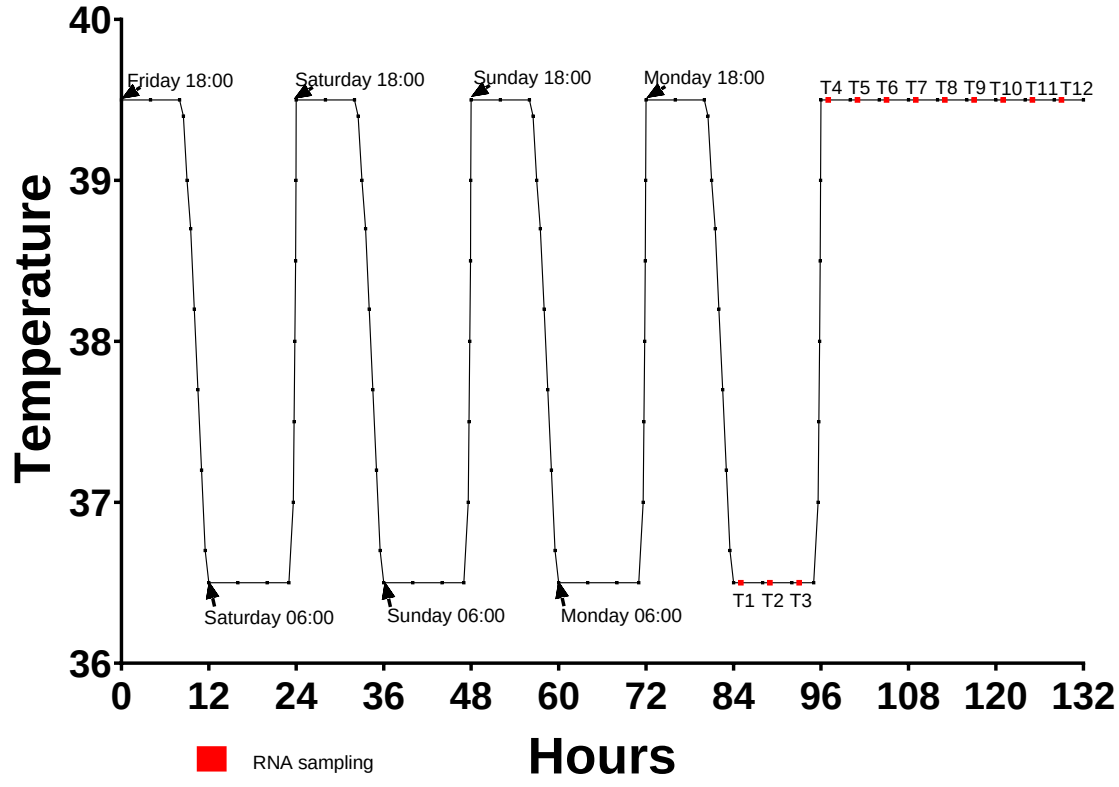

Figure 12 **Experimental design and collection timepoints for temperature cycling at a constant temperature.** The cells were kept under temperature cycle for 84 hours before the experiment. The experiment started for the first 12 hours at 36.5°C and continued with a constant temperature of 39.5 for the remaining 36 hours. Red dots mark the sampling times

2.7.5 Temperature cycle with collection at cycling temperature

For this experiment, 12 six wells plates were exposed to a temperature cycle. Each plate had 4 wells filled with confluent cells at the time of the experiment. 12 T175 flasks were used for the SUIT Protocol experiment (see Methods 2.8.2) and 12 plates were used for protein collection.

The cells were exposed to 5 cycles of temperature variation between 39.5°C and 36.5°C of 12h each, from the growing phase until they reached confluency and the start of the experiment. At the end of the 3rd cycle, the media of all plates and flasks was changed (Figure 13). This operation was done quickly and the time outside the incubator for each experimental unit was minimised to reduce the effect of the external temperature on the cell synchronicity.

The plates were collected from the second half of the 6th cycle (36.5°C) for 12 sampling points with a 4h resolution over 2 cycles (Figure 13). For collection, the plates were washed with PBS and directly frozen on dry ice before storage at -80°C for further mRNA extraction.

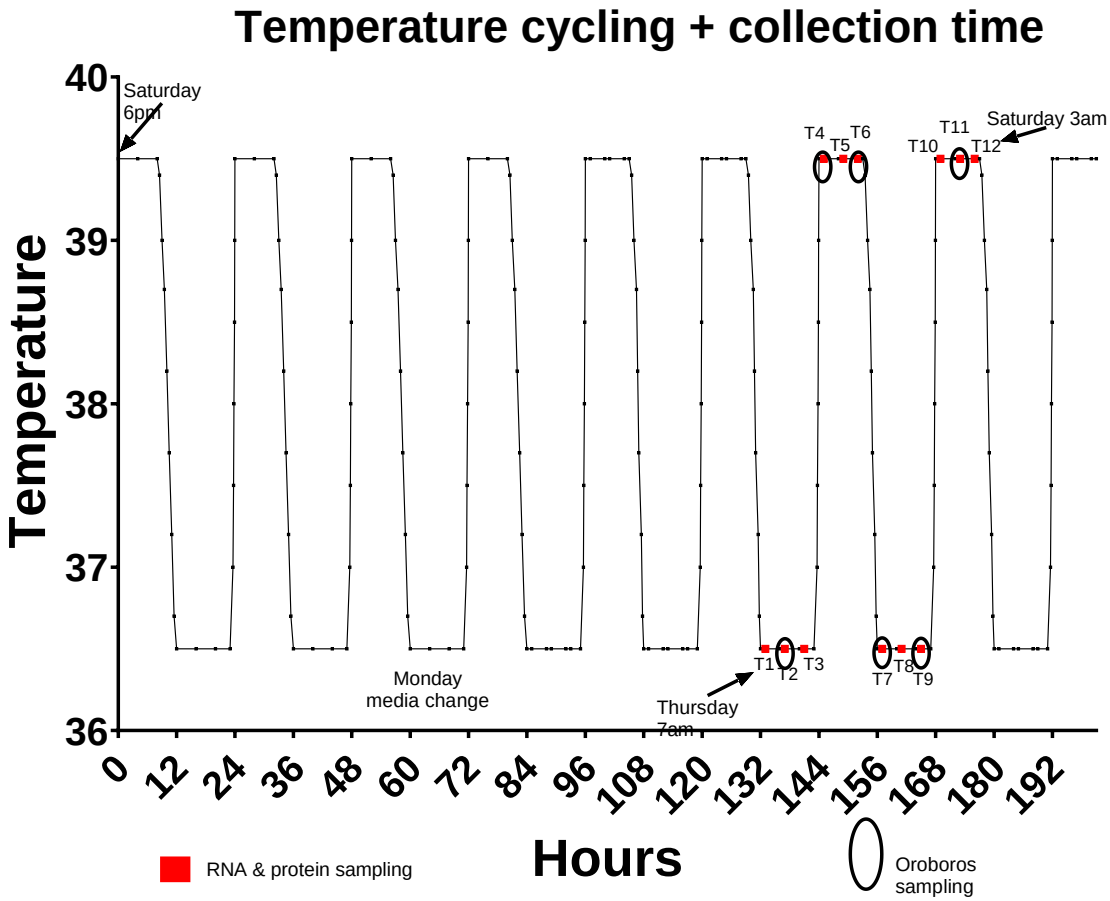

Figure 13 **Experimental design and collection timepoints for temperature cycling at cycling temperature.** The cells were kept in temperature cycles for 132 hours before the experiment and the media was changed at 72 hours. The cells were sampled across 2 temperature cycles with a 4-hour resolution for the RNA and protein sampling while the sampling for the respiration measurement (ororboros experiment) was collected with an 8 hours resolution except between T6 and T7.

2.8 Mitochondrial respiration measure protocol

2.8.1 Preparation of the O2k fluo respirometer Oroboros instrument

The 2 Oxygraph 2K high-resolution respirometer (Oroboros Instruments, Innsbruck, Austria) with each 2 oxygraph chambers were calibrated the day before the experiment and left running overnight to stabilise the oxygen level sensors. The calibration was done following the calibration protocol. The temperature of the oxygraph chambers receiving the cells was the same as the temperature of the incubator at the timepoints of the experiment (36.5°C or 39.5°C)

The oxygen consumption was recorded in real-time using the experiment using the Datlab software (Oroboros Instruments) and the different injections of drugs were annotated simultaneously on the graphs (Figure 14).

To ensure a high enough concentration in the oroboros chamber, the cells were cultured in T175 flasks and 2 flasks were cultured for 1 timepoint. The resolution of the oroboros experiment was 8 hours between each experiment, and it was repeated 6 times throughout the 2 collection cycles (Figure 13), thus giving data around a full cycle with only 1 repetition for each timepoint.

The flasks were taken out from the incubator, washed with PBS to remove residual media. The cells were detached from the flask with trypsin that was let to incubate at an experimental temperature from 1 to 5 minutes. The cells were then collected in culture media, counted, and centrifugated for 5 minutes. The pellet was then resuspended in respiration media MIRO5 (see 2.8.2) to match the concentration needed in the oxygraph chamber.

2.8.2 Substrate-uncoupler-inhibitor titration protocol (SUIT)

The mitochondrial respiration experiment protocol was based on a protocol previously done on northern elephant seals (Chicco et al. 2014) to measure the capacity and leak of complex I and complex II.

The cells were introduced in the chamber with a concentration of $0.6x10^6$ cells/ml and a volume of 2.620 ml. 0.5ml were sampled for protein quantification and 2 x 10 µl were taken out for cell counting. The final volume in the oroboros chamber was 2.1ml. of cells and respiration solution MIRO5 (0.5 mM EGTA, 3 mM MgCl2*6H2O, 60 mM K-lactobionate,

20 mM taurine, 10 mM KH2P04, 20 mM HEPES, 110 mM sucrose, and 1 g/L bovine serum albumin pH = 7). The chamber was then closed and the O2 flow per cell was let to stabilize before starting the experiment.

The different respiratory states were measured as an average of approximately 5 min record of oxygen flow per cell once the flow stabilized from the injection of chemicals in the chamber. (Figure 14) (Table 4).

The first step to measure mitochondrial respiration was to permeabilize the cells with 0.6 µl of Digitonin at 3 µgram/ml. Cell permeabilization keeps the mitochondrial membrane intact and enables measurement of respiration as if the mitochondria were isolated. It also allows the chemicals to interact with the mitochondria. The digitonin concentration was determined in another experiment by Chiara Ciccone.

5 µl of pyruvate [5mM] and 10 µl of malate [2mM] were then added to measure the leak respiration due to pyruvate and malate alone. The pyruvate and malate are the substrates of the tricarboxylic acid cycle. The leak state is the measure of the protons that do not participate in energy production. (state PM-L Figure 14)

The next chemical added was 10 µl of ADP [2.5mM] to measure the respiration capacity with pyruvate and malate. ADP is used in the cycle to be transformed in ATP and the respiration at this state is the contribution of pyruvate and malate to the respiration. (state PM- P Figure 14)

The next chemical added was glutamate to measure the oxidative phosphorylation, also called OXPHOS capacity of the complex I (CI-P Figure 14). The glutamate is enabling the production of NADH+H which is used by the complex I, the NADH dehydrogenase.

20 µl of succinate[10mM] were added to the chamber to measure the respiration at complex I and II. (states CI + CII – P Figure 14). Succinate is the substrate of complex II and because the SUIT protocol addition the different treatments, the respiration of both complexes can be measured at the same time.

To verify that the mitochondria were still intact and had not been damaged by the digitonin, 5 µl of cytochrome C [10 µM] were added. A dramatic rise in oxygen consumption per cell means that the mitochondria are damaged, while an unchanged respiration rate means that

they are intact. If the mitochondria are intact, the oxygraph chamber is reoxygenated to be sure that the oxygen is not a limiting factor (Figure 14).

the experiment can continue and 1 µl of Rotenone [0.5 µM] was added to measure the respiration of complex II. (state CII-P Figure 14). The rotenone inhibits complex I respiration.

To measure the leak due to complex II (state CII-L Figure 14), 2 µl of oligomycin [10nM] were added. Its action inhibits the action of the ATP synthase and only the leak due to complex II is measured.

Finally, 2 µl of the uncoupler Carbonyl cyanide-*4*(trifluoromethoxy) phenylhydrazone (FCCP) [1microM] were added to measure the uncoupled state of the mitochondria, which measures the enzymatic capacity of the mitochondria to transport hydrogen atoms (state CII-E Figure 14). This concentration was determined in a separate experiment to have the highest uncoupling effect without inhibition of the oxygen consumption. as the FCCP is an uncoupler that bypasses the ATP synthase and disrupts the proton gradient and thus forces the other elements of the respiratory transport system to restore the proton gradient at their maximum rate.

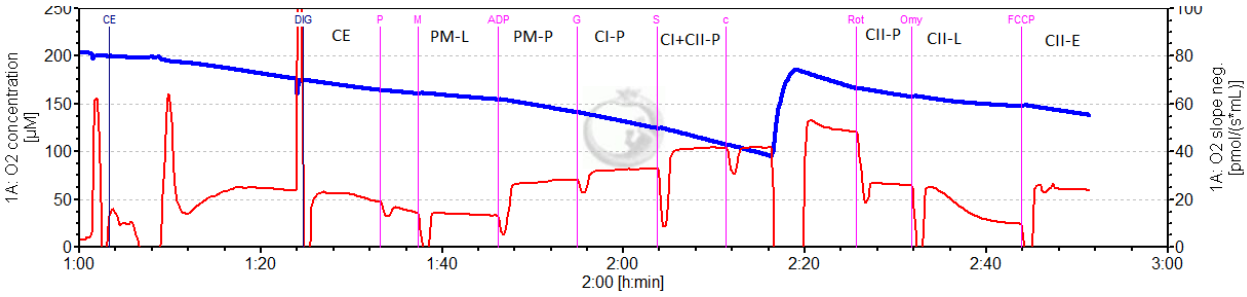

Figure 14 **Datlab oxygraph**: the blue line represent the O2 concentration in [µM] the red line is the variation in O2 flow per cell in [pmol/(s*Mill)] the injection of different titration products is marked by the blue and pink vertical lines. The respiratory states are measured between the different injections.

Chemical	Abreviation	Concentration	Quantity [µl]	State *
	Ce	0.6x10^6 cells/ml	2.620 ml *	
Digitonin	Dig	3 µg/ml	0.6 µl	
Pyruvate	P	5 mM	5	PM -L
Malate	M	2 mM	10	
ADP	D	2.5 mM	10	PM-P
Glutamate	G	10mM	10	CI -P
Succinate	S	10 mM	20	CI + CII - P
Cytochrome C	c	10 µM	5	
Rotenon	Rot	0.5 µM	1	CII - P
Oligomycin	Omy	5-10 nM	1-2	CII - L
FCCP	U	1 µM	2	CII - E

Table 4 **The different titration products for the SUIT protocol and the respiratory state they induce.** The products were successively added to the chamber to measure respiration at different states.

2.9 Use of statistics

The statistical analyses were done using GraphPad Prism 9.0.0 (121) software for most of the statistical analysis. One-way ANOVA was used to compare a control sample to multiple other samples with multiple comparison Tukey tests. The unpaired T-tests were used to compare 2 samples between each other. The Pearson correlation matrixes were used to observe the correlation between different experimental measures.

Outliers were visually identified and retrospectively confirmed by calculation. Values that were deviating of 20% variance from the mean were considered an outlier and excluded.

The analysis of the circadian oscillations was done using JTK cycle (Hughes, Hogenesch, and Kornacker 2010) (Miyazaki et al. 2011) in Rstudio version 1.2.5033 software. It detects cyclic patterns in datasets that are designed with regular intervals between each measure.

3 RESULTS

3.1 Identification of hooded seal clock genes

The hooded seal genome has not been sequenced and very little research has been done on the clock genes of seals in general. Therefore, we took an in-silico approach to identify potential clock genes in the Hooded seal and validated these predictions using qPCR, cloning, and Sanger sequencing.

3.1.1 *In-silico* prediction of hooded seal clock genes

The Weddell seal and Hooded seal are very closely related and we were confident these Weddell seal sequences would be very similar to the hooded seal, not least since clock genes, in general, are highly conserved across species (Bhadra et al. 2017). However, the Weddell seal genome has only been sequenced and is not annotated, therefore we do not know the identity of the genes, we only have the sequences. Pinnipeds and dogs are relatively close in the phylogenetic tree, they both belong to the *Caniformia* (Figure 15). The dog genome is annotated, therefore the identity of the clock genes is known. The clock genes from the dog were obtained and were aligned to the Weddell seal genome (see Methods 2.5.1). The different exons of the seal genes were then identified by alignment to the dog and cross-checked to other species to correctly identify the predicted coding sequence for the seal (Figure 16).

Table 5 summarises the clock genes identified, whether a match was found in the Weddell seal genome and whether the coding region was identified. All the core clock genes and the housekeeping genes were successfully identified using this *in-silico* approach.

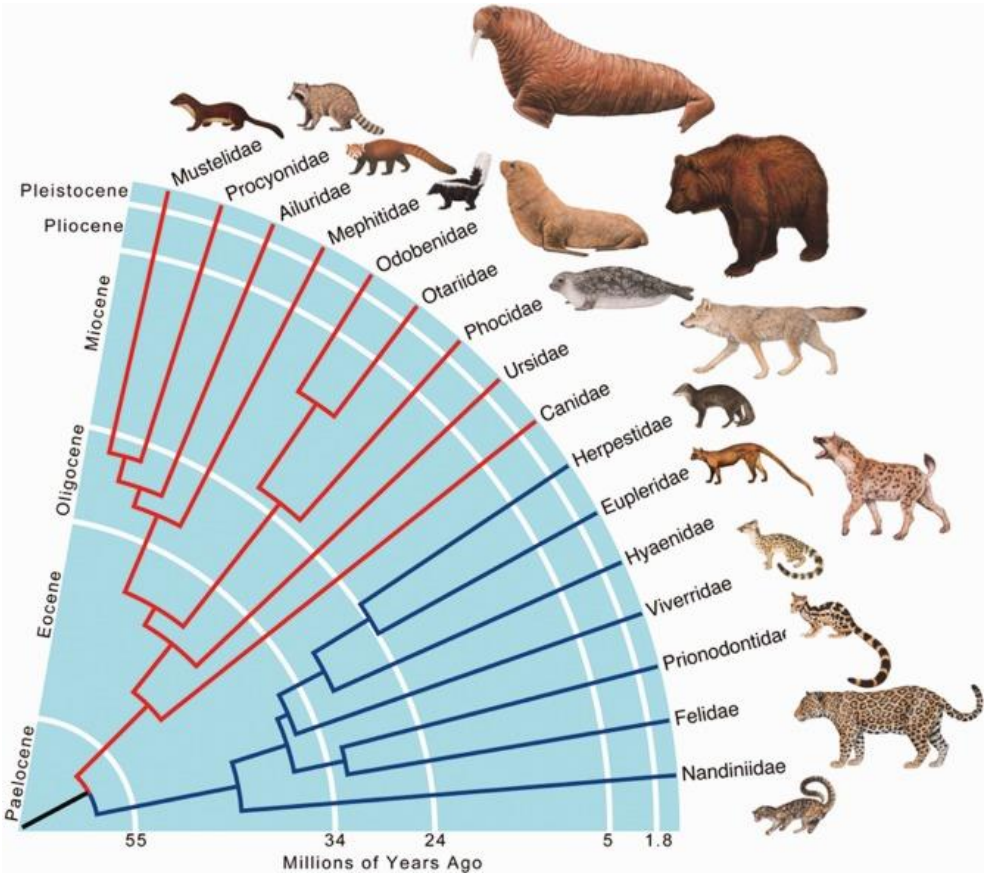

Figure 15 **phylogeny of the Hooded seal**. Reprinted from (Van Valkenburgh et al. 2014). The phylogenetic tree of the Caniformia branch (red) the Hooded and Weddell seals are Phocidae and closely related to the dog, Canidae, making the dog a good reference gene to identify genes in the Weddell seal.

3.1.2 Validation of *in-silico* predicted clock genes by cloning and sequencing

To test if the *in-silico* predicted clock genes could be detected in the hooded seal genome, we designed specific quantitative PCR (qPCR) primers for each clock gene to both quantify and amplify a PCR product. This required that the primers met certain criteria (see methods section 2.5) and efficiently (above 90%) produced the PCR product (Table 1). Using RNA extracted from hooded seal fibroblasts we converted it to cDNA and amplified it by PCR (Methods 2.4.5/2.6). The PCR products were then sequenced to confirm whether the PCR product matched the predicted clock gene sequence. Several criteria must be met to determine if a clock gene had been correctly identified, these are summarised in

Table 5 and Methods 2.5. All the six core clock genes products were more than 90% similar to the predicted target region in the Weddell seal, these results confirm that the primers are efficiently reporting the gene of interest. In addition, three reference genes for qPCR were identified (see Figure 16 and Methods 2.5). The appendix Figure 41 lists all the alignments from the sequencing.

```
DOG         CCCCAGGGGGTCTACAAGTGGCCCTGGAAGATAGTAGCCGAGTGTCCCCCAGCAAGAGCA
      830
SEAL        CCCCAGGGGGTCTACAAGTGGCCCTGGAAGATAGCAGCCGAGTGTCCCCCAGCAAGAGCA
      840
            ********************************** ************************

DOG         CCAGCAACATCACCAAGCTGAATGGCATGGTGCTACTGTGTAAAGTGTGTGGGGATGTTG
      890
SEAL        CCAGCAACATCACCAAGCTGAATGGCATGGTGCTCCTGTGTAAAGTGTGCGGGGACGTGG
      900
            ********************************** ************** ***** ** *

DOG         CCTCAGGCTTCCACTATGGCGTGCATGCCTGTGAGGGCTGCAAG---GGCTTTTTCCGTC
      947
SEAL        CCTCGGGCTTCCACTATGGCGTGCATGCCTGTGAGGGCTGCAAGGAGGGCTTTTTCCGTC
      960
            **** ***************************************   **************

DOG         GGAGCATCCAGCAGAATATCCAGTACAAGAGGTGTCTGAAAAATGAAAATTGTTCCATTG
     1007
SEAL        GGAGCATCCAGCAGAACATCCAGTACAAAAGGTGTCTGAAGAACGAGAACTGCTCCATTG
     1020
            ***************** ************ ************ ** ** ** ** ********

DOG         TCCGCATCAACCGGAACCGCTGCCAGCAGTGTCGCTTCAAGAAGTGTCTCTCCGTGGGCA
     1067
SEAL        TCCGCATCAATCGGAACCGCTGCCAACAGTGTCGCTTCAAGAAGTGTCTCTCCGTGGGCA
     1080
            ********** ************** **********************************
```

Figure 16 **Sequence alignment of NR1D1 in the dog and seal genome**. The dog and Weddell seal genome were aligned together to identify conserved regions. "*"sign represents a match between both dog and seal nucleotides. *Forward* primer and *reverse* primer are selected in a conserved region of the genome

in silico prediction				wet lab validation					
gene	clock gene sequence found in the dog?	Aligned to Weddell genome?	coding region identified?	primer design criteria met	efficient qPCR?	ligation	successful ligation and transformation?	DNA extraction	% similarity of PCR product to the Weddell genome
ARNTL	✓	✓	✓	✓	✓	✓	✓	✓	97.09
CLOCK	✓	✓	✓	✓	✓	✓	✓	✓	99.27
NR1D1	✓	✓	✓	✓	✓	✓	✓	✓	97.14
PER-2	✓	✓	✓	✓	✓	✓	✓	✓	99.09
PPIB	✓	✓	✓	✓	✓	✓	✓	✓	97.54
RORA	✓	✓	✓	✓	✓	✓	✓	✓	94.34
CRY1 1	✓	✓	✓	✓	✓	✓	✓	✓	96.3
RPLPO	✓	✓	✓	✓	✓	✓	✓	✓	90.79
TBP	✓	✓	✓	✓	✗	✗	✗	✗	✗

Table 5 **Gene identification and confirmation.** Summary table of the different steps in the identification of the clock genes and housekeeping genes in hooded seal and the similarity between the sequenced product and the predicted qPCR target to confirm the qPCR results.

3.2 Validation and quantification of predicted clock genes in multiple tissues from the hooded seal in the mid-light and mid-dark phase

Having successfully predicted and identified clock genes in the hooded seal (3.1) we now wished to test which tissues in the hooded seal expressed these clock genes and whether there was a time of day difference in the amount of expression. To achieve this, hooded seals kept under 12 hours of light and 12 hours of dark were sampled at the mid-light and mid-dark phase, which represents zeitgeber time ZT6 and ZT18 respectively (Methods 2.3). The seals were kept under a light/dark cycle for at least 18 days (Table 1). Table 6 lists the tissues sampled and whether the RNA extraction was successful. The liver, kidney, heart, lungs, and skin were collected for the peripheral tissues. The brain tissues collected were the cerebellum CE, the visual cortex VC, the bulbus olfactorius BO, the hippocampus H, and the somatosensory cortex SC (Figure 7).

Only very low amounts of RNA (0 ng/µl to 36.4 ng/µl) could be extracted from the heart and skin samples therefore, they were removed from the analysis (Table 6). Samples successfully

extracted were then converted to cDNA and quantified by qPCR (primers, percentage efficiencies and products are in Methods2.5 /appendix Table 7).

	peripheral tissue					brain tissue				
individual	liver	kidney	lungs	heart	skin	CE	VC	BO	H	SC
K1	✓	✓	✓	✗	✗	✓	✓	✓	✓	✓
K2	✗	✓	✓	✗	✗	✓	✓	✓	✓	✓
K3	✓	✓	✓	✗	✗	✓	✓	✓	✓	✓
K4	✓	✓	✓	✗	✗	✓	✓	✓	✓	✓
K5	✓	✓	✓	✗	✗	✓	✓	✓	✓	✓
K6	✓	✓	✓	✗	✗	✓	✓	✓	✓	✓

Table 6 **Sucess of RNA extraction in different hooded seal tissues.** The mRNA extraction from the tissue samples in the 6 seals that were culled was effective in most of the samples, except for the heart and skin samples, and the liver sample for K2 individual.

The first observation from the qPCR of the clock genes on the different tissue samples shows that all the clock genes are expressed *in-vivo* in hooded seals. This rejects the hypothesis that as arctic animals, the hooded seals could have lost the genes or completely silenced their expression. The CT values of the qPCR for the clock genes are between 25 and 30 cycles, indicating a low expression of the genes. Reference genes for the qPCR quantification were also run (see methods 2.6 for an explanation of the need for reference genes).

3.2.1 Clock gene expression varies between hooded seal tissues

To assess the tissue differences in the expression level of the clock genes each tissue relative to the mean expression of five of the liver samples were used. The sample K3 for the liver was excluded from the study on the basis that it did not provide coherent results compared to the other liver samples. For example, the CT values for the housekeeping gene RPLPO for that sample were abnormally low (CT value= 36.08; 34.90) compared to the other liver samples (CT values around 22.5). For all the other tissues, all the samples were used in the calculations (n=6). Figure 17 shows the expression level in each individual relative to the mean expression in the liver as a heatmap, the darker the colour the higher the expression.

The tissues were compared to the mean of the liver samples using an ordinary one-way ANOVA. The peripheral tissues, kidneys, and lungs did not show a difference in the mean level of expression in any of the 6 clock genes compared to the liver (Figure 17)

The brain tissues however presented a marked difference to those in the periphery. The expression level of NR1D1 (Figure 17e), CRY1 (Figure 17c), CLOCK (Figure 17a), and ARNTL (Figure 17b) were significantly different in all the brain samples, namely the cerebellum CE, the visual cortex VC, the bulbus olfactorius BO, the hippocampus H, and the somatosensory cortex SC (Figure 17).

The difference was less pronounced for PER-2 and RORA (Figure 17d,f), where the brain samples with a significantly higher expression were limited to the cerebellum, the visual cortex, and the somatosensory cortex.

There is overall a higher expression of the clock genes in the brain tissues than in the peripheral tissues regardless of the sampling time. It is an encouraging finding. If there is a relation between the clock and the hypoxia metabolism, it is in the brain that the interactions could be more critical.

Validation and quantification of predicted clock genes in multiple tissues from the hooded seal in the mid-light and mid-dark phase

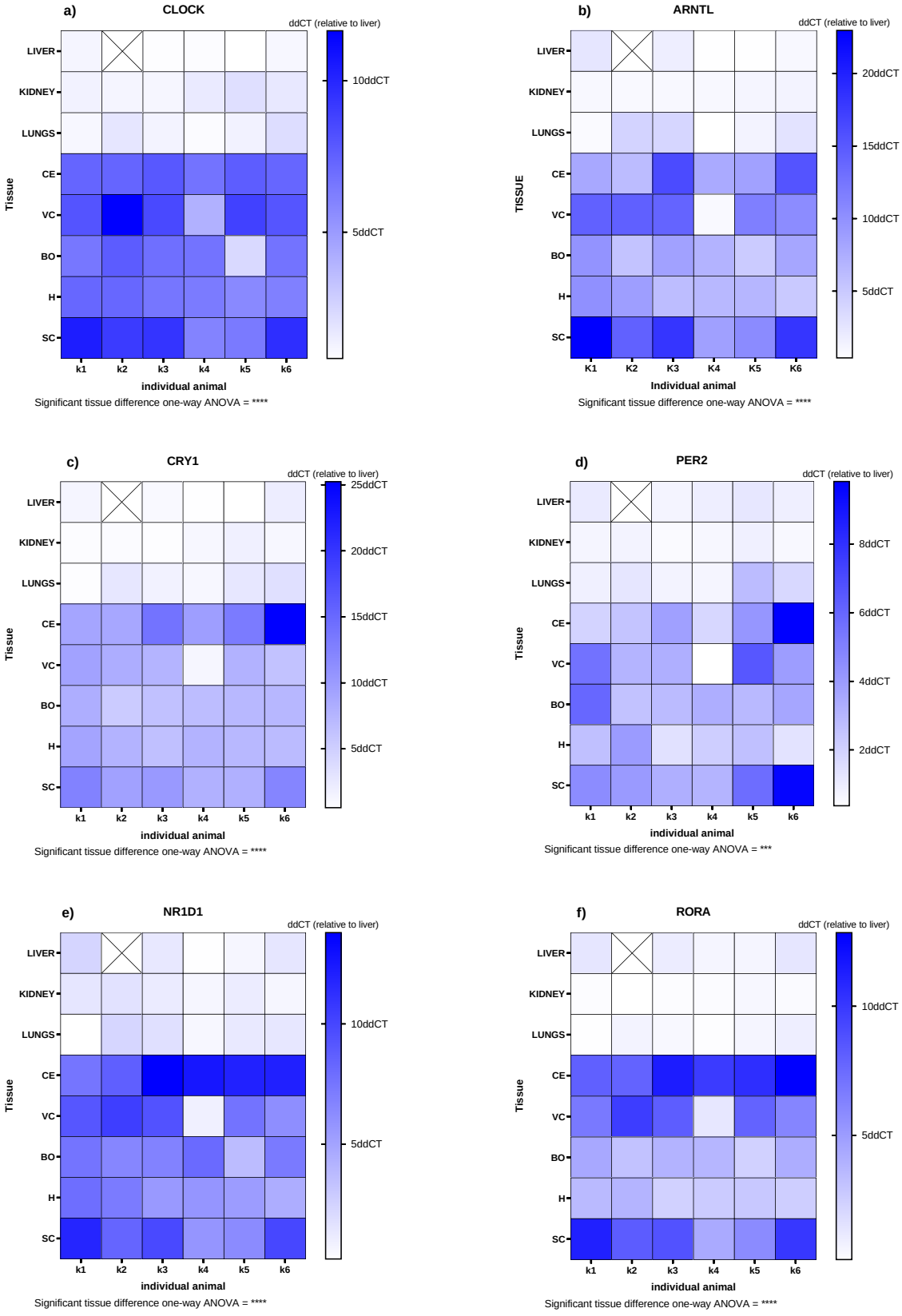

Figure 17 **heatmap representing the level of expression of seal clock genes**: the level of gene expression in different tissues, expressed in ddCT is relative to the gene expression in the liver of the animals The difference of expression across tissues is significant between the peripheral tissues (liver, kidney, lungs) and all the brain tissues (the cerebellum CE, the visual cortex VC, the bulbus olfactorius BO, the hippocampus H, and the somatosensory cortex SC) for CRY1, CLOCK, and ARNTL. It is significant between the peripheral tissues and the cerebellum, the visual cortex and the somatosensory cortex for PER-2 and RORA ***p<0.0005; ****p<0.0001 using one-way ANOVA

3.2.2 The majority of clock genes do not show time of day differences when comparing mid-light and mid-dark samples within hooded seal tissues

The individual animal gene expression for each clock relative to the liver gives no clear indication of a consistent time of day effect. The time of day is defined by the zeitgeber time, ZT=0 corresponding to the onset of light (Figure 17, k2, k4 and k6 – sampled ZT6, k1, k3, k5 – sample ZT18). However, the nature of qPCR analysis and the different expression levels across tissues means that to test the effect of the time of day we must compare expression within tissues and between time points. Therefore, the level of expression within tissues was compared between ZT6 and ZT18 relative to the mean of the ZT6 within each tissue (Appendix Figure 32- Figure 37).

To statistically test the effect of time of day on expression an unpaired T-test was used since there were only two groups to compare. Only four results of the 48 comparisons were significant. Therefore the majority (91.67%) is not significant (Appendix Figure 32-Figure 37). The most likely explanation is that a resolution of 12 hours and sampling at mid-day and mid-night, means it is easy to sample in the middle of the gene cycle rather than at its peak and trough. A greater time resolution would give a better idea of the potential time of day differences, but that was not possible given limited animal numbers.

Nevertheless, ARNTL in the liver showed a higher expression at ZT18 than at ZT6 (P=0.02) and CRY1 has a higher expression at ZT6 than at ZT18 in the kidney (P=0.045) (Figure 18a & b). The tissues in which the difference of expression is significant between ARNTL and CRY1 are not the same, no conclusion can be drawn from this analysis, but the two genes

have an opposite level of expression, which is what is expected for those clock genes when the circadian clock is entrained. CLOCK in the hippocampus has a higher expression at ZT18 than at ZT6 (Figure 18c). The difference of ddCT between the two time points is not bigger than 0.20 but the spread within each timepoint is so small that the difference between the two groups is significant, just below the significant threshold (P=0.04). In the kidney, CLOCK has a higher expression at ZT6 than at ZT18 (P=0.01) (Figure 18d). This illustrates that the expression of the same gene can be different between different tissues. It accentuates that the opposite expression of ARNTL and CRY1 is only an interesting observation.

In conclusion, there is a greater difference in expression across tissues than between the 2 sampling points ZT6 and ZT18 within the same tissue, and the clock genes are more expressed in the brain tissues than in the peripheral tissues.

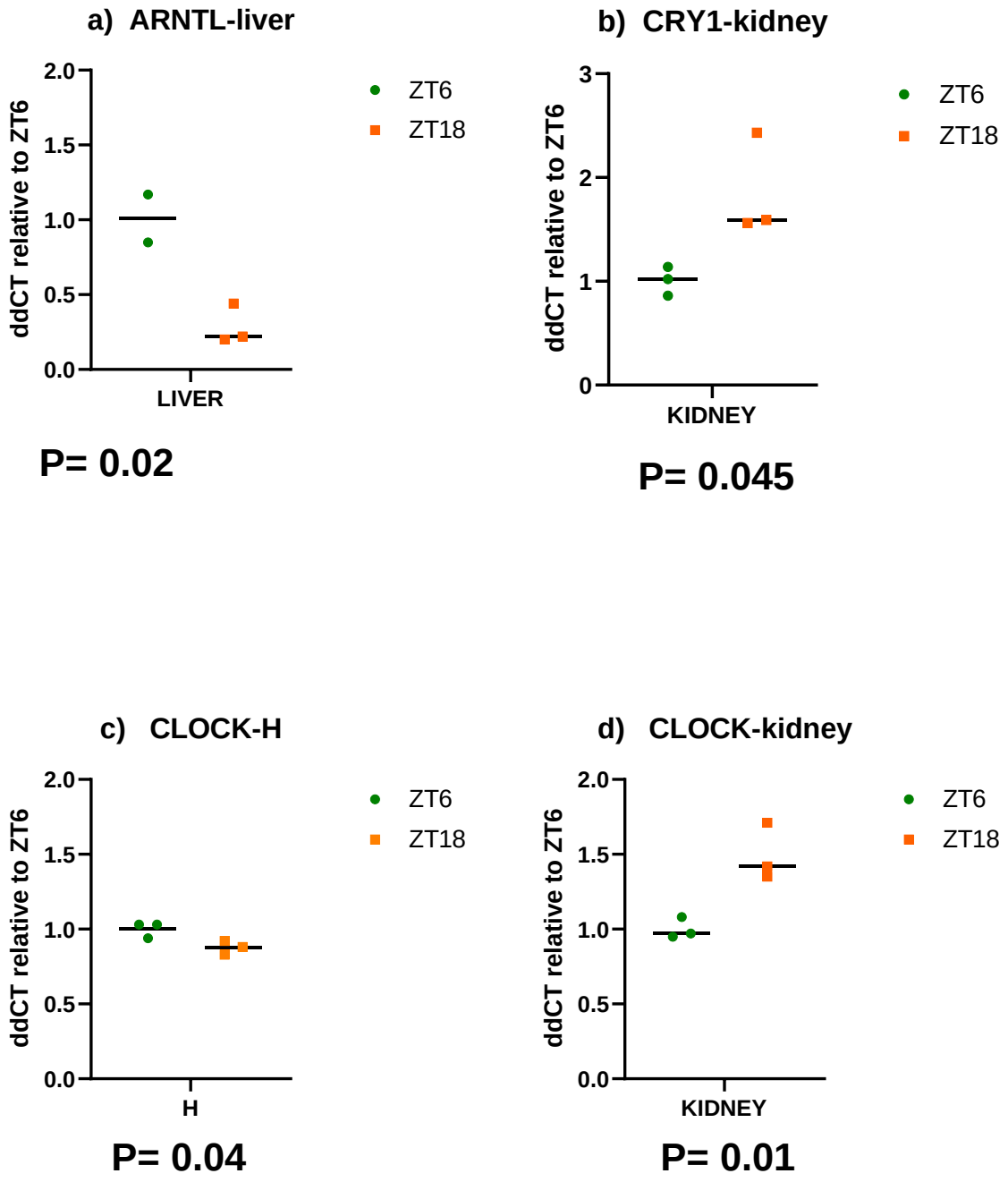

Figure 18 **Difference in the clock gene expression between ZT6 and ZT18 within a tissue**. The ddCT is relative to the average of ZT6 within the tissue samples liver, kidney, and hippocampus(H). P values were calculated using an unpaired T-test.

3.3 Development of a hooded seal cell culture model to characterise circadian clock genes

Given the limitations on animal numbers and the need for increased sampling resolution to investigate clock gene expression, we decided to develop and characterise an *in-vitro* cell culture model. Skin fibroblasts being relatively easy to sample and culture, have been used to characterize the circadian clock in rat cells in the founding papers of chronobiology (Aurélio Balsalobre, Damiola, and Schibler 1998). These cells are easy to culture under standard conditions and are an excellent substitute to the animal model as the mechanisms can be described at the cellular level without the need for an extensive physiological response. Treatments susceptible to interact with the clock are also more precisely controlled in the context of cell culture than *in-vivo* experiments, where external factors are much more likely to interfere. Therefore, to investigate the molecular clock in hooded seals, cell cultures of hooded seals' skin fibroblasts were established, allowing a series of experiments to provide insight into the circadian clockwork of the hooded seal to be undertaken.

3.3.1 PER-2 expression is stimulated in hooded seal skin fibroblast culture

It is well established that factors such as serum(Aurélio Balsalobre, Damiola, and Schibler 1998), forskolin(Yagita and Okamura 2000), dexamethasone (A. Balsalobre 2000) and melatonin (Mcarthur, Gillette, and Prosser 1991) can be used in cell culture to synchronise/stimulate clock gene rhythms in cells in multiple species. Therefore, directly stimulating cells with any one of these factors can induce clock gene expression. We treated our hooded seal skin fibroblasts with serum, forskolin, dexamethasone, melatonin and compared the clock gene expression by qPCR after 1 hour of treatment. Because each of these factors is prepared in different vehicle solutions, we also performed a number of controls; no treatment control (NTC), ethanol (melatonin is dissolved in ethanol), DMSO (forskolin, dexamethasone are dissolved in DMSO). Each treatment is compared to the relevant control i.e. DMSO versus dexamethasone. The effect of the vehicle is also assessed relative to the NTC. All samples were analysed by qPCR for all 6 clock genes.

It should be noted that one of the DMSO treated wells was a systematic outlier and was not included in the calculations therefore n=3, for that group in all genes. In the PER-2 comparison, the qPCR result from one of the replicates from the non-treated control presented an outlier value (Methods 2.9) and was removed from the calculations lowering the number of replicates to n=3. All the other treatments and gene measures were done using the 4 wells replicates of the treated plate (n=4).

CLOCK, CRY1, RORA, and ARNTL showed no significant differences relative to NTC for any of the treatments (Appendix Figure 39). There was an effect of the different treatments on the expression of the clock PER-2 (Figure 19) and NR1D1 (Figure 20 & Appendix *Figure 38*).

The expression of PER-2 did not vary between the DMSO treatment and the non-treated control group, therefore the DMSO is a valid control because it did not affect the cells (Figure 19a). This means it is valid to assess the effect of dexamethasone and forskolin by comparison to their DMSO control (Figure 19b). This shows a clear induction of PER-2 gene expression on treatment with both treatments (approximately 1,5 fold). Figure 19a shows that there is also a significant effect of ethanol on PER-2 expression, the amount of ethanol used was not expected to produce an effect. As ethanol was the vehicle for the melatonin treatment if we compared melatonin to NTC it would appear that we have an effect but it would be due to the ethanol, therefore we compare ethanol to melatonin (Figure 19c) and show no effect. Dissolving melatonin in an alternative vehicle may be a way to overcome this.

The serum shock showed a significant increase in PER-2 expression compared to the non-treated control (Figure 19a). This means that the serum shock influences the expression of PER-2 compared to its control and it is a positive result.

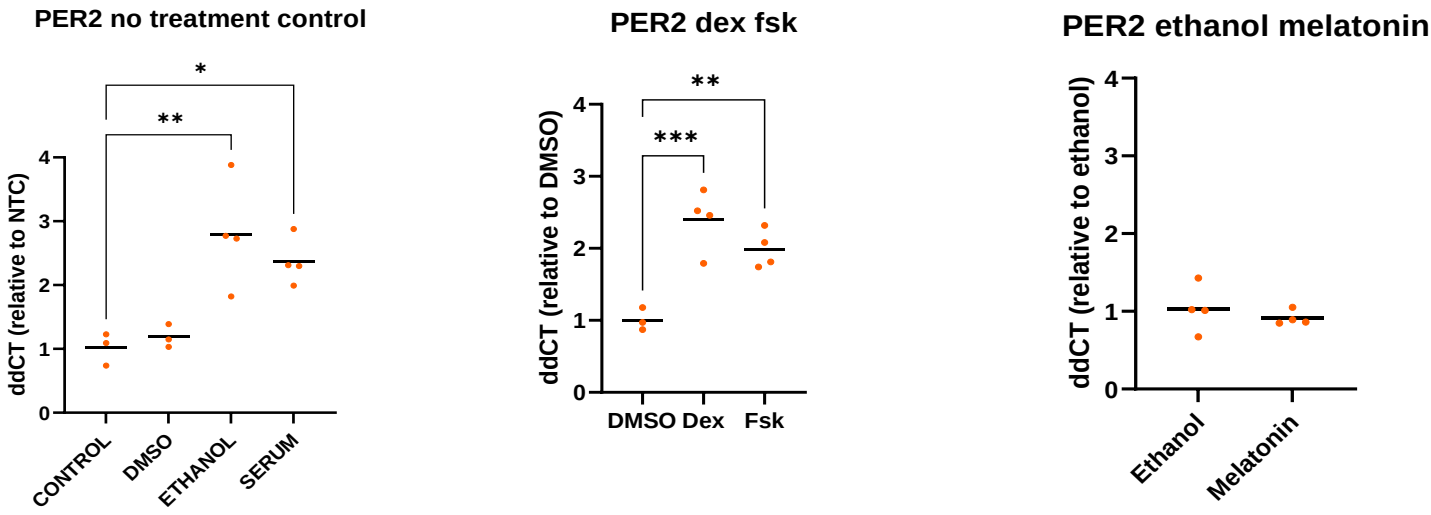

Figure 19 **expression of PER-2 under different cell stimulation treatments.** The cells were exposed to different treatments for 1 hour their gene expression was measured. The different treatments were DMSO, ethanol, dexamethasone (Dex), forskolin (Fsk) and melatonin. a) compares the DMSO and ethanol control, as well as the Serum treatment. There is a significant difference between the control and the ethanol and serum, there is no effect of the DMSO. b) compares the DMSO control with dexamethasone (Dex) and forskolin (Fsk). Both show a significant effect. c) there is no effect of the melatonin compared to the ethanol control. ddCT values are relative to the average of the control group *p<0.05; **p<0.01; ***p<0.001 using one-way ANOVA

NR1D1 gave intriguing results, all treatments showed a significant and consistently lower expression of NR1D1 relative to NTC (Figure 20). The key difference between all treatments and the NTC is that the NTC was in the incubator during the entire experiment, whereas the treatment plates were removed briefly to be treated.

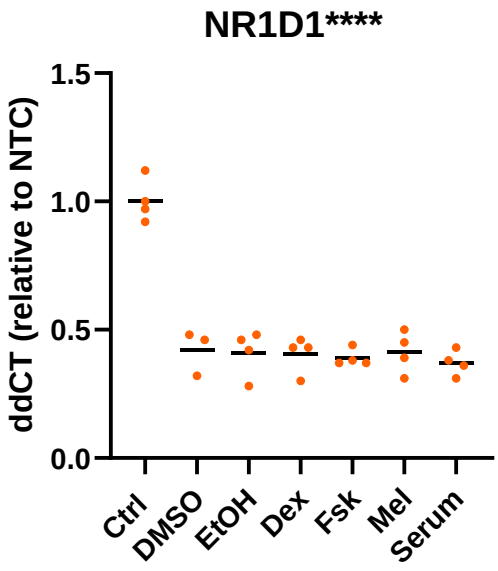

Figure 20 **expression of NR1D1 under different cell stimulation treatments.** The cells were exposed to different treatments for 1 hour their gene expression was measured. The different treatments were DMSO, ethanol, dexamethasone (Dex), forskolin (Fsk), and melatonin there is a significant difference between the control (ctrl) and all the other treatments ddCT values are relative to the average of the control group. ****$p<0.0001$ using one-way ANOVA

In conclusion, PER 2 expression can be induced by treatments that are known to affect the clock genes. This result supports the hypothesis of a functioning circadian clock in hooded seal skin fibroblasts. PER-2 acute response to the treatments is similar to the results found by Yagita and Okamura (Yagita and Okamura 2000). This acute response could entrain the clock and other genes would show a variation in their gene expression if they were sampled later on the cycle.

The results from NR1D1 unusual. It seems that a factor other than the treatment has affected the cells because the reduction in the gene expression level is the same for all the plates compared to the non-treated control. The other most obvious factor that could explain the variation between the 2 groups is the reduction in temperature when removed from the incubator.

3.3.2 NR1D1 expression is affected by acute cold shock

Temperature is known to reset and synchronise the clock but usually, this is a result of multiple temperature cycles to entrain the clock(Buhr, Yoo, and Takahashi 2010). However, recent studies have shown acute responses to cold (Fischl et al. 2020). To test if NR1D1 expression was affected by acute cold shock as suggested by the previous cell stimulation experiment, the cells exposed to cold temperature (18°C) for half an hour and collected at different timepoint (30, 60, 90, 120 min) after the exposure (Methods 2.7.3). Clock gene expression for NR1D1, PER-2, and ARNTL was measured by qPCR.

The only clock gene that seemed affected by the treatment was NR1D1, which showed a significant increase in its expression that peaked an hour after the cold exposure and was still significant 90 minutes after it (Figure 21a). The other genes did not show any effect of the cold shock on their level of expression (Figure 21b & c).

Surprisingly, the response of NR1D1 to changes in temperature was the opposite of the effect in the cell stimulation (Figure 20 compared to Figure 21a). The expression of NR1D1 increased when it was exposed to cold for half an hour, while it decreased during the cell stimulation experiment when the cells were exposed to cold for a very short time. However, in both experiments, NR1D1 showed sensitivity to temperature changes even though the response is divergent. This may reflect the more complex role of temperature in entraining the clock (Sandu et al. 2015).

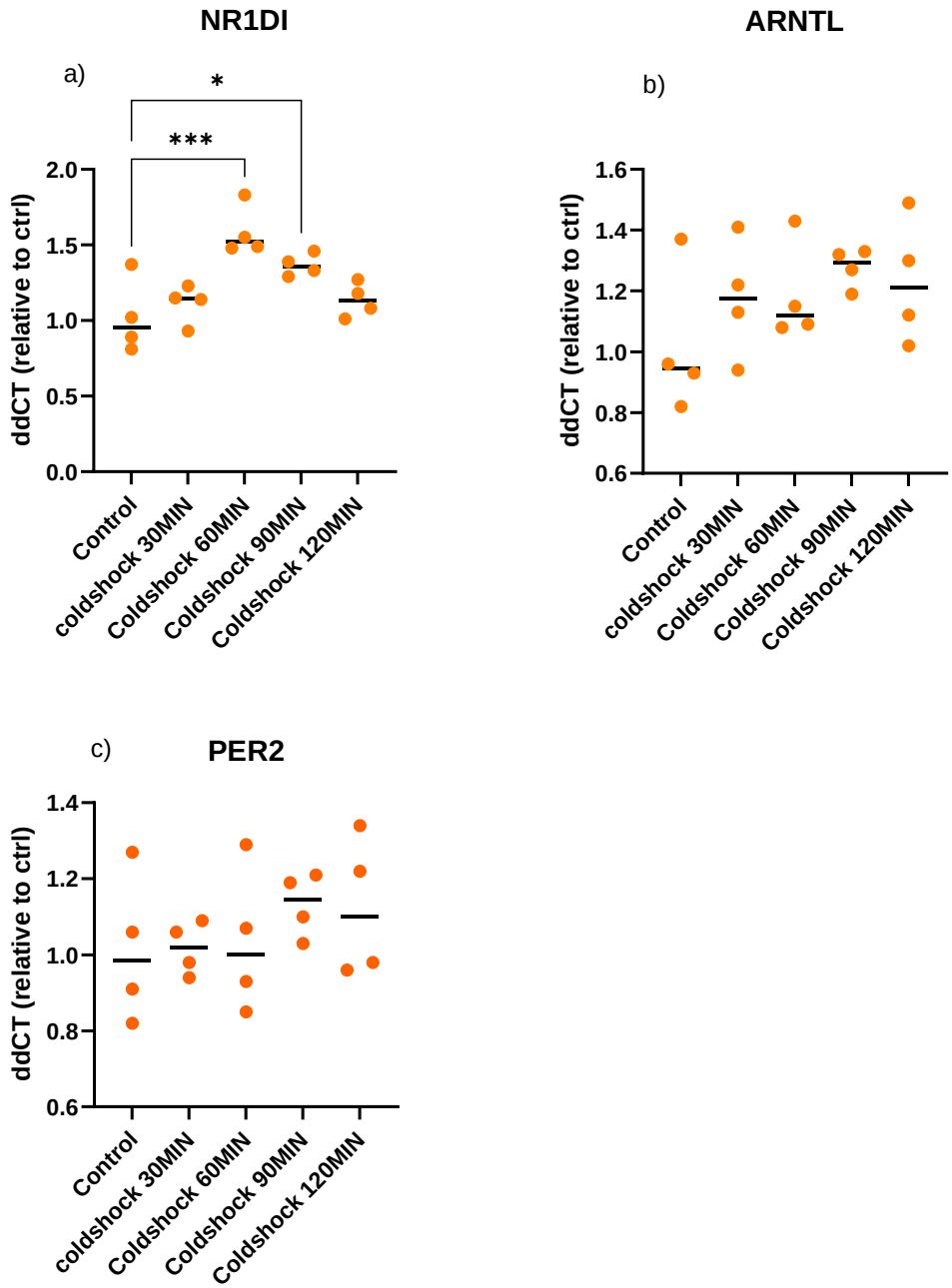

Figure 21 **clock gene expression of cells under cold shock experiment**. The cells were exposed to 18°C for 30minutes and placed back at 37°C and collected at different time points. a) there is a significant difference in the expression of NR1D1 60 and 90 minutes after the cold treatment compared to the control. The other genes b) ARNTL and c) PER-2 did not show any significant change in their expression compared to the control. ddCT is relative to the average of the control group. *p<0.05; ***p<0.001 using one-way ANOVA.

3.3.3 Can the seal circadian clockwork entrain to a temperature cycle and persist in constant conditions?

Temperature cycling has previously been used to synchronise and entrain circadian clockwork in cell culture (Brown et al. 2002) (Prolo 2005), (Tsuchiya, Akashi, and Nishida 2003; Buhr, Yoo, and Takahashi 2010). Therefore, to characterise the response and phase relationships between the clock genes in hooded seals we undertook to conduct two experiments. The first experiment tested whether the clock gene expression became synchronised and entrained to the temperature cycle and whether the predicted phase relationships were maintained between the clock genes. The second experiment was to test whether circadian oscillations persisted in constant conditions, thereby establishing if the clockwork in a seal maintained circadian rhythmicity.

3.3.3.1 The hooded seal clock genes can entrain to a temperature cycle and the core clock genes show the correct phase relationships

We used a series of 12-hour cycles switching between 36.5C to 39.5 degrees for 5 cycles before sampling every 4 hours for 48 hours in the 6^{th} and 7^{th} cycles (Figure 13). The gene expression was assessed by qPCR for the core clock genes (ARNTL, CRY1, PER-2, NR1D1, and CLOCK).

Using JTK cycle (Hughes, Hogenesch, and Kornacker 2010) (Miyazaki et al. 2011) all genes apart from CLOCK were found to significantly oscillate with a period of 24 hours (Figure 22). It is not unusual for CLOCK gene expression to not oscillate (Yu 2006). Importantly, the phase relationship between ARNTL and PER-2 is in anti-phase which is the expected relationship if there was a functional circadian clockwork (Figure 22a & d). The other pair of genes oscillating in antiphase is CRY1 and NR1D1 (Figure 22c & e). This demonstrates that all the genes are modifying their expression at different times with different patterns, this excludes a simple q10 effect on the gene expression and suggests an interaction between different clock genes.

In conclusion, the clock genes are entrained by a temperature cycle and appear to maintain the correct phase relationships, indicating a functional clockwork rather than a passive response to temperature.

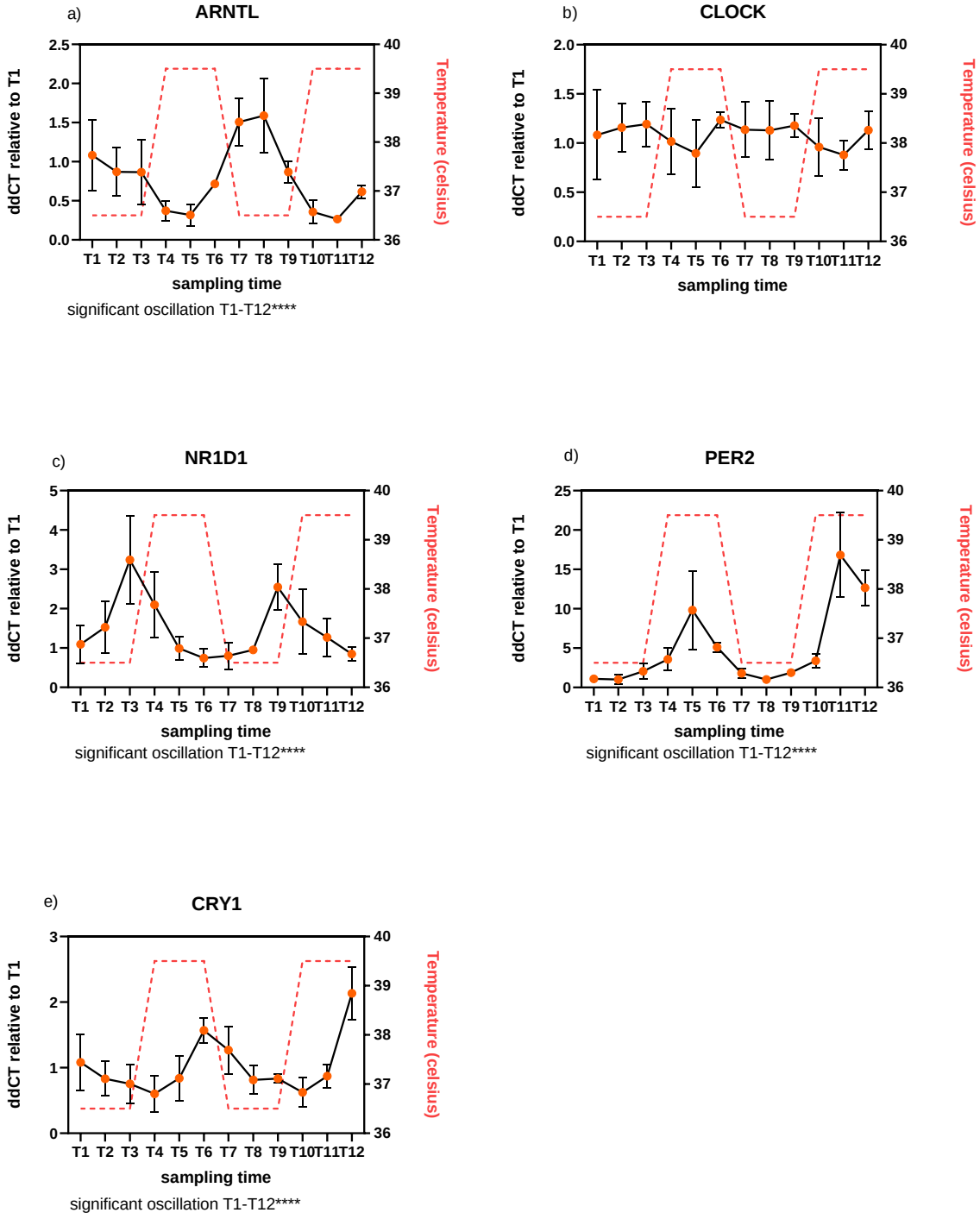

Figure 22 **Expression of the molecular clock genes in cultured skin fibroblasts from hooded seals on temperature cycling**. Genes measured are a)ARNTL b)CLOCK c)NR1D1 d)CRY1 e)PER-2 at different timepoint. ddCT relative to T1: level of gene expression relative to the gene expression at the sampling time T1. Cells wells were collected (replicate n=4) for each sampling time. The temperature

curve indicates the temperature in the incubator at the collection time. The experimental design is detailed in Figure 13. Statistical analysis inform if the genes are cycling within a 20h-24h period over the 48 hours sampling time using JTK cycle (Hughes, Hogenesch, and Kornacker 2010)*p<0.05; **p<0.001; ****p<0.0001

3.3.3.2 Strong evidence for circadian rhythmicity in hooded seal fibroblasts

Our second temperature cycling experiment was designed to entrain the clock genes and then test whether they continued to oscillate when kept at a constant temperature. This is important because it demonstrates circadian-ness in constant conditions, and not a simple hourglass mechanism (Nagoshi et al. 2004) .

The cells were exposed to temperature cycles between 36.5°C and 39.5°C of 12h for 84 hours. The sampling lasted 48h overall and was done at 36.5°C for the first 12 hours and at 39.5°C for the remaining 36 hours. Cells were collected every 4 hours (Figure 12). qPCR was used to assess gene expression.

The results of this experiment can be analysed for the entire length of the experiment from T1 to T12 to assess if the clock is oscillating overall. They also can be looked at as a temperature cycle of 12h at 36,5°C and 12h at 39,5°C for the first 24h (from T1 to T6). The last alternative to analyse the results of this experiment is to consider the 36 hours at a constant temperature of 39.5°C, from T4 to T12.

ARNTL was significantly oscillating with a 20 hours period for the entire experiment (T1-T12 p= 3,37 $x10^{-05}$) (Figure 23a), when just looking at the oscillation under constant temperature (T4-T12p= 1.33 $x10^{-08}$) it was also significant with a period of 24h (Figure 23a).

As previously noted (3.3.3.2) the oscillation of CLOCK is less significant (Figure 23b). However, in this experiment, there is a significant oscillation with a 24 hours period if we consider the entire experiment (T1 -T12 p=0.036). And in contradiction to the first experiment CLOCK shows a significant oscillation with a 20 hours period during the first half of the experiment T1-T6 when the temperature is cycling. The difference in the period between the entire experiment and the T1-T6 timepoint question the strength of the

oscillation. When CLOCK expression is looked through the constant temperature frame, T4-T12, the oscillation has a 24h period but is not significant (Figure 23b).

PER-2 (Figure 23e) and NR1D1 (Figure 23c) showed oscillations with a period of 24h was detected for the entire collection time (T1-T12 PER-2 $p=2.72\ x^{10-7}$, NR1D1 $p=1.17\ x10^{-09}$), the temperature cycling (T1-T6 PER-2 $p=3.8\ x10^{-6}$ NR1D1 $p=3.08\ x10^{-8}$), and at constant temperature (T4-T12 PER-2 p=0.001 NR1D1 $p=6.5\ x10^{-7}$). These two genes gave the most consistent result of this experiment.

CRY1 1 is not significantly oscillating (Figure 23e), except when looked for the first 24h (T1-T6 p=O.012) where it shows an oscillation of 24h period. The same 24h period is detected for the entire experiment (T1-T12) and when the temperature is constant (T4-T12). It makes it a coherent observation, but the P-values are above the significance threshold, which limits the strength of this result. Even if there was a significant oscillation detected in the CLOCK and CRY1 expression, the amplitude of their cycle was very low (Figure 23)

In conclusion, this experiment demonstrated that the clock genes are oscillating in a circadian pattern. That this oscillation can be entrained by the temperature cycle and in some cases persists in constant conditions.

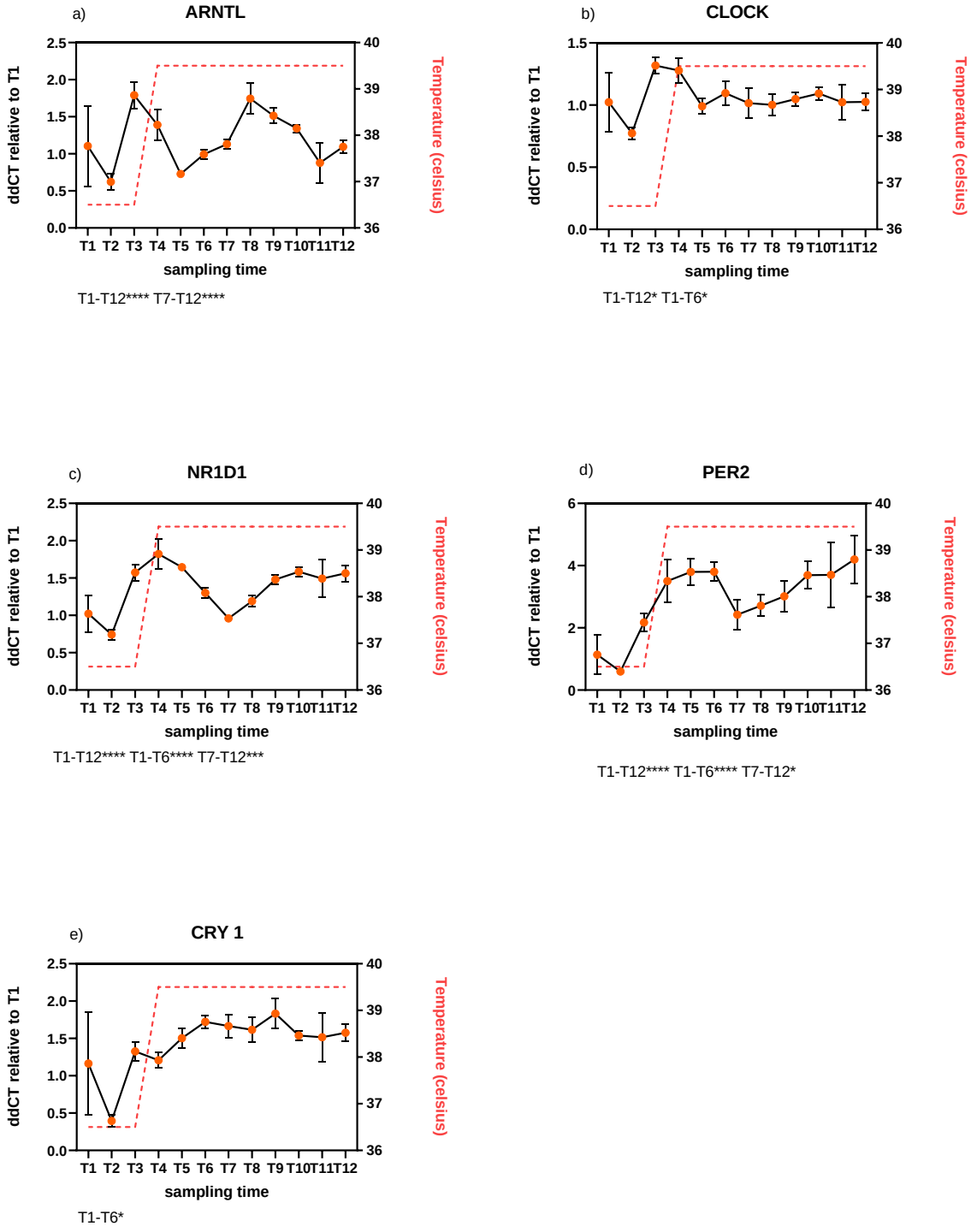

Figure 23 **Expression of the molecular clock genes in cultured skin fibroblasts from the hooded seal on temperature cycling**. Genes measured are a)ARNTL b)CLOCK c) NR1D1 d) PER-2 e) CRY1 under different cell treatments. Cells wells were collected (replicate n=4) for each sampling

time. The temperature curve indicates the temperature in the incubator at the collection time. The statistical analysis informs if the genes are cycling within a 20h-24h period, T1-12 for the entire length of the experiment, T1-T6 for the first half of the experiment, during a temperature cycle, T7-T12 for the second half of the experiment at a constant temperature. The experimental design is detailed in Figure 12. ddCT relative to T1: level of gene expression relative to the gene expression at the sampling time T1. the statistical analysis is done using JTK cycle (Hughes, Hogenesch, and Kornacker 2010) *p<0.05; **p<0.001; ****p<0.0001

3.4 Characterisation of the mitochondrial metabolism in relation to circadian phase using the seal cell culture model

3.4.1 Evidence for a time of day variation in the metabolic capacity of hooded seal mitochondria

To investigate the mitochondrial metabolism of hooded seals we used the O2k fluo respirometer Oroboros instrument. It measures oxygen consumption as a proxy of the oxidative phosphorylation (OXPHOS) activity of different complexes in the respiratory system. By measuring the oxygen flux per cell using the known cell concentration in the chamber, as well as the volume of the chamber, the instrument senses direct increases or decreases in the oxygen flow. An increase in the oxygen flow means that the cells have a higher oxidative phosphorylation rate.

The respiration measure experiment measured the mitochondrial metabolism from hooded seals cells that were under the same temperature cycle as the cells used in experiment 3.3.3.1 (Figure 13), this is because it allows clear predictions about the phase of the clock genes to be made as the cells are entrained.

Cellular respiration (CE) indicates the basal respiration capacity of the mitochondria before any drug injection. The first experimental respiratory state to be measured (PM-L) was the leak respiration mostly due to the complex I, in the presence of pyruvate and malate. PM-P is the second measured stage. It measures the OXPHOS capacity when the mitochondria have pyruvate and malate available to use in the presence of ADP. CI is the respiration due to the complex I at its maximal capacity. CI + CII-P is the maximal phosphorylation with both

complexes I and II working at the maximum of their capacity. CII-P is the state where the OXPHOS capacity is only supported by complex II. CII-L is the leak respiration of complex II. CII-E, the uncoupled state is the enzymatic turnover capacity of the different complexes in the mitochondria. It is the maximal respiration capacity of the cell. (Methods 2.8.2)

While the phosphorylation states measure the capacity of different parts of the electron transport system to produce energy as ATP, the leak state gives information on the loss of energy in the protons that will not participate in the production of ATP while they dissipate the proton gradient. (Cheng et al. 2017)

Due to the length of the respiration measurement protocol, it was only possible to sample 6 times over 48 hours. Referencing the design in Figure 13, this meant that T2, T4, T6, T7, T9, and T11 were sampled. T6 and T7 only had 4 hours between sampling whereas the rest had 8 hours. The choice of sampling was also so it was possible to shuffle the timepoints into a 24-hour cycle to be used for JTK cycle analysis, which needs an even distribution of sampling points. JTK cycle indicated that the final uncoupled state CII-E showed a significant oscillation over a period of 20 hours.

However, due to variation in gene expression levels with each subsequent cycle, we decided this was not the correct way to handle these data and present the data in the order of collection time and statistically asked if there were any significant effects due to sampling point using one way ANOVA (Figure 24).shows the circadian clock genes replotted on the same time axis as the respiration measure (Appendix Figure 40 and Figure 24).

When plotting the respiration measures data (Figure 24) and conducting one-way ANOVA tests CE, PM-L, CII-L, CII-E all show a significant timepoint difference (Figure 24 a, b, g,f). These data suggest that there is a time-of-day variation in the metabolic capacity of the mitochondria in the hooded seal.

Note: the experiment was done with 4 replicates chambers containing cells except for T7 and T9 where only 3 chambers were used. The injection of digitonin on one of the oroboros chambers did not give the expected effect during those time points, and the mitochondria

were not responsive to the other treatments. Data from this chamber were excluded from the analysis.

From all the different respiratory states, only CE, PM-L, CII-L CII-E presented differences between the different time points. There was a recurrent difference in respiration between T4 and T9 for PM-L($p=0.0095$), CII-L($p=0.0125$),CII-E(0.0108). There are 20 hours between the peak T4 and trough T9 but this period should not be looked at closely as there is an 8 hours resolution between the samples.

CE and PM-L presented a common difference in respiration between T2 and T9 (CE $p=0.0191$; PM-L $p=0.0003$). PM-L also presents a difference in the respiratory capacity between T2 and T11($p=0.0182$), as well as between T7 and T9(0,0125).

The other respiratory state with multiple significant differences in paired timepoints is CII-E. Not only T4 is different from T9, but it is also different from T6 ($p=0.0058$) and T2 ($p=0.0072$). T4 is a peak in the oxygen consumption and the multiples differences with other timepoints enhance a variation of the oxygen consumption at different times of the cycle. The CII-E respiratory state measures the maximal oxygen consumption and thus the maximal turnover of the enzymes in complex I and II. It is an interesting result because many variations between time points mean that the capacity of the enzymes has changed over the sampling times in cells entrained by the temperature cycle.

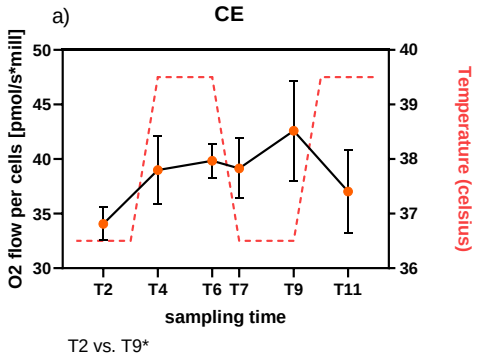
a)
CE
O2 flow per cells [pmol/s*mill]
Temperature (celsius)
sampling time
T2 T4 T6 T7 T9 T11
T2 vs. T9*

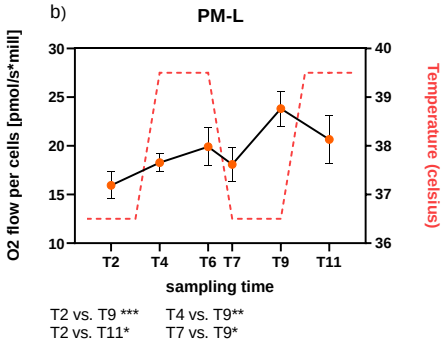
b)
PM-L
O2 flow per cells [pmol/s*mill]
Temperature (celsius)
sampling time
T2 T4 T6 T7 T9 T11
T2 vs. T9 ***
T2 vs. T11*
T4 vs. T9**
T7 vs. T9*

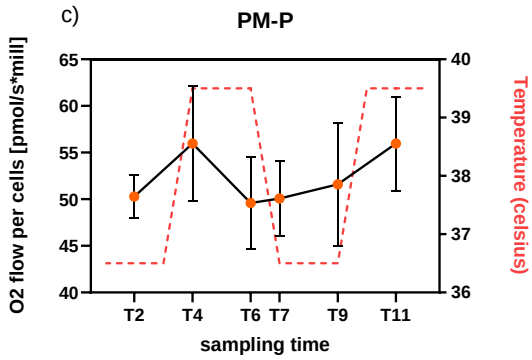
c)
PM-P
O2 flow per cells [pmol/s*mill]
Temperature (celsius)
sampling time
T2 T4 T6 T7 T9 T11

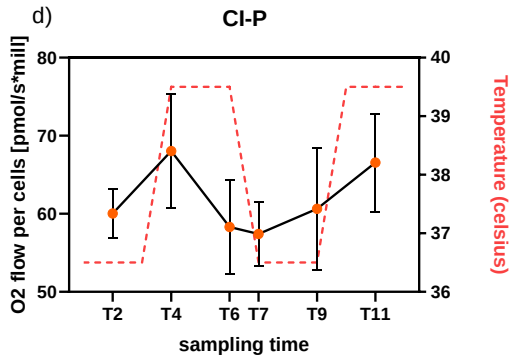
d)
CI-P
O2 flow per cells [pmol/s*mill]
Temperature (celsius)
sampling time
T2 T4 T6 T7 T9 T11

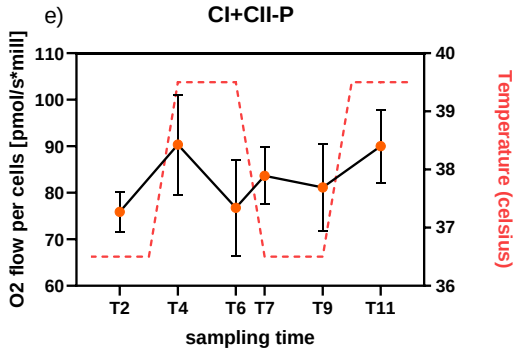
e)
CI+CII-P
O2 flow per cells [pmol/s*mill]
Temperature (celsius)
sampling time
T2 T4 T6 T7 T9 T11

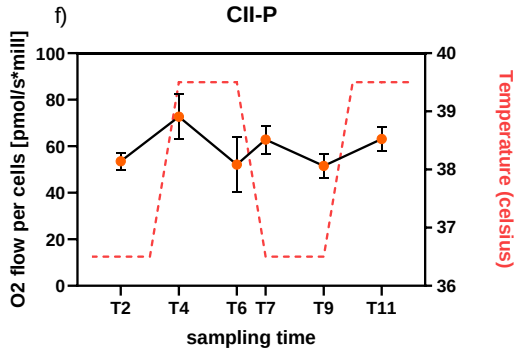
f)
CII-P
O2 flow per cells [pmol/s*mill]
Temperature (celsius)
sampling time
T2 T4 T6 T7 T9 T11

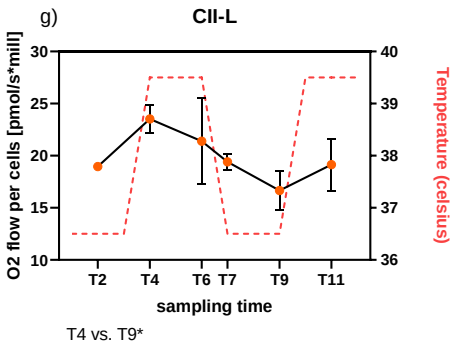
g)
CII-L
O2 flow per cells [pmol/s*mill]
Temperature (celsius)
sampling time
T2 T4 T6 T7 T9 T11
T4 vs. T9*

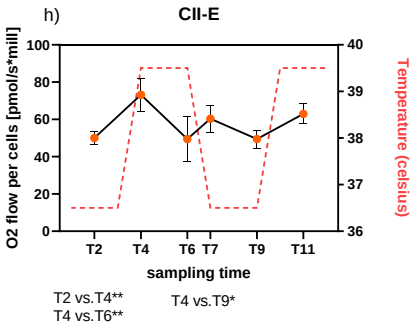
h)
CII-E
O2 flow per cells [pmol/s*mill]
Temperature (celsius)
sampling time
T2 T4 T6 T7 T9 T11
T2 vs.T4**
T4 vs.T6**
T4 vs.T9*

Figure 24 **Measurement of the O2 flow per cells of cultured skin fibroblasts from the hooded seal at different respiratory states**: the control state CE, the leak due to pyruvate OXPHOS capacity, PM-L, the respiration due to pyruvate and malate PM-P, the respiration due to complex I CI-P, and due to combined complex I and complex II CI+CII-P. the respiration at complex II is measured at CII-P, the leak due to complex II is measured at CII-L, and the final uncoupled state of the mitochondria measures the enzymatic capacity CII-E. The sampling time points have an 8h resolution over 48 hours, except for T6 and T7 that separated by only 4h. The temperature curve indicates the temperature in the incubator at the collection time. The experimental design is detailed in Figure 13. The statistical analysis is a one way ANOVA *p<0.05; **p<0.001; ***p<0.001

3.4.2 Oscillations in the mitochondrial gene MFN1

To further investigate a circadian pattern in mitochondrial metabolism, we looked at the expression of some genes involved in mitochondrial physiology. The fusion and fission dynamics in the mitochondria are responsible for changes in respiratory capacity (Sardon Puig et al. 2018). They were measured by qPCR using the samples from the temperature cycling experiment with collection under the temperature cycle (3.3.3.1). Primers were designed and sequenced using the same approach as for the clock genes (Methods2.5) (appendix Table 8)

The different mitochondrial genes tested are involved in the fusion (MFN1, MFN2, OPA1) and fission (DNM1L) of mitochondria and NAD+ production (NAMPT).

Mitochondrial fusion changes the morphology of mitochondria, making them longer. The physiological benefit from fusion is higher efficiency at ATP production (Schmitt et al. 2018). Mitochondrial fission is the counterpart of fusion It fragments the mitochondria to dissipate energy production (Jacobi et al. 2015). NAD+ promotes SIRT protein activity. The proteins are involved in circadian mechanisms, energy metabolism, and mitophagy (Sardon Puig et al. 2018) .

Only MFN1 has a significant oscillation with a period of 24h (Figure 25a), all the other genes did not show a significant circadian oscillation, even though a period of 24h was detected (Figure 25b-e). MFN1 is plotted to match the respiratory measures timepoints (Figure 25f)

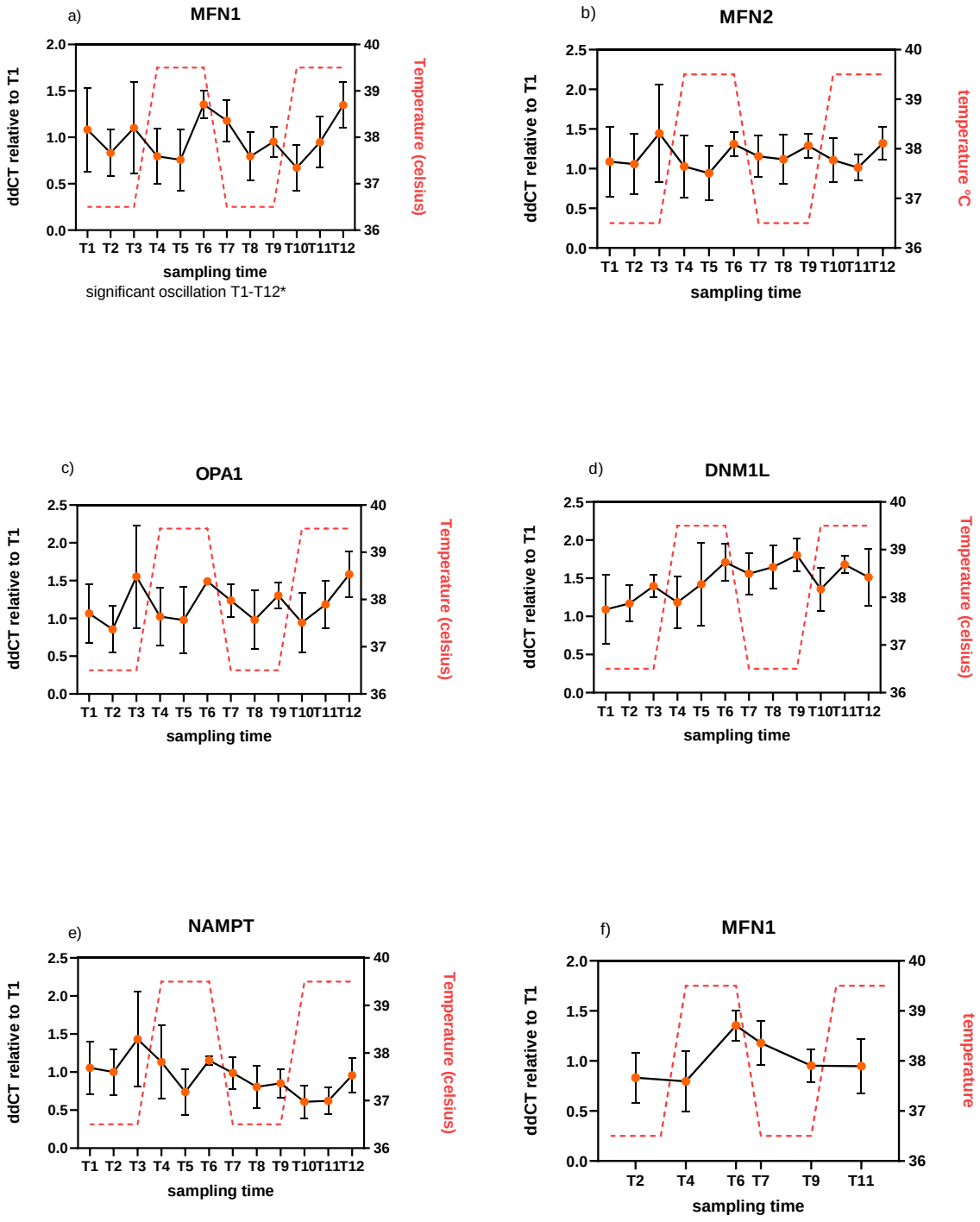

Figure 25 **Expression of the mitochondrial genes from hooded seal skins fibroblasts under temperature cycle**. The genes are involved in the fusion a)MFN1 b)MFN2 c)OPA1 and fission d)DNM1L and mitophagy e)NAMPT at different timepoint in cultured skin fibroblasts from hooded seals. f)MFN1 plotted according to the mitochondrial respiratory states. Cells wells were collected

(replicate n=4) for each sampling time. The temperature curve indicates the temperature in the incubator at the collection time. Data are presented as the mean *p<0.05; f) Experimental design is detailed in Figure 13: the cells were kept in the incubator in temperature cycles for 120 hours before the experiment. The red dots represent the collection times. ddCT relative to T1: level of gene expression relative to the gene expression at the sampling time T1. The statistical analysis informs if the genes are cycling within a 20h-24h period over the 48 hours sampling time. it is done using JTK cycles (Hughes, Hogenesch, and Kornacker 2010) *p<0.05

3.4.3 Mitochrondrial status correlates with circadian clock gene expression

Having identified a time of day difference in mitochondrial activity we next asked whether there was any evidence that mitochondrial activity related to the circadian clock phase (or gene expression). As we had 5 mitochondrial genes, 8 mitochondrial measures, and 6 clock genes we decided to use correlation matrices to indicate if there were any relationships between the measurements and then follow up on the strongest correlations. Figure 26 shows the full correlation matrices of the clock genes and the respiratory states. The correlation matrix between the clock genes and the respiratory rates shows a strong negative correlation between the OXPHOS capacity and the clock genes ARNTL and CLOCK and CRY1. On the other hand, there is a positive correlation between the respiratory states and PER-2 and NR1D1. PER 2 is in antiphase with ARNTL (Figure 22) and their matching opposite correlation with the respiratory states incites to look at the relation between rhythms and energy metabolism.

The high correlation between CI-P and CI+CII-P is not surprising because CI-P is comprised in the calculation of CI+CII-P. PM-P is the OXPHOS capacity of pyruvate-malate in the mitochondria, which is also included in the two other states CI-P and CI+CII-P (Figure 26).

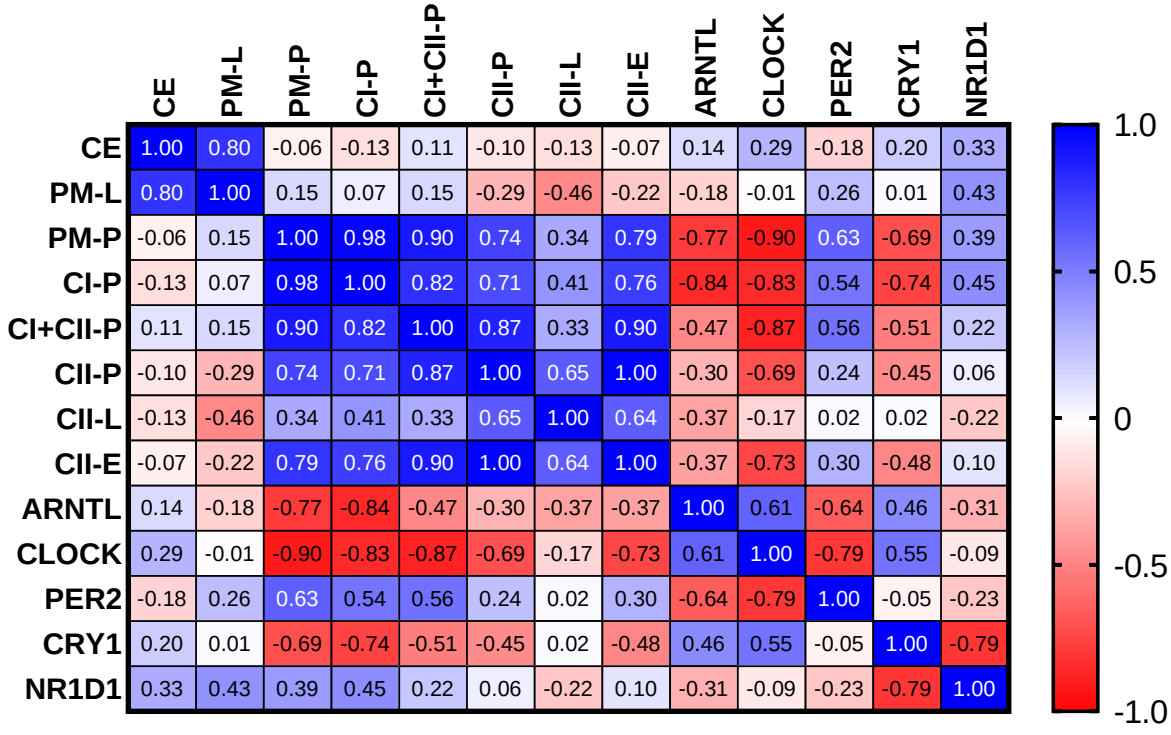

Figure 26 **correlation matrix between the different respiratory states and the clock genes**. The correlation matrix presents the relationship between the respiratory states and the clock genes. A correlation close to 1 means a positive correlation between two elements while a correlation close to -1 represents a negative correlation. The matrix was done using Pearson correlation. There is a high correlation between the different respiration states CI-P and CI+CII-P and PM-P, as well as between the OXPHOS states and clock genes PER-2 and NR1D1. There is a strong negative correlation between the respiratory states and ARNTL and CLOCK and CRY1.

3.4.4 Correlations of mitochondrial gene expression relates to known functions in the respiratory status of the cell

We then asked if mitochondrial gene expression was related to mitochondrial activity. Using Pearson correlation again we show that the respiration rates at complex I and complex II measurements show a strong positive correlation between each other (Figure 27). The mitochondrial genes also present a positive correlation with each other, except NAMPT, which is neutral when correlated to OPA1 and negatively correlated to DNM1L. The positive correlation between the fusion genes MFN1 and MFN2 and OPA1 is the strongest and

coherent as the genes are involved in the same metabolic process. The correlation between those fusion genes and NAMPT is still positive but has the lowest values, which is encouraging considering that they have the opposite function. The negative correlation between NAMPT and DNM1L is also supporting the opposition of function. NAMPT favors mitochondrial fusion through a metabolic link with OPA1, while DNM1L is promoting fission of the mitochondria.

The different respiratory states of the mitochondria are negatively related to the expression of all mitochondrial genes. The only consistent positive correlation is at the initial state, where the basal OXPHOS capacity of the cells is measured, and when the leak respiration due to pyruvate malate is measured. In the 2 states, the mitochondrial genes have a positive correlation with the oxygen consumption of the different respiratory states.

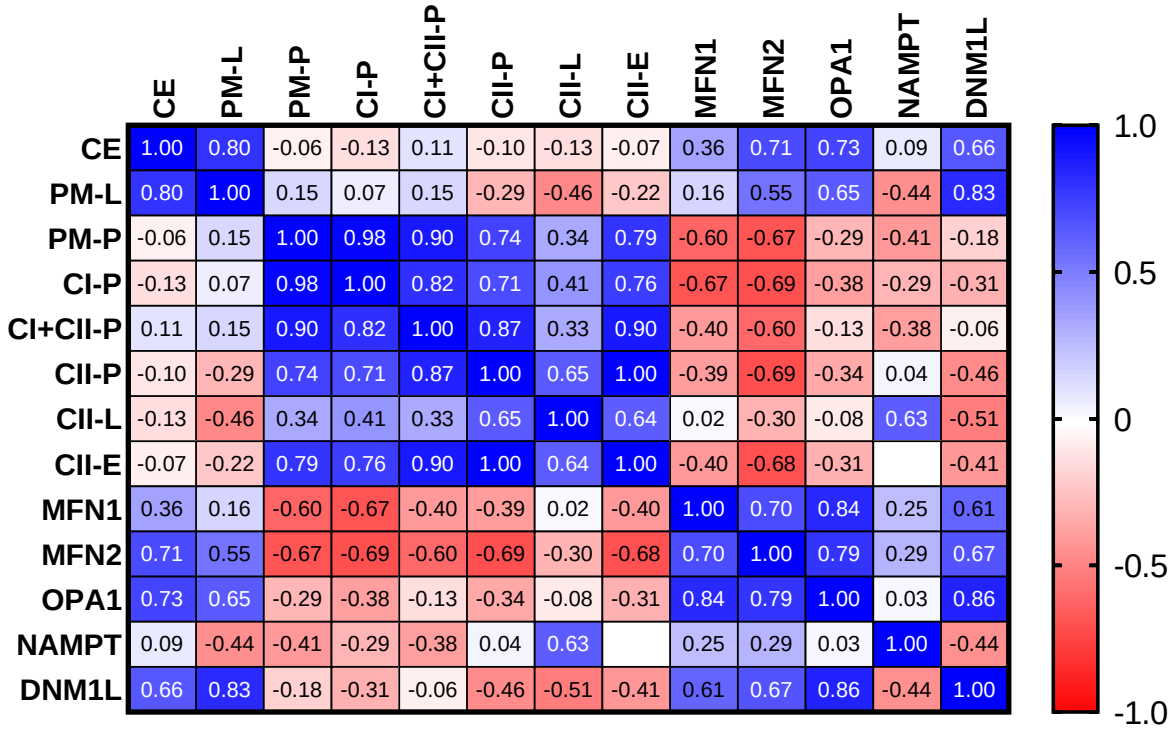

Figure 27 **Correlation matrix between the different respiratory states and the genes involved in mitochondrial dynamics.** A correlation close to 1 means a positive correlation between two elements while a correlation close to -1 represents a negative correlation. The matrix was done using Pearson correlation. There is a positive correlation between MFN1 MFN2 and OPA1 and a negative correlation between DNM1L and NAMPT.

3.4.5 Phase relationships between CRY1 and ARNTL expression, MFN1, and mitochondrial activity

The respiratory states, clock genes, and mitochondrial genes that presented the highest correlation were selected and are presented in Figure 28. The only mitochondrial gene selected was MFN1 which was also the only oscillating mitochondrial gene (Figure 25).

It is interesting to note that the highest correlation in the respiration measures is in the OXPHOS states and not in the leak states of the experiment. The OXPHOS states are the ones reporting the energy capacity in the mitochondria, which is of interest. The Clock genes that were highly correlated with those OXPHOS states are ARNTL, CLOCK, and CRY1 in antiphase with PER-2.

CRY1 and PER-2 expression are not correlated, it is thus difficult to extrapolate a relation between their expression and the OXPHOS capacity.

The negative correlation between the respiratory states and the expression of the clock genes could be representative of this dynamic balance and when the clock genes expression decrease, the OXPHOS capacity is increasing, as mitochondrial fusion occurs.

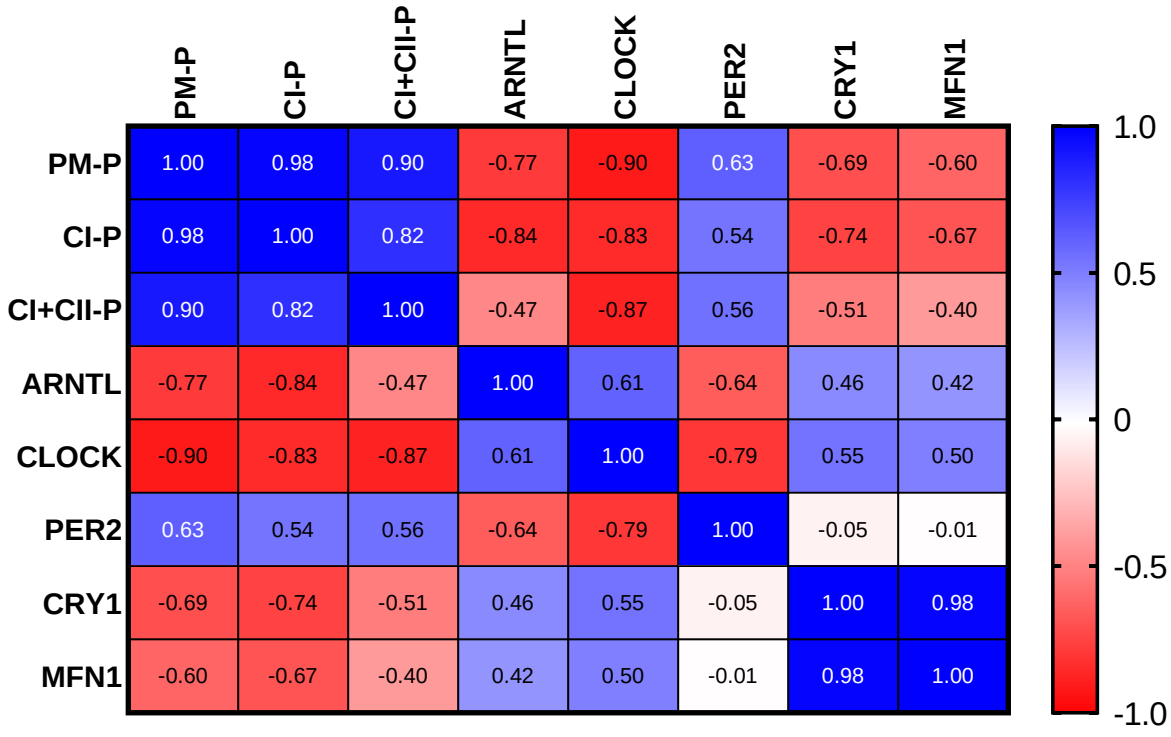

Figure 28 **Strongest correlation between the different respiratory states the clock genes and mitochondrial gene**. A correlation close to 1 means a positive correlation between two elements while a correlation close to -1 represents a negative correlation. The matrix was done using Pearson correlation. There is a high positive correlation between the respiratory states while ARNTL, CLOCK, and CRY1 are negatively correlated to the respiratory states.

To further investigate the phase relationships between gene expression and mitochondrial activity the data were overlaid (Figure 29). The Pearson correlation informs about the strengths of the relationship between the 2 groups. The strength of the relation is the same from one group to the other and an external factor influencing both groups can be responsible for the strong correlation. Because correlation does not imply causation or direction of effect, we decided to overlay the genes and respiratory states that had a strong correlation. The overlays give a better representation of the relationship but do not inform further about the causation.

The PM-P ARNTL overlay (Figure 29 f) shows that the gene expression and the respiratory rate are opposing each other over time. It confirms the strong negative correlation observed (-77) in Figure 28.

The PM-P CRY1 overlay (Figure 29 e) is opposing the peak and trough of the clock gene and the respiratory state. The opposition is however less marked than for PM-P ARNTL overlay (Figure 29 f). This observation matches the lower negative correlation (-69) for PM-P CRY1 (Figure 28). Because ARNTL and CRY1 are in opposite phases with PMP, they are closely in phase with each other, even if CRY1 peaks before ARNTL and its amplitude are smaller. Those differences are translated in the low positive correlation between each other (+0.46 Figure 28).

The different respiratory rates are in phase with each other. PM-P and CI-P (Figure 29a), as well as PM-and CI+CII-p (Figure 29 b) variate the same manner between the different time points. This observation confirms the strong positive correlation observed between the different respiratory rates (Figure 28).

One of the strongest correlations of these metrics is between CRY1 and MFN1. MFN1 seems to be peaking at the end of the high-temperature phase (Figure 25a) and it coincides with the peak time of CRY1 (Figure 29d). Both genes are regulated by AMPK (Lamia et al. 2009). AMPK is involved in the mitochondrial fusion process when ATP levels are decreasing compare to NAD+. The activity of AMPK could be crucial between the mitochondrial dynamic and the clock gene expression. (Jordan and Lamia 2013)

In conclusion, there appears to be a relationship between circadian gene expression and mitochondrial activity, and in the case of CRY1 and ARNTL there is a relationship between the phases of peak expression and mitochondrial activity, however, a lot of work remains to determine the causal relationships.

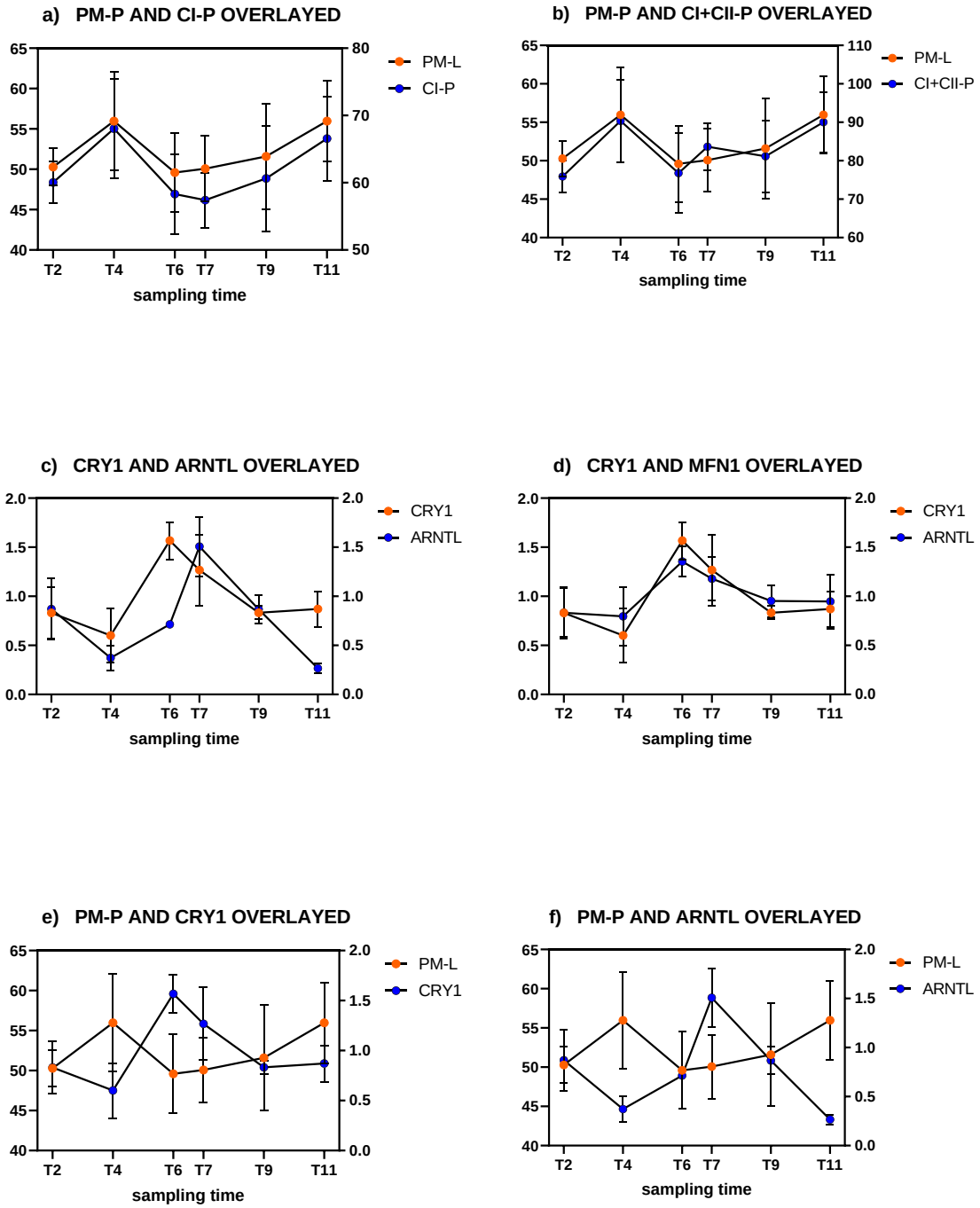

Figure 29 **overlays of different respiratory states, clock, and mitochondrial genes that presented a strong correlation**. There is an overlay of the phases between different respiratory rates a) PM-P and CI-P, b) PM-P and CI+CII-P, but also between clock genes c)CRY1 and ARNTL as well as between d) clock gene CRY1 and mitochondrial gene MFN1. e) The respiratory state PM-P and the clock gene CRY1 are in antiphase as well as f) PM-P and ARNTL.

4 DISCUSSION

In this thesis, I have identified circadian clock genes in the hooded seal, measured expression levels in multiple tissues, established a cell culture model, demonstrated the capacity of hooded seal cells to have a functional clockwork, then attempted to relate the function of this clockwork to mitochondrial activity. This work lays the foundation for further research into the relationship between clocks, metabolism, and hypoxia.

4.1 Genes identification and basic expression

Genes identification *in-silico* showed that the genes were conserved in Weddell seal and sequencing showed that they were conserved from Weddell seal to hooded seals. Despite living in an arctic aquatic environment where the light regime is disrupted, the coding sequence is still present in their genome (3.1). This was a reassuring result because the clock genes are normally conserved across species (Bhadra et al. 2017) and closely related species living at the same latitudes maintain rhythms (Ware et al. 2020).

4.2 A sampling of live tissues limits the time resolution

We found the expression of the clock genes in the different tissues; they are expressed at some level (3.2.1). This expression was the first proof that the genes are not only present in the genome but may play a role in the physiology of the animal because they are transcribed into mRNA.

The poor resolution of the tissue sample experiments with only 2-time points within 24 hours makes it difficult to detect any circadian rhythm.

To repeat the same type of experiment with a greater resolution would require a lot more animals to be used as replicates with more time points. It is not the direction that is considered. Following the principle of the 3Rs, the use of animals in science tends to be Reduced, Replaced, or Refined. The animals used in this experiment were not only used to determine if there was or not a difference in the clock gene expression across tissues. It was

rather an opportunity taken, as the animals were culled for brain samples dedicated to research on hypoxia. Using the same animal for different experiments participates in reducing their numbers. Furthermore, Hooded seals are a very special model. They are not bred in captivity to become laboratory models, like rats and mice. They are taken from their natural environment and brought into captivity. This does not affect the Hooded seal population, but it should be limited to the strict minimum for ethical reasons.

The poor resolution of the experiment can explain why the difference in gene expression between the ZT6 and ZT18 groups was non-significant for the majority of the samples (3.2.2.). If the genes are not at their peak and trough during both sampling times, but in the same phase, we will not detect a difference, but the clock could be oscillating anyway.

A conclusion from this experiment is that the gene expression was higher in the brain tissues than in the peripheral tissues. It has been shown previously that there is a higher expression of the clock genes in the brain than in peripheral tissues in salmon (West et al. 2020). There is direct neuronal integration of the clock messages from the SCN to the other brain regions controlling physiological parameters, whereas peripheral tissues receive information from the brain centers via hormones and indirect pathways, and it could explain why they have a lower clock expression. It is a promising result for further research if the circadian approach of seal physiology aims to explore the relation between clockwork and brain resistance to hypoxia.

The nature of the tissues is different and could partially explain the different success of RNA extraction between tissues. The peripheral tissues might have more connective tissues and enzymatic activities than the brain samples and could have affected the mRNA quality. The tissue lysis performed better on the brain samples than on the skin sample for example. The brain is a soft tissue easy to disrupt, while a skin punch offers more resistance. Peripheral tissue could have degraded faster during the sampling. The blood-brain barrier could also protect the brain samples from circulating RNase in the vascular system (Ohashi et al. 2017) that could have affected peripheral tissues, like the heart, whose RNA extraction did not succeed.

While this experiment did not provide precise information about the clockwork, it proved that the clock genes are expressed *in-vivo* in hooded seals. It supports the further work done on cell cultures with the possibility of physiological implications.

Establishing cell lines from the multiple tissues would be the direction to take to explore the clockwork and its difference across tissues. it would allow a greater resolution without the unnecessary use of many animals to precisely characterize the clockwork in different tissues. To grow neurons and glial cells will be a great opportunity to couple the historic study of hypoxia on seals with the circadian approach.

Animals could be used for physiological measures to support the in vitro circadian and metabolic measures. Hooded seal's activity has been measured in their natural environment and even though there was a difference in the dive depth between day and night, the experiment was not designed to assess the circadian nature of their activity (Folkow, Mårtensson, and Blix 1996). *In-vivo* experiments measuring physiological parameters and activity under controlled light, the environment would give physiological cues of what has been observed *in-vitro*. Temperature recording of the core body temperature, hormone levels, and activity recording around the clock would help define both physiological and behavioral possible rhythms of the hooded seal.

Such validation of the cell culture model from the animal model would encourage further development of *in-vitro* experiments. It would also help define its limits and place it in the perspective of the integrative biology of hooded seal on rhythm, mitochondrial metabolism, and hypoxia.

4.3 Hooded seal skin fibroblasts are a great model to study the clockwork and metabolism *in-vitro*

The study of circadian mechanisms requires sampling around the clock, preferably during multiple cycles. As discussed in 4.2, the extensive use of animals is not appropriate for this type of experiment for ethical and technical reasons. To continue the exploration, we used an *in-vitro* model of hooded seals skin fibroblasts. They are fairly robust cells to culture. Under

normal conditions, the cells are confluent within 3 days, compared to Pia Mater cells of the same animal model who did not proliferate as easily as the fibroblasts (Kante unpublished data). Using cell culture implements the Replacement principle of the 3 R's. It is also a more direct approach to study cellular clockwork. There is no possible interaction with other physiological processes and the environment is tightly controlled. It gives results less subject to interpretation than tissue sampling. Skins fibroblasts have been used previously in chronobiological experiments to characterize the clockwork of animal models, using Rat 1 fibroblasts for example (Aurélio Balsalobre, Marcacci, and Schibler 2000; Yagita and Okamura 2000; Sandu et al. 2015). By using the same cell type, it is possible to demonstrate the existence and characteristics of the clock. It is also possible to compare it with other models.

4.3.1 Cell treatment and temperature affect the clock

Balsalobre et al. showed in their experiment on rat 1 fibroblasts cells that after serum shock, the genes involved in the clockwork presented an oscillation that lasted for 3 days, using RNase protection assay (Balsalobre, Damiola et al. 1998).

In our experiment, the cells exposed to the serum shock were collected an hour after the treatment (3.3.1). We did not collect cells over 3 days to measure an oscillation. We wanted to know if there was an acute response to the treatment as a first step in describing the clockwork in the seal cells (3.3.1). We induced an acute increase in the expression of *PER-2*. This result coincide with the finding of Balsalobre (Aurélio Balsalobre, Damiola, and Schibler 1998). They observed induction of *rper1* and *rPER-2* at the beginning of their experiment followed by a decrease of the gene expression in the 12 following hours.

Glucocorticoids are hormones produced in the adrenal glands and regulated by the hypothalamic-pituitary-adrenal (HPA) axis. This axis is regulated by circadian rhythms, and the hormones are acting on a wide range of physiological responses (Timmermans, Souffriau, and Libert 2019). Dexamethasone is a glucocorticoid that has been used in similar treatment experiments on rat 1 fibroblast (Balsalobre 2000). After 1 hour exposed to the treatment, the cells responded with an increase in *per1* expression but the *PER-2* expression just above the reaction induced by the solvent, ethanol. In our experiment, we used DMSO as a solvent and there was an induction of *PER-2* in the seal fibroblasts (3.3.1).

Forskolin has been used by Yagita and Okamura to highlight the pathway which leads to the expression of *per1* and *PER-2*. Forskolin induces the expression of cAMP (Yagita and Okamura 2000), which induces the activation of CREB through the PKA pathway (Gonzalez and Montminy 1989). CREB has been linked with the expression of PER1 and PER-2, a lower expression of CREB resulted in lower PER expression (B. Lee et al. 2010). Yagita and Okamura showed an acute mRNA expression of *per1* but the induced expression of *PER-2* started 4 hours after exposure. In our experiment, *PER-2* mRNA expression showed an acute response to forskolin (Yagita and Okamura 2000).

In rat 1 fibroblast, *per1* mRNA expression is more sensitive to dexamethasone and forskolin treatment than *PER-2*. Our experiments did not include *per1* in the panel of genes tested. *PER-2* was induced after serum shock in the seal cells, like the *rat1* cells. The seal cells responded with the same induced mRNA expression under dexamethasone and forskolin treatment (3.3.1). This result could suggest a difference in the pathways used by the rat and seal cells. *PER-2* in seal cells could be induced by CREB phosphorylation by the cAMP/PKA pathway.

Melatonin is capable to reset the clock in rat brain slices of the suprachiasmatic nucleus when administrated around the day-night transition (Mcarthur, Gillette, and Prosser 1991). It has been used in the culture of synchronized rat 1 fibroblasts to explore its capacity to interact with the clockwork (Sandu et al. 2015). This study showed that melatonin can increase the amplitude of the *per1* expression when administrated during the day to night transition.

The response to melatonin seems to be limited to the day/ night transition. In cell culture, the cells need to be synchronized to be responsive during that transition phase. The seal cells that we treated with melatonin were not synchronized, and the administration time was not planned to a hypothetical day/ night cycle (3.3.1). In these conditions, an increase in *PER-2* expression would have been surprising according to the literature.

The solvent used to dilute the melatonin influenced the expression of *PER-2*. This would have ruled out any positive result. Another solvent is to be used in further experiments with melatonin to measure only its effect and not the vehicle effect.

This treatment experiment was the first step to explore the clockwork in seal cells. We decided to design the sampling point to detect an acute response to the treatment. One outlier of the DMSO treated cells was masking the significance of the result for *PER-2* expression if it was not removed from the analysis.

This experiment should be followed and repeated using not measuring *PER-2* expression but also *per1*. This could inform about the dynamic between *per1* and *PER-2* compared to what has been observed. A control with rat 1 fibroblast cells would also strengthen the result and help exclude experimental error.

Another axis to pursue this experiment could be to extend the measure not only the acute response to the treatment but also its capacity to entrain the clock over cycles. It would change the conclusions and help define a circadian effect of the treatment rather than a simple effect of the treatment on the gene expression.

4.3.2 NR1D1 shows sensitivity to temperature variations

The only reason for the difference in NR1D1 expression between the cells that stayed in the incubator and the other plates is the effect of temperature (Figure 20, 3.3.1). There is no variation between the treated groups but the non-treated control group has a strong higher expression compared to all of them. Such a strong effect of temperature on gene expression was surprising. NR1D1 has however been reported to be sensitive to cold exposure. In an experiment, brown adipose tissues were exposed from 29°C to 4°C and NR1D1 (Rev-erba) expression was downregulated (Gerhart-Hines et al. 2013). In this case, the cells were exposed to extreme cold temperatures for hours. The treated plates in our experiment were exposed to room temperature, approximately 22°C for less than 5 minutes and it seems to have affected them (3.3.1). The 2 experimental conditions should not be compared, but it underlines the temperature sensitivity of NR1D1.

The cold-shock experiment was designed to confirm the hypothesis of the temperature effect on NR1D1 and possibly other genes. The result confirmed the temperature sensitivity of NR1D1 (3.3.2). Instead of a downregulation observed during the treatment experiment and similar to the brown adipose tissue (Gerhart-Hines et al. 2013), NR1D1 was upregulated after mild cold exposure to 18°C (3.3.2). The upregulation of NR1D1, when exposed to 18°C, is

supported by Fischl et al. (Fischl et al. 2020), who shows that there is an upregulation of Rev-erba when exposed at 18°C for 5 hours. This temperature might not be cold enough to induce the same downregulation shown by Gerhart-Hines, even though brown adipose tissue has a major role in thermogenesis and might present a different phenotype.

This result is not consistent with the observation from the cell treatment either. The exposure time to the cold is not the same. It is possible that a short exposure downregulates the expression of NR1D1 and a longer one upregulates it. To clarify the effect of temperature on the gene expression, a group should be exposed to cold for less than 5 minutes to confirm the result from the treatment experiment (3.3.1). The cells should also be exposed to 4°C to be compared with the expression in brown adipose tissue. We know that the seal fibroblasts are resistant to this kind of cold temperature exposure and would persist in this experiment (data not shown).

From this experiment, we can conclude that temperature affects NR1D1 expression. The cells were collected a maximum of 2 hours after the cold shock. It is not sufficient to detect an oscillation on other genes if their peak or trough is to happen later in the cycle.

4.4 Temperature cycles entrain seal skin fibroblasts

The previous experiments have shown that the clock genes, especially PER-2 and NR1D1 are acutely responding to treatments. Those experiments were not designed to prove circadian oscillation of the genes because the collection times were restricted to a maximum of 2 hours after treatment.

Because we did not know how strong the clockwork would be maintained in seal fibroblasts, we decided to measure the clock gene oscillation on cells exposed to temperature cycles. The clocks are temperature compensated. It means that external temperature cannot influence the frequency of the oscillator. However, some oscillators are more affected by temperature changes than others. The master clock is known to be insensitive to temperature changes. This property lies in the neuronal interaction in the Supra Chiasmatic Nucleus, which protects the master clock from temperature resetting. The clocks in peripheral tissues can however be

entrained by an internal temperature cycle in homeotherms and it is considered a universal cue for mammalian circadian oscillators (Buhr, Yoo, and Takahashi 2010).

Temperature is a zeitgeber that has a strong effect on seal skin fibroblasts (3.3.3). Variation of temperatures in the incubator can be programmed without interacting with the cells. It is a great way to limit the experimental bias compared to entrainment induced by treatments that require more manipulation. Our experiment indicates that the molecular clock did not lose its function in the arctic animal. This could suggest that endogenous rhythms are an advantage for the hooded seals. The major outputs of the clock in seals are not established. We can speculate that it would give them an advantage in their environment, adapting alertness and physiological abilities to the prey availability for example. It could also be an advantage for the internal physiology of the animal. Synchronising core body temperature and digestion or clearance for example could be a way for the seal to save energy.

The cells entrained to the temperature cycle and the clock genes dynamic happened according to known clock mechanisms (3.3.3.1/1.5) ARNTL was oscillating in antiphase with PER-2 and CRY1. While ARNTL peaks before the rise in temperature from 36.5°C to 39.5°C, PER-2 peaks in the middle of the warm phase. CRY1 peaks before the onset of the cold phase. The activation of the transcription factor dimer formed by ARNTL-clock activates the transcription of PER-2 and CRY1. They are translated into protein in the cytoplasm and reintroduced in the nucleus to suppress their own expression by preventing the activity of the ARNTL-clock dimer.

In our experiment, because we see an antiphase relation between ARNTL and PER-2/CRY1, we can conclude that there is a circadian mechanism in place, and it is not only an effect of temperature on molecular interactions. CLOCK was not significantly cycling during the experiment. We can however extrapolate a pattern from its expression, and it seems that the trough follows the same synchronicity as ARNTL (Figure 22). Moreover, the expression of CLOCK is not always cyclic. In drosophila with a described functional clock, there is a constant expression of the equivalent CLK (Gallego and Virshup 2007), and the regulation comes from the phosphorylation of the protein (Yu 2006).

To prove the circadian nature of the oscillation, we designed an experiment where the cells were partly collected at a constant temperature (3.3.3.2). Because the cells maintained rhythm at a constant temperature, there is a circadian clockwork in the hooded seal cells. It is not only the representation of an hourglass mechanism entrained by external cues but an endogenous rhythm generated in the cells (Rensing, Meyer-Grahle, and Ruoff 2001).

The results showed that there is a circadian oscillation under constant temperature. The amplitude of the cycle is not as marked as the amplitude of the same genes collected while the temperature was cycling (3.3.3.1). The cells in this experiment were exposed to a shorter number of temperature cycle before collection. This could explain the lower amplitude of the cycle. The circadian entrainment in this configuration might be weaker and gene oscillation is less important. This experiment could be repeated with a longer exposition to temperature cycles before collection, and with more collection timepoints at a constant temperature to observe the variation over 2 to 3 cycles.

4.5 A relationship between clockwork, respiratory states, and mitochondrial morphology

Because of its length, the respiratory measure experiment could not be repeated with a 4 hours resolution for 48 hours. This low resolution combined with the important difference between replicates is not ideal to fully comprehend the mitochondrial dynamics. A greater time resolution with replicates timepoints would be more informative. It would also allow us to use the JTK cycle analysis (Hughes, Hogenesch, and Kornacker 2010) to detect an oscillation in the different respiratory states. Due to the shift in sampling time between T6 and T7, we were not able to use the JTK cycle when the data are organised linearly by the time of the experiment. Because there were only 4 hours between the 2-time points compared to the 8 hours for the other intervals, the analysis could not be made. We reorganised the timepoints to have them on a theoretical 24h cycle with a 4 hours resolution that would allow us to analyse the cyclic activity with JTK.

The only respiratory state with a significant oscillation determined by JKT cycle was CII-E. It was also one of the two-state that had the most variation between time points according to the one-way ANOVA analysis for the linear data (3.4). This result is very interesting because it measures the overall maximum OXPHOS capacity of the mitochondria. The uncoupler FCCP is a weak acid that uncouple the oxidation from phosphorylation and permit the transport of protons across cell membranes (Benz and McLaughlin 1983). It bypasses the ATP synthase and lets the hydrogen protons back in the matrix without limitation. It disrupts the proton gradient and forces the enzymes of complexes in the electron transport system to work at their maximum capacity. Variation in this measure at different time points could mean that the mitochondria are more efficient during some time of the day. A different capacity to utilize oxygen and to produce energy could be determinant for an animal subject to limited oxygen most of his time.

The other respiratory state with multiple significant differences between time points using the one-way ANOVA analysis was the leak respiration due to pyruvate and malate. It means that at different times of the day, mitochondria are more or less regulating the protons that can slip through the proton gradient without producing energy. The proton leak participates in reactive oxygen species (ROS) production (Cheng et al. 2017). ROS production and clock function could be regulated by the availability of NAD, conditioned by NAMPT expression (Sundar, Sellix, and Rahman 2018) (Figure 30).

There is little evidence of the direct effect of the clockwork on the respiratory system itself. An experiment by Andrews et al. showed that KO mice models *BMAL1*$^{-/-}$ presented a lower respiration capacity, mostly due to PM-P state on mitochondria from gastrocnemius and diaphragm muscles compared to the wild type (Andrews et al. 2010).

Another experiment showed that there is an effect of Rev-erba (*NR1D1)* on the oxidative capacity of the entire respiratory system. *NR1D1*$^{-/-}$ mutants mice have lower endurance and physical activity. At the respiratory system level, there was a lower DNA and protein content and a lower respiratory capacity compared to the wild-type mice at different respiratory rates (Woldt et al. 2013).

This direct link between the clockwork and the respiratory system has been associated in both studies with the shape and distribution of the mitochondria (Sardon Puig et al. 2018)(Figure 30). This mitochondrial dynamic is a fusion-fission mechanism known to influence respiratory capacity and is regulated by circadian rhythms (De Goede et al. 2018).

We decided to analyze the expression of some mitochondrial genes involved in the fusion-fission dynamic to highlight a possible correlation between the respiratory states and the expression of the clock genes. The genes involved in fusion are MFN1, MFN2, and OPA1. The genes involved in the fission of mitochondria are DNM1L (DRP1) (De Goede et al. 2018)(Figure 30). We also measured the expression level of NAMPT, a protein involved in the acetylation state of the complex I by mediating NAD SIRT1/3 activity. (Cela et al. 2016). NAMPT is regulated by the core clock genes (Ramsey et al. 2009) and strongly relates the clockwork with the OXPHOS capacity.

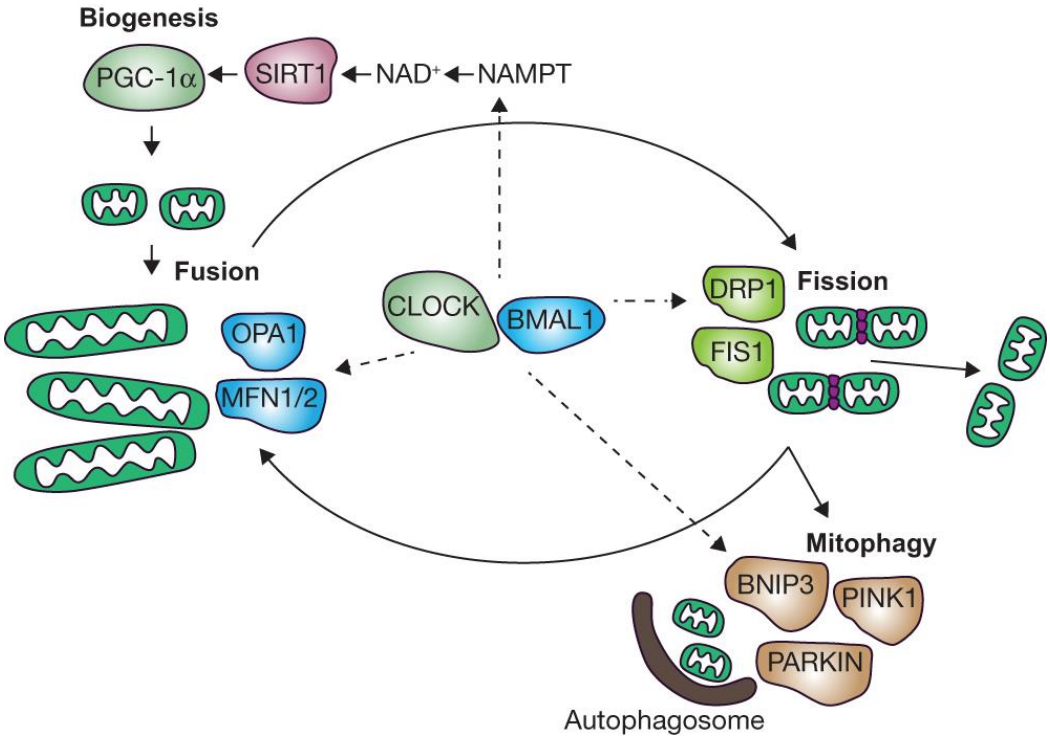

Figure 30 **The interactions between the clock genes and the mitochondrial-related genes influence the mitochondrial shape**. Reprinted from (De Goede et al. 2018) the clock genes Clock and BMAL1 are affecting the expression of MFN1/2 and OPA1 genes involved in the mitochondrial fusion, as well as DRP1 (NR1D1) and FIS1 involved in mitochondrial fission. The clock genes are also regulating genes promoting mitophagy. Finally, they influence the expression of NAMPT, necessary for the production of NAD+, an element of the TCA cycle, and influencing the OXPHOS capacity.

MFN1 expression is negatively correlated to respiratory capacity (3.4.4). It may seem contradictory because it promotes mitochondrial fusion (Figure 30) which is related to higher energy production (Sardon Puig et al. 2018), it is however important to remember that the fusion-fission dynamic needs expression of the different genes that evolved at all time and no conclusion could be drawn from the correlation.

It is also important to remember the mRNA expression of the gene is different from the actual protein content in the cell. The mRNA gives an idea of the gene expression while the protein content would be more informative about the mechanisms occurring in the cells at a given

time. This is especially important for clock genes as their posttranslational phosphorylation state plays a major role in the clockwork (C. Lee et al. 2001).

The dimer ARNTL-CLOCK is negatively correlated to the OXPHOS capacity of the mitochondria (3.4.5). Upon high expression of the dimer, ARNTL-CLOCK, there is a lower respiratory capacity in complex I and II. High expression of the dimer induces NAMPT expression is linking the circadian dimer to the mitochondrial dynamics through NAD+. When the NAD+ concentration is at its highest, it promotes SIRT expression and mitochondrial fusion processes. the upregulation of SIRT will in return downregulate the expression of BMAL1 and phosphorylation delays could explain why we find a negative relation between high ARNTL and low OXPHOS capacity, while it is promoting mitochondrial fusion (Sardon Puig et al. 2018). A further measure of the protein phosphorylation would be informative to relate the mRNA expression level with the active protein state.

The negative correlation between ARNTL (BMAL1) and OXPHOS capacity has previously been observed by Jacobi et al. in BMAL1 KO hepatocytes. (Jacobi et al. 2015). They showed that BMAL1 influenced the daily changing shape of the mitochondria in hepatic cells. Those changes were not happening in BMAL1 KO mice, showing the importance of BMAL1 in mitochondrial dynamics. It is reported that BMAL1 was targeting fission genes and proteins in hepatic cells, but not fusion genes lie MFN1 and 2 as well as OPA1 and DRP1 (DNM1L). The hepatocytes showed lower mitochondrial respiration, notably from the complex I (Jacobi et al. 2015). This result could be compared to a study on embryonic stem cells where high expression of BMAL1 maintained low mitochondrial functions (Ameneiro et al. 2020). This study however showed that BMAL1 function was regulating mitochondrial fission without dimerization with clock and in the absence of functional clockwork. It suggests that BMAL1 could have an action on mitochondrial metabolism without involving the clock. This result invites us to consider other interactions in the correlations between clock and respiration. There is no correlation when ARNTL expression is compared between fusion and fission genes. This could suggest that the interaction between ARNTL and the mitochondrial genes is more subtle. The mitochondrial genes were not cycling except MFN1. The genes are acting on mitochondrial fission, a dynamic that has a fairly observable phenotype. Combination of

observation of mitochondrial phenotype of live mitochondria (Jakobs 2006) and fusion/ fission gene expression would clarify the sensitivity of qPCR of mitochondrial genes as a proxy to measure mitochondrial dynamics.

The oxidative phosphorylation in the mitochondria is using oxygen as the last electron acceptor in aerobic conditions. If there is a circadian regulation in the OXPHOS capacity of the different complexes in the mitochondria, there is also a regulation of the oxygen sensing capacity of the cells and the entire organism. The protein HIF-1α is affected by oxygen levels. in normoxic conditions, the protein is degraded by the proteasome. The proline hydroxylation binds oxygen to HIF-1α and ubiquitin is recruited through von Hippel-Lindau (VHL) protein to mark the protein and direct it to the proteasome. Under hypoxic conditions, the VHL protein is not recruited and HIF-1α is translocated in the nucleus where it heterodimerizes with Hif1b and act as a transcription factor on the hypoxia response elements (Figure 31).

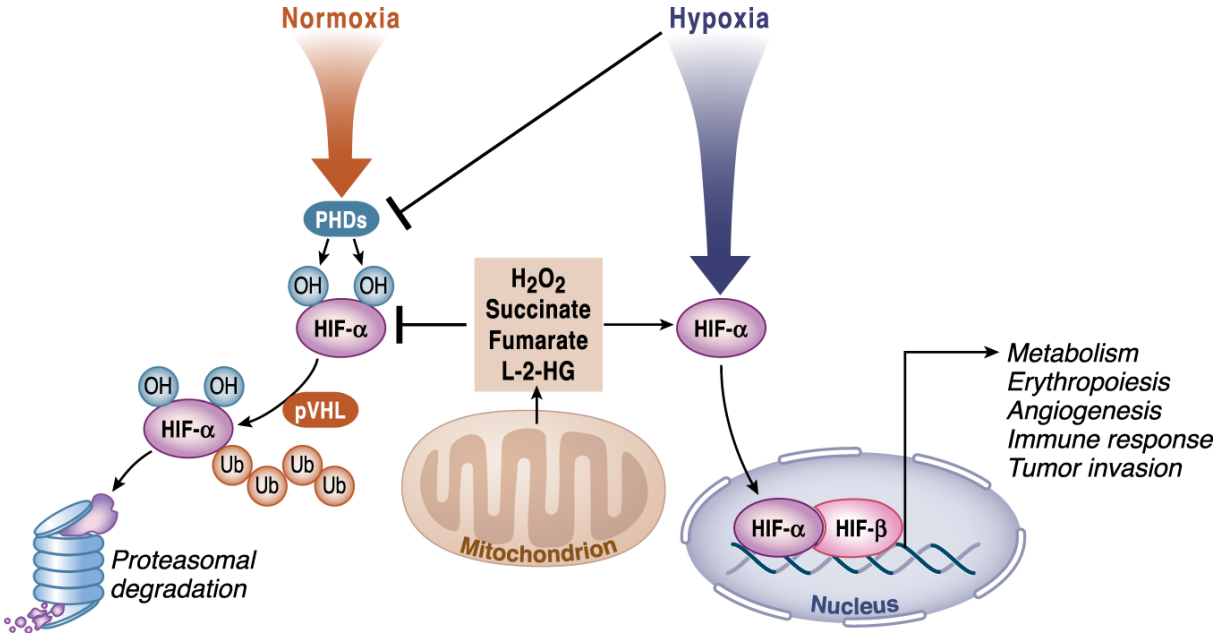

Figure 31 **Mechanism of HIF-1α in normoxia and hypoxia and the interaction with mitochondrial by-products**. Reprinted from (Martínez-Reyes and Chandel 2020) under normoxia, HIF-1α is targeted by the von Hippel-Lindau and degraded by the proteasome. Under hypoxic conditions, it binds to Hif1b in the nucleus to engage hypoxia response-related genes, promoting metabolism, erythropoiesis, and angiogenesis for example.

Hypoxic condition is likely to happen during the active phase, and because HIF-1α has a constitutive expression and is permanently degraded, circadian regulation of this element could be an advantage for an organism. Upregulation during the active period when it is most needed and downregulation during the resting phase would save metabolic energy. There is a direct regulation between HIF-1α and the clock gene BMAL1 in the nucleus, but there is also an action of HIF-1α on the mitochondrial dynamic in the cytoplasm (Peek et al. 2017). Further work to measure the expression level of HIF-1α in cell cultures that are rhythmically entrained would be informative of the constitutive expression of the gene. Because HIF-1α is constantly degraded, a measure of the protein content using western blot and localization, either in the nucleus or the cytoplasm using immunohistochemistry (Heikal et al. 2018) would help understand its dynamic.

4.6 Laboratory tools development

The quantitative PCRs that measured the expression of the different genes were analysed against only one housekeeping gene. The housekeeping gene is used as a reference gene whose expression is not changing between the different experimental conditions. The stability of this gene can vary across species, tissues, and even cell types (Wood et al. 2008).

We designed primers for 3 reference genes: RPLPO, PPIB and TBP. We could only use one of them, RPLPO. The primer efficiency for PPIB was below 90% and the expression of TBP was not considered to be stable enough. The genes have been used and proven to be stable in human synovial fibroblasts (Nazet et al. 2019). TBP and RPLPO have been identified to be suitable reference genes in human mammary epithelial cells in the context of circadian studies. The use of only one reference gene could have affected the strength of the qPCR results. A refinement of qPCR primers for housekeeping genes could give a more precise picture of the expression of the different genes in the future.

The efficiency of the primers for the mitochondrial genes was close to 100% and was which makes the efficiency difference with the reference gene close to 10%. Such a difference could influence the ct values and mask a difference between samples by an overall higher efficiency of the primer pair.

The limitation of measuring clock gene oscillation by the qPCR method is the time resolution. Because cells have to be collected for each time point, a better resolution on a longer timeframe requires more cells to be cultured. This is a cost and time-consuming strategy. An experiment with a 1-hour resolution over 48 hours using 4 replicates would mean 192 RNA extraction and 4 96 wells qPCR for one gene. While using qPCR to apprehend the expression of the clock genes was suitable, we should not aim to use it with a greater resolution. It could be used to sample only the peak and trough of gene expression defined in the temperature cycle experiment 3.3.3.1. This could be informative of the amplitude of the gene cycle, under different zeitgeber for example. This would require a strong and precise oscillation model of the genes involved.

The development of alternative cellular tools to measure gene expression is to be developed. Transfection of fibroblast and pia mater from hooded seals have been tested with a mcherry reporter integrated with different transfection reagents (Appendix Figure 43-Figure 45). We used the Invitrogen Lipofectamine 3000 and Promega viafect transfection reagents with mcherry reporter construct. This experiment did not work and there was no fluorescence detected on both the skin fibroblasts and pia matter hooded seal cells. Other transfection reagents were more successful. We used the TransIT 2020 and TransIT-LT1 transfection reagents with mcherry constructs. The TransIT 2020 reagents successfully transfected the fibroblasts (Appendix Figure 45) and pia mater cells (Appendix Figure 43), while the TransIT-LT1 successfully transfected the pia mater cells only (Appendix Figure 44). Validation of transfection reagents opens possibilities to measure the gene translation in protein. Live-cell imaging would enable us to study the rhythmic expression of genes with a better resolution and allow more complex experimental designs. The treatment experiments were done with serum, forskolin, and dexamethasone could be repeated to measure the expression of PER-2 over several cycles instead of an acute response measure.

A greater resolution in the clockwork cycle also enables us to identify the peak and trough in the cycle and time the respiratory measures accordingly, and they would be coupled with qPCR analysis of the clock and mitochondrial genes.

5 Conclusion

Circadian rhythms are present across all taxa and they are essential for living organisms to organize their metabolism around the day. In polar regions, the notion of the day as a light-dark cycle is greatly disturbed. Arctic organisms are exposed to constant light and constant darkness for parts of the year. In this study, we demonstrate that despite this peculiar environment, hooded seals can express the genes involved in the molecular clockwork, with a higher presence in the brain than in peripheral tissues. We established fibroblasts hooded cell cultures and showed that the clock of the cells responds to different stimulation treatments. We further demonstrated that the clock can entrain to temperature cycles. There is a daily difference in the respiratory capacity of the mitochondria, as well as in MFN1 involved in mitochondrial dynamic. A functional clock and a successful measure of mitochondrial respiration make hooded seal cell culture a great model to study oxygen metabolism with a circadian approach. Hooded seals have been a historic model in the research in hypoxia. Characterization of their circadian clock, coupled with mitochondrial studies is an opportunity to gain knowledge in the 2 awarded research fields.

Works cited

.Aarseth, J., T. Van'T Hof, and K.-A. Stokkan. 2003. "Melatonin is rhythmic in newborn seals exposed to continuous light." *Journal of Comparative Physiology B* 173 (1): 37-42. https://doi.org/10.1007/s00360-002-0307-7.

Abrahamson, E. E., R. K. Leak, and R. Y. Moore. 2001. "The suprachiasmatic nucleus projects to posterior hypothalamic arousal systems." *NeuroReport* 12 (2): 435-440. https://journals.lww.com/neuroreport/Fulltext/2001/02120/The_suprachiasmatic_nucleus_projects_to_posterior.48.aspx.

Ameneiro, Cristina, Tiago Moreira, Alejandro Fuentes-Iglesias, Alba Coego, Vera Garcia-Outeiral, Adriana Escudero, Daniel Torrecilla, Sonia Mulero-Navarro, Jose Maria Carvajal-Gonzalez, Diana Guallar, and Miguel Fidalgo. 2020. "BMAL1 coordinates energy metabolism and differentiation of pluripotent stem cells." *Life Science Alliance* 3 (5): e201900534. https://doi.org/10.26508/lsa.201900534.

Andersen, Julie M., Mette Skern-Mauritzen, Lars Boehme, Yolanda F. Wiersma, Aqqalu Rosing-Asvid, Mike O. Hammill, and Garry B. Stenson. 2013. "Investigating Annual Diving Behaviour by Hooded Seals (Cystophora cristata) within the Northwest Atlantic Ocean." *PLoS ONE* 8 (11): e80438. https://doi.org/10.1371/journal.pone.0080438. http://research.library.mun.ca/6316/1/Investigating.Annual.Diving.pdf.

Andrews, J. L., X. Zhang, J. J. Mccarthy, E. L. Mcdearmon, T. A. Hornberger, B. Russell, K. S. Campbell, S. Arbogast, M. B. Reid, J. R. Walker, J. B. Hogenesch, J. S. Takahashi, and K. A. Esser. 2010. "CLOCK and BMAL1 regulate MyoD and are necessary for maintenance of skeletal muscle phenotype and function." *Proceedings of the National Academy of Sciences* 107 (44): 19090-19095. https://doi.org/10.1073/pnas.1014523107. http://www.pnas.org/content/107/44/19090.full.pdf.

Appenroth, Daniel, Gabriela C. Wagner, David G. Hazlerigg, and Alexander C. West. 2021. "Evidence for circadian-based photoperiodic timekeeping in Svalbard ptarmigan, the northernmost resident bird." *Current Biology*. https://doi.org/https://doi.org/10.1016/j.cub.2021.04.009. https://www.sciencedirect.com/science/article/pii/S0960982221005224.

Arnold, Walter, Thomas Ruf, Leif Egil Loe, R. Justin Irvine, Erik Ropstad, Vebjørn Veiberg, and Steve D. Albon. 2018. "Circadian rhythmicity persists through the Polar night and midnight sun in Svalbard reindeer." *Scientific Reports* 8 (1). https://doi.org/10.1038/s41598-018-32778-4. https://www.ncbi.nlm.nih.gov/pmc/articles/PMC6160466.

Balsalobre, A. 2000. "Resetting of Circadian Time in Peripheral Tissues by Glucocorticoid Signaling." *Science* 289 (5488): 2344-2347. https://doi.org/10.1126/science.289.5488.2344.

Balsalobre, Aurélio, Francesca Damiola, and Ueli Schibler. 1998. "A Serum Shock Induces Circadian Gene Expression in Mammalian Tissue Culture Cells." *Cell* 93 (6): 929-937. https://doi.org/10.1016/s0092-8674(00)81199-x. http://linkinghub.elsevier.com/retrieve/pii/S009286740081199X.

Balsalobre, Aurélio, Lysiane Marcacci, and Ueli Schibler. 2000. "Multiple signaling pathways elicit circadian gene expression in cultured Rat-1 fibroblasts." *Current Biology* 10 (20): 1291-1294. https://doi.org/10.1016/s0960-9822(00)00758-2.

Begemann, Kimberly, Anne-Marie Neumann, and Henrik Oster. 2020. "Regulation and function of extra-SCN circadian oscillators in the brain." *Acta Physiologica* 229 (1):

e13446. https://doi.org/https://doi.org/10.1111/apha.13446. https://doi.org/10.1111/apha.13446.

Bell-Pedersen, Deborah. 2002. "Circadian rhythms in Neurospora crassa." *MYCOLOGY SERIES* 15: 187-214.

Benz, R., and S. McLaughlin. 1983. "The molecular mechanism of action of the proton ionophore FCCP (carbonylcyanide p-trifluoromethoxyphenylhydrazone)." *Biophysical Journal* 41 (3): 381-398. https://doi.org/https://doi.org/10.1016/S0006-3495(83)84449-X. https://www.sciencedirect.com/science/article/pii/S000634958384449X.

Bhadra, Utpal, Nirav Thakkar, Paromita Das, and Manika Pal Bhadra. 2017. "Evolution of circadian rhythms: from bacteria to human." *Sleep Medicine* 35: 49-61. https://doi.org/10.1016/j.sleep.2017.04.008.

Blix, A. S., L. Walloe, E. B. Messelt, and L. P. Folkow. 2010. "Selective brain cooling and its vascular basis in diving seals." *Journal of Experimental Biology* 213 (15): 2610-2616. https://doi.org/10.1242/jeb.040345. http://jeb.biologists.org/content/213/15/2610.full.pdf.

Blix, Arnoldus Schytte. 2018. "Adaptations to deep and prolonged diving in phocid seals." *The Journal of Experimental Biology* 221 (12): jeb182972. https://doi.org/10.1242/jeb.182972. https://jeb.biologists.org/content/jexbio/221/12/jeb182972.full.pdf.

Blix, Arnoldus Schytte, John K. Kjekshus, Ivar Enge, and Anstein Bergan. 1976. "Myocardial Blood Flow in the Diving Seal." *Acta Physiologica Scandinavica* 96 (2): 277-280. https://doi.org/10.1111/j.1748-1716.1976.tb10196.x.

Bron, Klaus M., H. V. Murdaugh, J. Eugene Millen, Ronald Lenthall, Philip Raskin, and Eugene D. Robin. 1966. "Arterial Constrictor Response in a Diving Mammal." *Science* 152 (3721): 540-543. https://doi.org/10.1126/science.152.3721.540. https://science.sciencemag.org/content/sci/152/3721/540.full.pdf.

Brown, Steven A, Gottlieb Zumbrunn, Fabienne Fleury-Olela, Nicolas Preitner, and Ueli Schibler. 2002. "Rhythms of Mammalian Body Temperature Can Sustain Peripheral Circadian Clocks." *Current Biology* 12 (18): 1574-1583. https://doi.org/10.1016/s0960-9822(02)01145-4.

Buhr, E. D., S.-H. Yoo, and J. S. Takahashi. 2010. "Temperature as a Universal Resetting Cue for Mammalian Circadian Oscillators." *Science* 330 (6002): 379-385. https://doi.org/10.1126/science.1195262. http://europepmc.org/articles/pmc3625727?pdf=render.

Buijs, Ruud M., and Andries Kalsbeek. 2001. "Hypothalamic integration of central and peripheral clocks." *Nature Reviews Neuroscience* 2 (7): 521-526. https://doi.org/10.1038/35081582. https://doi.org/10.1038/35081582.

Cagnacci, A., J. A. Elliott, and S. S. Yen. 1992. "Melatonin: a major regulator of the circadian rhythm of core temperature in humans." *J Clin Endocrinol Metab* 75 (2): 447-52. https://doi.org/10.1210/jcem.75.2.1639946.

Cela, Olga, Rosella Scrima, Valerio Pazienza, Giuseppe Merla, Giorgia Benegiamo, Bartolomeo Augello, Sabino Fugetto, Marta Menga, Rosa Rubino, Luise Fuhr, Angela Relógio, Claudia Piccoli, Gianluigi Mazzoccoli, and Nazzareno Capitanio. 2016. "Clock genes-dependent acetylation of complex I sets rhythmic activity of mitochondrial OxPhos." *Biochimica et Biophysica Acta (BBA) - Molecular Cell Research* 1863 (4): 596-606. https://doi.org/10.1016/j.bbamcr.2015.12.018. https://doi.org/10.1016/j.bbamcr.2015.12.018.

Work cited

Challet, Etienne. 2019. "The circadian regulation of food intake." *Nature Reviews Endocrinology* 15 (7): 393-405. https://doi.org/10.1038/s41574-019-0210-x. https://www.nature.com/articles/s41574-019-0210-x.pdf.

Cheng, Jiali, Gayani Nanayakkara, Ying Shao, Ramon Cueto, Luqiao Wang, William Y. Yang, Ye Tian, Hong Wang, and Xiaofeng Yang. 2017. "Mitochondrial Proton Leak Plays a Critical Role in Pathogenesis of Cardiovascular Diseases." In *Advances in Experimental Medicine and Biology*, 359-370. Springer International Publishing.

Chicco, A. J., C. H. Le, A. Schlater, A. Nguyen, S. Kaye, J. W. Beals, R. L. Scalzo, C. Bell, E. Gnaiger, D. P. Costa, D. E. Crocker, and S. B. Kanatous. 2014. "High fatty acid oxidation capacity and phosphorylation control despite elevated leak and reduced respiratory capacity in northern elephant seal muscle mitochondria." *Journal of Experimental Biology* 217 (16): 2947-2955. https://doi.org/10.1242/jeb.105916. http://jeb.biologists.org/content/217/16/2947.full.pdf.

De Goede, Paul, Jakob Wefers, Eline Constance Brombacher, Patrick Schrauwen, and Andries Kalsbeek. 2018. "Circadian rhythms in mitochondrial respiration." *Journal of Molecular Endocrinology* 60 (3): R115-R130. https://doi.org/10.1530/jme-17-0196.

Dijk, D. J., J. F. Duffy, E. J. Silva, T. L. Shanahan, D. B. Boivin, and C. A. Czeisler. 2012. "Amplitude reduction and phase shifts of melatonin, cortisol and other circadian rhythms after a gradual advance of sleep and light exposure in humans." *PLoS One* 7 (2): e30037. https://doi.org/10.1371/journal.pone.0030037.

Dodd, A. N. 2005. "Plant Circadian Clocks Increase Photosynthesis, Growth, Survival, and Competitive Advantage." *Science* 309 (5734): 630-633. https://doi.org/10.1126/science.1115581.

Edgar, Rachel S., Edward W. Green, Yuwei Zhao, Gerben Van Ooijen, Maria Olmedo, Ximing Qin, Yao Xu, Min Pan, Utham K. Valekunja, Kevin A. Feeney, Elizabeth S. Maywood, Michael H. Hastings, Nitin S. Baliga, Martha Merrow, Andrew J. Millar, Carl H. Johnson, Charalambos P. Kyriacou, John S. O'Neill, and Akhilesh B. Reddy. 2012. "Peroxiredoxins are conserved markers of circadian rhythms." *Nature* 485 (7399): 459-464. https://doi.org/10.1038/nature11088. http://europepmc.org/articles/pmc3398137?pdf=render.

Erecińska, Maria, and Ian A. Silver. 2001. "Tissue oxygen tension and brain sensitivity to hypoxia." *Respiration Physiology* 128 (3): 263-276. https://doi.org/10.1016/s0034-5687(01)00306-1.

Falke, K., R. Hill, J Qvist, R. Schneider, M Guppy, G. Liggins, P. Hochachka, R. Elliott, and W. Zapol. 1985. "Seal lungs collapse during free diving: evidence from arterial nitrogen tensions." *Science* 229 (4713): 556-558. https://doi.org/10.1126/science.4023700.

Fischl, Harry, David Mcmanus, Roel Oldenkamp, Lothar Schermelleh, Jane Mellor, Aarti Jagannath, and Andre Furger. 2020.

Folkow, Lars P., Per-Erik Mårtensson, and Arnoldus Schytte Blix. 1996. "Annual distribution of hooded seals (Cystophora cristata) in the Greenland and Norwegian seas." *Polar Biology* 16 (3): 179-189. https://doi.org/10.1007/BF02329206. https://doi.org/10.1007/BF02329206.

Gallego, Monica, and David M. Virshup. 2007. "Post-translational modifications regulate the ticking of the circadian clock." *Nature Reviews Molecular Cell Biology* 8 (2): 139-148. https://doi.org/10.1038/nrm2106.

Gerhart-Hines, Zachary, Dan Feng, Matthew J. Emmett, Logan J. Everett, Emanuele Loro, Erika R. Briggs, Anne Bugge, Catherine Hou, Christine Ferrara, Patrick Seale, Daniel A. Pryma, Tejvir S. Khurana, and Mitchell A. Lazar. 2013. "The nuclear receptor Rev-erbα controls circadian thermogenic plasticity." *Nature* 503 (7476): 410-413.

https://doi.org/10.1038/nature12642.
https://www.ncbi.nlm.nih.gov/pmc/articles/PMC3839416.

Gonzalez, G. A., and M. R. Montminy. 1989. "Cyclic AMP stimulates somatostatin gene transcription by phosphorylation of CREB at serine 133." *Cell* 59 (4): 675-80. https://doi.org/10.1016/0092-8674(89)90013-5.

Guillaumond, F., H. Dardente, V. Giguère, and N. Cermakian. 2005. "Differential control of Bmal1 circadian transcription by REV-ERB and ROR nuclear receptors." *J Biol Rhythms* 20 (5): 391-403. https://doi.org/10.1177/0748730405277232.

Hastings, Michael H., Elizabeth S. Maywood, and Marco Brancaccio. 2018. "Generation of circadian rhythms in the suprachiasmatic nucleus." *Nature Reviews Neuroscience* 19 (8): 453-469. https://doi.org/10.1038/s41583-018-0026-z.

Hastings, Michael H., Akhilesh B. Reddy, and Elizabeth S. Maywood. 2003. "A clockwork web: circadian timing in brain and periphery, in health and disease." *Nature Reviews Neuroscience* 4 (8): 649-661. https://doi.org/10.1038/nrn1177.

Heikal, Lamia, Pietro Ghezzi, Manuela Mengozzi, and Gordon Ferns. 2018. "Assessment of HIF-1α expression and release following endothelial injury in-vitro and in-vivo." *Molecular medicine (Cambridge, Mass.)* 24 (1): 22-22. https://doi.org/10.1186/s10020-018-0026-5.
https://pubmed.ncbi.nlm.nih.gov/30134815

https://www.ncbi.nlm.nih.gov/pmc/articles/PMC6016879/.

Hughes, Michael E., John B. Hogenesch, and Karl Kornacker. 2010. "JTK_CYCLE: An Efficient Nonparametric Algorithm for Detecting Rhythmic Components in Genome-Scale Data Sets." *Journal of Biological Rhythms* 25 (5): 372-380. https://doi.org/10.1177/0748730410379711.
https://www.ncbi.nlm.nih.gov/pmc/articles/PMC3119870.

Iitaka, Chisato, Koyomi Miyazaki, Toshihiro Akaike, and Norio Ishida. 2005. "A Role for Glycogen Synthase Kinase-3β in the Mammalian Circadian Clock*." *Journal of Biological Chemistry* 280 (33): 29397-29402. https://doi.org/https://doi.org/10.1074/jbc.M503526200.
https://www.sciencedirect.com/science/article/pii/S0021925820563618.

Irving, Laurence, P. F. Scholander, and S. W. Grinnell. 1941. "Significance of the heart rate to the diving ability of seals." *Journal of Cellular and Comparative Physiology* 18 (3): 283-297. https://doi.org/https://doi.org/10.1002/jcp.1030180302.
https://onlinelibrary.wiley.com/doi/abs/10.1002/jcp.1030180302.

Jacobi, David, Sihao Liu, Kristopher Burkewitz, Nora Kory, H. Knudsen, Nelson, K. Alexander, Ryan, Ugur Unluturk, Xiaobo Li, Xiaohui Kong, L. Hyde, Alexander, R. Gangl, Matthew, B. Mair, William, and Chih-Hao Lee. 2015. "Hepatic Bmal1 Regulates Rhythmic Mitochondrial Dynamics and Promotes Metabolic Fitness." *Cell Metabolism* 22 (4): 709-720. https://doi.org/10.1016/j.cmet.2015.08.006.
http://europepmc.org/articles/pmc4598294?pdf=render.

Jakobs, Stefan. 2006. "High resolution imaging of live mitochondria." *Biochimica et Biophysica Acta (BBA) - Molecular Cell Research* 1763 (5-6): 561-575. https://doi.org/10.1016/j.bbamcr.2006.04.004. http://hdl.handle.net/11858/00-001M-0000-0012-E5EB-2.

Jordan, Sabine D., and Katja A. Lamia. 2013. "AMPK at the crossroads of circadian clocks and metabolism." *Molecular and Cellular Endocrinology* 366 (2): 163-169. https://doi.org/10.1016/j.mce.2012.06.017.
http://europepmc.org/articles/pmc3502724?pdf=render.

Judge, Ayesha, and S. Dodd, Michael. 2020. "Metabolism." *Essays in Biochemistry* 64 (4): 607-647. https://doi.org/10.1042/ebc20190041.

Work cited

Kala, R., F. Fyhrquist, and A. Eisalo. 1973. "Diurnal Variation of Plasma Angiotensin II in Man." *Scandinavian Journal of Clinical and Laboratory Investigation* 31 (4): 363-365. https://doi.org/10.3109/00365517309084318. https://doi.org/10.3109/00365517309084318.

Keijzer, Henry, Marcel G. Smits, Jeanne F. Duffy, and Leopold M. G. Curfs. 2014. "Why the dim light melatonin onset (DLMO) should be measured before treatment of patients with circadian rhythm sleep disorders." *Sleep Medicine Reviews* 18 (4): 333-339. https://doi.org/https://doi.org/10.1016/j.smrv.2013.12.001. https://www.sciencedirect.com/science/article/pii/S1087079213001135.

Kerem, D, D.D Hammond, and R Elsner. 1973. "Tissue glycogen levels in the Weddell seal, Leptonychotes weddelli: A possible adaptation to asphyxial hypoxia." *Comparative Biochemistry and Physiology Part A: Physiology* 45 (3): 731-736. https://doi.org/10.1016/0300-9629(73)90076-5.

Kooyman, G. L., M. A. Castellini, R. W. Davis, and R. A. Maue. 1983. "Aerobic diving limits of immature Weddell seals." *Journal of comparative physiology* 151 (2): 171-174. https://doi.org/10.1007/BF00689915. https://doi.org/10.1007/BF00689915.

Kooyman, G. L., E. A. Wahrenbrock, M. A. Castellini, R. W. Davis, and E. E. Sinnett. 1980. "Aerobic and anaerobic metabolism during voluntary diving in Weddell seals: Evidence of preferred pathways from blood chemsitry and behavior." *Journal of comparative physiology* 138 (4): 335-346. https://doi.org/10.1007/BF00691568. https://doi.org/10.1007/BF00691568.

Koronowski, Kevin B., and Paolo Sassone-Corsi. 2021. "Communicating clocks shape circadian homeostasis." *Science* 371 (6530): eabd0951. https://doi.org/10.1126/science.abd0951.

Lamia, K. A., U. M. Sachdeva, L. Ditacchio, E. C. Williams, J. G. Alvarez, D. F. Egan, D. S. Vasquez, H. Juguilon, S. Panda, R. J. Shaw, C. B. Thompson, and R. M. Evans. 2009. "AMPK Regulates the Circadian Clock by Cryptochrome Phosphorylation and Degradation." *Science* 326 (5951): 437-440. https://doi.org/10.1126/science.1172156. http://europepmc.org/articles/pmc2819106?pdf=render.

Lee, B., A. Li, K. F. Hansen, R. Cao, J. H. Yoon, and K. Obrietan. 2010. "CREB influences timing and entrainment of the SCN circadian clock." *J Biol Rhythms* 25 (6): 410-20. https://doi.org/10.1177/0748730410381229.

Lee, Choogon, Jean-Pierre Etchegaray, Felino R.A. Cagampang, Andrew S.I. Loudon, and Steven M. Reppert. 2001. "Posttranslational Mechanisms Regulate the Mammalian Circadian Clock." *Cell* 107 (7): 855-867. https://doi.org/10.1016/s0092-8674(01)00610-9.

Legates, Tara A., Diego C. Fernandez, and Samer Hattar. 2014. "Light as a central modulator of circadian rhythms, sleep and affect." *Nature Reviews Neuroscience* 15 (7): 443-454. https://doi.org/10.1038/nrn3743. http://europepmc.org/articles/pmc4254760?pdf=render.

Lestyk, Keri C., L. P. Folkow, A. S. Blix, M. O. Hammill, and J. M. Burns. 2009. "Development of myoglobin concentration and acid buffering capacity in harp (Pagophilus groenlandicus) and hooded (Cystophora cristata) seals from birth to maturity." *Journal of Comparative Physiology B* 179 (8): 985-996. https://doi.org/10.1007/s00360-009-0378-9.

Lewy, AJ, TA Wehr, FK Goodwin, DA Newsome, and SP Markey. 1980. "Light suppresses melatonin secretion in humans." *Science* 210 (4475): 1267-1269. https://doi.org/10.1126/science.7434030. https://science.sciencemag.org/content/sci/210/4475/1267.full.pdf.

Work cited

Lowrey, P. L., K. Shimomura, M. P. Antoch, S. Yamazaki, P. D. Zemenides, M. R. Ralph, M. Menaker, and J. S. Takahashi. 2000. "Positional syntenic cloning and functional characterization of the mammalian circadian mutation tau." *Science* 288 (5465): 483-92. https://doi.org/10.1126/science.288.5465.483.

Lu, Weiqun, Qing-Jun Meng, Nicholas J. C. Tyler, Karl-Arne Stokkan, and Andrew S. I. Loudon. 2010. "A Circadian Clock Is Not Required in an Arctic Mammal." *Current Biology* 20 (6): 533-537. https://doi.org/https://doi.org/10.1016/j.cub.2010.01.042. https://www.sciencedirect.com/science/article/pii/S0960982210000850.

Martínez-Reyes, Inmaculada, and Navdeep S. Chandel. 2020. "Mitochondrial TCA cycle metabolites control physiology and disease." *Nature Communications* 11 (1). https://doi.org/10.1038/s41467-019-13668-3.

Mcarthur, Angela J., Martha U. Gillette, and Rebecca A. Prosser. 1991. "Melatonin directly resets the rat suprachiasmatic circadian clock in vitro." *Brain Research* 565 (1): 158-161. https://doi.org/10.1016/0006-8993(91)91748-p.

McMullan, C. J., E. S. Schernhammer, E. B. Rimm, F. B. Hu, and J. P. Forman. 2013. "Melatonin secretion and the incidence of type 2 diabetes." *Jama* 309 (13): 1388-96. https://doi.org/10.1001/jama.2013.2710.

Mitz, S.A., S. Reuss, L.P. Folkow, A.S. Blix, J.-M. Ramirez, T. Hankeln, and T. Burmester. 2009. "When the brain goes diving: glial oxidative metabolism may confer hypoxia tolerance to the seal brain." *Neuroscience* 163 (2): 552-560. https://doi.org/10.1016/j.neuroscience.2009.06.058.

Miyazaki, Mitsunori, Elizabeth Schroder, Stephanie E. Edelmann, Michael E. Hughes, Karl Kornacker, C. William Balke, and Karyn A. Esser. 2011. "Age-Associated Disruption of Molecular Clock Expression in Skeletal Muscle of the Spontaneously Hypertensive Rat." *PLoS ONE* 6 (11): e27168. https://doi.org/10.1371/journal.pone.0027168. https://journals.plos.org/plosone/article/file?id=10.1371/journal.pone.0027168&type=printable.

Morf, Jörg, and Ueli Schibler. 2013. "Body temperature cycles: gatekeepers of circadian clocks." *Cell cycle (Georgetown, Tex.)* 12 (4): 539-540. https://doi.org/10.4161/cc.23670. https://pubmed.ncbi.nlm.nih.gov/23343768

https://www.ncbi.nlm.nih.gov/pmc/articles/PMC3594249/.

Morris, Christopher J., Jessica N. Yang, Joanna I. Garcia, Samantha Myers, Isadora Bozzi, Wei Wang, Orfeu M. Buxton, Steven A. Shea, and Frank A. J. L. Scheer. 2015. "Endogenous circadian system and circadian misalignment impact glucose tolerance via separate mechanisms in humans." *Proceedings of the National Academy of Sciences* 112 (17): E2225-E2234. https://doi.org/10.1073/pnas.1418955112. https://www.pnas.org/content/pnas/112/17/E2225.full.pdf.

Nagoshi, Emi, Camille Saini, Christoph Bauer, Thierry Laroche, Felix Naef, and Ueli Schibler. 2004. "Circadian Gene Expression in Individual Fibroblasts." *Cell* 119 (5): 693-705. https://doi.org/10.1016/j.cell.2004.11.015.

Nazet, Ute, Agnes Schröder, Susanne Grässel, Dominique Muschter, Peter Proff, and Christian Kirschneck. 2019. "Housekeeping gene validation for RT-qPCR studies on synovial fibroblasts derived from healthy and osteoarthritic patients with focus on mechanical loading." *PLOS ONE* 14 (12): e0225790. https://doi.org/10.1371/journal.pone.0225790.

Nonaka, Hidemi, Noriaki Emoto, Koji Ikeda, Hiroyuki Fukuya, Mohammad Saifur Rohman, Sunu Budhi Raharjo, Kazuhiro Yagita, Hitoshi Okamura, and Mitsuhiro Yokoyama. 2001. "Angiotensin II Induces Circadian Gene Expression of Clock Genes in Cultured Vascular Smooth Muscle Cells." *Circulation* 104 (15): 1746-1748. https://doi.org/10.1161/hc4001.098048.

Work cited

Oftedal, Olav, Daryl Boness, and William Bowen. 2011. "The composition of hooded seal (Cystophora cristata) milk: An adaptation for postnatal fattening." *Can J Zool* 66. https://doi.org/10.1139/z88-047.

Ohashi, Ayaka, Aya Murata, Yuichiro Cho, Shizuko Ichinose, Yuriko Sakamaki, Miwako Nishio, Osamu Hoshi, Silvia Fischer, Klaus T. Preissner, and Takatoshi Koyama. 2017. "The expression and localization of RNase and RNase inhibitor in blood cells and vascular endothelial cells in homeostasis of the vascular system." *PLOS ONE* 12 (3): e0174237. https://doi.org/10.1371/journal.pone.0174237. https://doi.org/10.1371/journal.pone.0174237.

Panda, Satchidananda, Marina P. Antoch, Brooke H. Miller, Andrew I. Su, Andrew B. Schook, Marty Straume, Peter G. Schultz, Steve A. Kay, Joseph S. Takahashi, and John B. Hogenesch. 2002. "Coordinated Transcription of Key Pathways in the Mouse by the Circadian Clock." *Cell* 109 (3): 307-320. https://doi.org/10.1016/s0092-8674(02)00722-5.

Partch, Carrie L., Carla B. Green, and Joseph S. Takahashi. 2014. "Molecular architecture of the mammalian circadian clock." *Trends in Cell Biology* 24 (2): 90-99. https://doi.org/10.1016/j.tcb.2013.07.002. https://www.ncbi.nlm.nih.gov/pmc/articles/PMC3946763.

Peek, Clara Bien, Daniel C. Levine, Jonathan Cedernaes, Akihiko Taguchi, Yumiko Kobayashi, Stacy J. Tsai, Nicolle A. Bonar, Maureen R. Mcnulty, Kathryn Moynihan Ramsey, and Joseph Bass. 2017. "Circadian Clock Interaction with HIF1α Mediates Oxygenic Metabolism and Anaerobic Glycolysis in Skeletal Muscle." *Cell Metabolism* 25 (1): 86-92. https://doi.org/10.1016/j.cmet.2016.09.010. http://europepmc.org/articles/pmc5226863?pdf=render.

Perrigault, Mickael, Hector Andrade, Laure Bellec, Carl Ballantine, Lionel Camus, and Damien Tran. 2020. "Rhythms during the polar night: evidence of clock-gene oscillations in the Arctic scallop

Chlamys islandica." *Proceedings of the Royal Society B: Biological Sciences* 287 (1933): 20201001. https://doi.org/10.1098/rspb.2020.1001.

Preitner, Nicolas, Francesca Damiola, Luis-Lopez-Molina, Joszef Zakany, Denis Duboule, Urs Albrecht, and Ueli Schibler. 2002. "The Orphan Nuclear Receptor REV-ERBα Controls Circadian Transcription within the Positive Limb of the Mammalian Circadian Oscillator." *Cell* 110 (2): 251-260. https://doi.org/10.1016/s0092-8674(02)00825-5.

Prolo, L. M. 2005. "Circadian Rhythm Generation and Entrainment in Astrocytes." *Journal of Neuroscience* 25 (2): 404-408. https://doi.org/10.1523/jneurosci.4133-04.2005.

Ralph, MR, RG Foster, FC Davis, and M Menaker. 1990. "Transplanted suprachiasmatic nucleus determines circadian period." *Science* 247 (4945): 975-978. https://doi.org/10.1126/science.2305266. https://science.sciencemag.org/content/sci/247/4945/975.full.pdf.

Ramsey, K. M., J. Yoshino, C. S. Brace, D. Abrassart, Y. Kobayashi, B. Marcheva, H.-K. Hong, J. L. Chong, E. D. Buhr, C. Lee, J. S. Takahashi, S.-I. Imai, and J. Bass. 2009. "Circadian Clock Feedback Cycle Through NAMPT-Mediated NAD+ Biosynthesis." *Science* 324 (5927): 651-654. https://doi.org/10.1126/science.1171641. http://europepmc.org/articles/pmc2738420?pdf=render.

Reiter, R. J., J. C. Mayo, D. X. Tan, R. M. Sainz, M. Alatorre-Jimenez, and L. Qin. 2016. "Melatonin as an antioxidant: under promises but over delivers." *J Pineal Res* 61 (3): 253-78. https://doi.org/10.1111/jpi.12360.

Work cited

Reiter, Russel J. 1991. "Pineal Melatonin: Cell Biology of Its Synthesis and of Its Physiological Interactions*." *Endocrine Reviews* 12 (2): 151-180. https://doi.org/10.1210/edrv-12-2-151. https://doi.org/10.1210/edrv-12-2-151.

Rensing, Ludger, Ulf Meyer-Grahle, and Peter Ruoff. 2001. "BIOLOGICAL TIMING AND THE CLOCK METAPHOR: OSCILLATORY AND HOURGLASS MECHANISMS." *Chronobiology International* 18 (3): 329-369. https://doi.org/10.1081/cbi-100103961.

Reppart, Steven M., David R. Weaver, and Catherine Godson. 1996. "Melatonin receptors step into the light: cloning and classification of subtypes." *Trends in Pharmacological Sciences* 17 (3): 100-102. https://doi.org/https://doi.org/10.1016/0165-6147(96)10005-5. https://www.sciencedirect.com/science/article/pii/0165614796100055.

Rosbash, Michael. 2009. "The Implications of Multiple Circadian Clock Origins." *PLoS Biology* 7 (3): e1000062. https://doi.org/10.1371/journal.pbio.1000062. https://journals.plos.org/plosbiology/article/file?id=10.1371/journal.pbio.1000062&type=printable.

Sadacca, L. A., K. A. Lamia, A. S. Delemos, B. Blum, and C. J. Weitz. 2011. "An intrinsic circadian clock of the pancreas is required for normal insulin release and glucose homeostasis in mice." *Diabetologia* 54 (1): 120-124. https://doi.org/10.1007/s00125-010-1920-8. http://europepmc.org/articles/pmc2995870?pdf=render.

Sandu, Cristina, Taole Liu, André Malan, Etienne Challet, Paul Pévet, and Marie-Paule Felder-Schmittbuhl. 2015. "Circadian clocks in rat skin and dermal fibroblasts: differential effects of aging, temperature and melatonin." *Cellular and Molecular Life Sciences* 72 (11): 2237-2248. https://doi.org/10.1007/s00018-014-1809-7.

Sardon Puig, Laura, Miriam Valera-Alberni, Carles Cantó, and Nicolas J. Pillon. 2018. "Circadian Rhythms and Mitochondria: Connecting the Dots." *Frontiers in Genetics* 9. https://doi.org/10.3389/fgene.2018.00452. https://www.frontiersin.org/articles/10.3389/fgene.2018.00452/pdf.

Schibler, Ueli, and Paolo Sassone-Corsi. 2002. "A Web of Circadian Pacemakers." *Cell* 111 (7): 919-922. https://doi.org/10.1016/s0092-8674(02)01225-4.

Schmitt, Karen, Amandine Grimm, Robert Dallmann, Bjoern Oettinghaus, Lisa Michelle Restelli, Melissa Witzig, Naotada Ishihara, Katsuyoshi Mihara, Jürgen A. Ripperger, Urs Albrecht, Stephan Frank, Steven A. Brown, and Anne Eckert. 2018. "Circadian Control of DRP1 Activity Regulates Mitochondrial Dynamics and Bioenergetics." *Cell Metabolism* 27 (3): 657-666.e5. https://doi.org/10.1016/j.cmet.2018.01.011. http://doc.rero.ch/record/309036/files/alb_ccd.pdf.

Schytte Blix, Arnoldus. 2007. "Arctic animals and their adaptations to life on the edge." *Polar Research* 26 (1): 88-89. https://doi.org/10.3402/polar.v26i1.6209. https://polarresearch.net/index.php/polar/article/view/2010.

St. John, Peter C., Tsuyoshi Hirota, Steve A. Kay, and Francis J. Doyle. 2014. "Spatiotemporal separation of PER and CRY posttranslational regulation in the mammalian circadian clock." *Proceedings of the National Academy of Sciences* 111 (5): 2040-2045. https://doi.org/10.1073/pnas.1323618111. http://europepmc.org/articles/pmc3918757?pdf=render.

Stokkan, Karl-Arne, Bob E. H. Van Oort, Nicholas J. C. Tyler, and Andrew S. I. Loudon. 2007. "Adaptations for life in the Arctic: evidence that melatonin rhythms in reindeer are not driven by a circadian oscillator but remain acutely sensitive to environmental photoperiod." *Journal of Pineal Research* 43 (3): 289-293. https://doi.org/10.1111/j.1600-079x.2007.00476.x.

Sundar, Isaac K., Michael T. Sellix, and Irfan Rahman. 2018. "Redox regulation of circadian molecular clock in chronic airway diseases." *Free Radical Biology and Medicine* 119:

121-128. https://doi.org/10.1016/j.freeradbiomed.2017.10.383. https://www.ncbi.nlm.nih.gov/pmc/articles/PMC5910271.

Thornton, S. J., and P. W. Hochachka. 2004. "Oxygen and the diving seal." *Undersea Hyperb Med* 31 (1): 81-95.

Timmermans, Steven, Jolien Souffriau, and Claude Libert. 2019. "A General Introduction to Glucocorticoid Biology." *Frontiers in Immunology* 10 (1545). https://doi.org/10.3389/fimmu.2019.01545. https://www.frontiersin.org/article/10.3389/fimmu.2019.01545.

Tsuchiya, Yoshiki, Makoto Akashi, and Eisuke Nishida. 2003. "Temperature compensation and temperature resetting of circadian rhythms in mammalian cultured fibroblasts." *Genes to Cells* 8 (8): 713-720. https://doi.org/10.1046/j.1365-2443.2003.00669.x.

Vacquie-Garcia, Jade, Christian Lydersen, Martin Biuw, Tore Haug, Mike A. Fedak, and Kit M. Kovacs. 2017. "Hooded seal Cystophora cristata foraging areas in the Northeast Atlantic Ocean—Investigated using three complementary methods." *PLOS ONE* 12 (12): e0187889. https://doi.org/10.1371/journal.pone.0187889. http://europepmc.org/articles/pmc5718402?pdf=render.

Van Oort, Bob E. H., Nicholas J. C. Tyler, Menno P. Gerkema, Lars Folkow, Arnoldus Schytte Blix, and Karl-Arne Stokkan. 2005. "Circadian organization in reindeer." *Nature* 438 (7071): 1095-1096. https://doi.org/10.1038/4381095a. https://www.rug.nl/research/portal/files/6691896/2005NaturevOortSupp.pdf.

Van Valkenburgh, Blaire, Benison Pang, Deborah Bird, Abigail Curtis, Karen Yee, Charles Wysocki, and Brent A. Craven. 2014. "Respiratory and Olfactory Turbinals in Feliform and Caniform Carnivorans: The Influence of Snout Length." *The Anatomical Record* 297 (11): 2065-2079. https://doi.org/10.1002/ar.23026.

Vielhaber, E., E. Eide, A. Rivers, Z. H. Gao, and D. M. Virshup. 2000. "Nuclear entry of the circadian regulator mPER1 is controlled by mammalian casein kinase I epsilon." *Mol Cell Biol* 20 (13): 4888-99. https://doi.org/10.1128/mcb.20.13.4888-4899.2000.

Voogel, A. J., M. G. Koopman, A. A. Hart, G. A. van Montfrans, and L. Arisz. 2001. "Circadian rhythms in systemic hemodynamics and renal function in healthy subjects and patients with nephrotic syndrome." *Kidney Int* 59 (5): 1873-80. https://doi.org/10.1046/j.1523-1755.2001.0590051873.x.

Ware, Jasmine V., Karyn D. Rode, Charles T. Robbins, Tanya Leise, Colby R. Weil, and Heiko T. Jansen. 2020. "The Clock Keeps Ticking: Circadian Rhythms of Free-Ranging Polar Bears." *Journal of Biological Rhythms* 35 (2): 180-194. https://doi.org/10.1177/0748730419900877.

Weaver, David R. 1998. "The Suprachiasmatic Nucleus: A 25-Year Retrospective." *Journal of Biological Rhythms* 13 (2): 100-112. https://doi.org/10.1177/074873098128999952. https://journals.sagepub.com/doi/abs/10.1177/074873098128999952.

West, Alexander C., Marianne Iversen, Even H. Jørgensen, Simen R. Sandve, David G. Hazlerigg, and Shona H. Wood. 2020. "Diversified regulation of circadian clock gene expression following whole genome duplication." *PLOS Genetics* 16 (10): e1009097. https://doi.org/10.1371/journal.pgen.1009097.

Williams, Cory T., Brian M. Barnes, Lily Yan, and C. Loren Buck. 2017. "Entraining to the polar day: circadian rhythms in arctic ground squirrels." *The Journal of Experimental Biology* 220 (17): 3095-3102. https://doi.org/10.1242/jeb.159889. https://jeb.biologists.org/content/jexbio/220/17/3095.full.pdf.

Woelfle, Mark A., Yan Ouyang, Kittiporn Phanvijhitsiri, and Carl Hirschie Johnson. 2004. "The Adaptive Value of Circadian Clocks." *Current Biology* 14 (16): 1481-1486. https://doi.org/10.1016/j.cub.2004.08.023. https://doi.org/10.1016/j.cub.2004.08.023.

Work cited

Woldt, Estelle, Yasmine Sebti, Laura A Solt, Christian Duhem, Steve Lancel, Jérôme Eeckhoute, Matthijs K C Hesselink, Charlotte Paquet, Stéphane Delhaye, Youseung Shin, Theodore M Kamenecka, Gert Schaart, Philippe Lefebvre, Rémi Nevière, Thomas P Burris, Patrick Schrauwen, Bart Staels, and Hélène Duez. 2013. "Rev-erb-α modulates skeletal muscle oxidative capacity by regulating mitochondrial biogenesis and autophagy." *Nature Medicine* 19 (8): 1039-1046. https://doi.org/10.1038/nm.3213. https://www.ncbi.nlm.nih.gov/pmc/articles/PMC3737409.

Wood, Shona H., Dylan N. Clements, Neil A. McEwan, Tim Nuttall, and Stuart D. Carter. 2008. "Reference genes for canine skin when using quantitative real-time PCR." *Veterinary Immunology and Immunopathology* 126 (3): 392-395. https://doi.org/https://doi.org/10.1016/j.vetimm.2008.08.006. https://www.sciencedirect.com/science/article/pii/S0165242708003218.

Yagita, Kazuhiro, and Hitoshi Okamura. 2000. "Forskolin induces circadian gene expression of rPer1

, rPER-2

and dbp

in mammalian rat-1 fibroblasts." *FEBS Letters* 465 (1): 79-82. https://doi.org/10.1016/s0014-5793(99)01724-x.

Yin, L., J. Wang, P. S. Klein, and M. A. Lazar. 2006. "Nuclear receptor Rev-erbalpha is a critical lithium-sensitive component of the circadian clock." *Science* 311 (5763): 1002-5. https://doi.org/10.1126/science.1121613.

Yu, W. 2006. "PER-dependent rhythms in CLK phosphorylation and E-box binding regulate circadian transcription." *Genes & Development* 20 (6): 723-733. https://doi.org/10.1101/gad.1404406. http://genesdev.cshlp.org/content/20/6/723.full.pdf.

Appendix

Appendix

Statistically non-significant difference in clock genes expression between ZT6 and ZT18 within a tissue

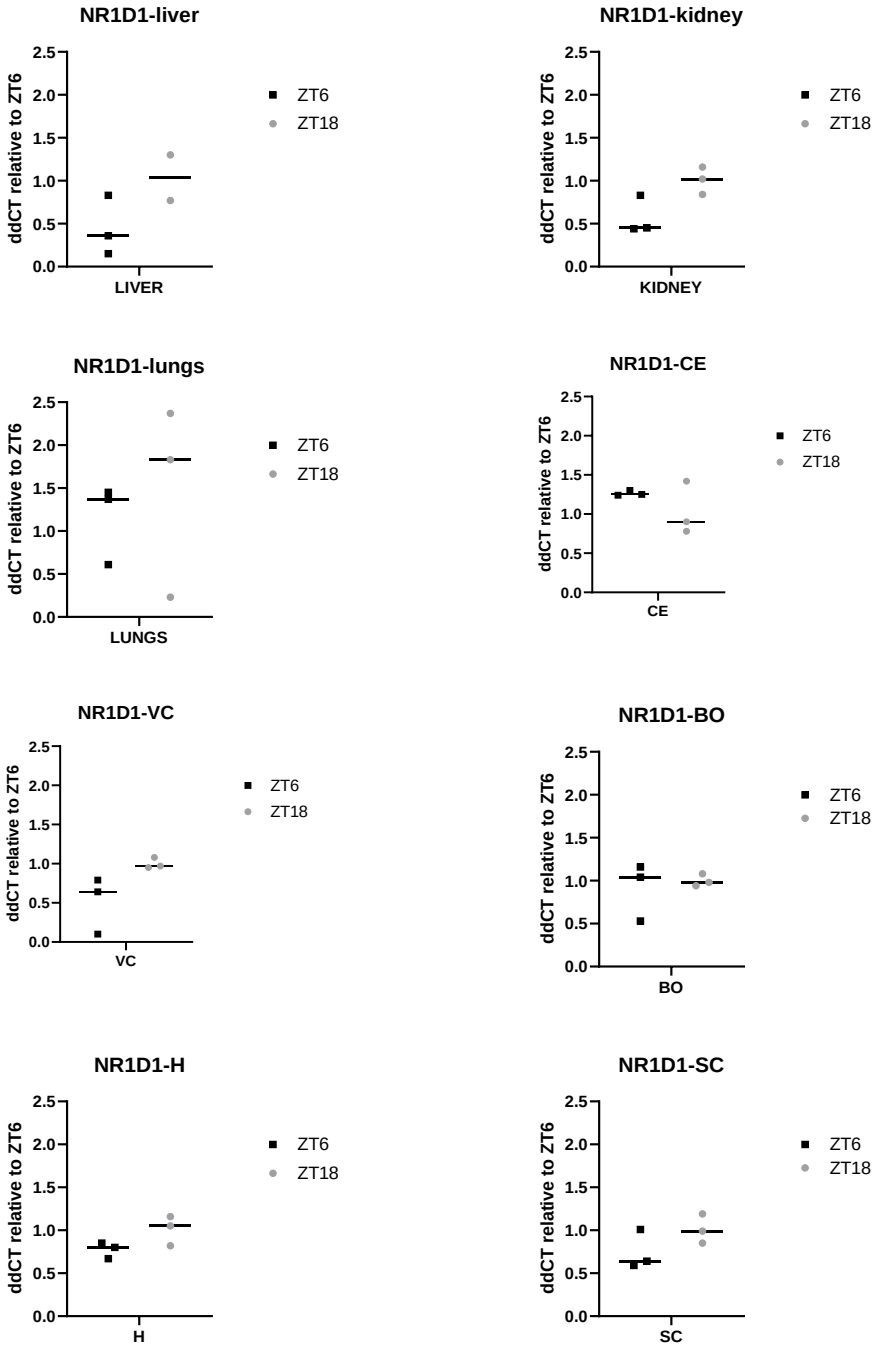

Figure 32 Difference in NR1D1 expression between ZT6 and ZT18 across the 8 hooded seal tissues sampled

Appendix

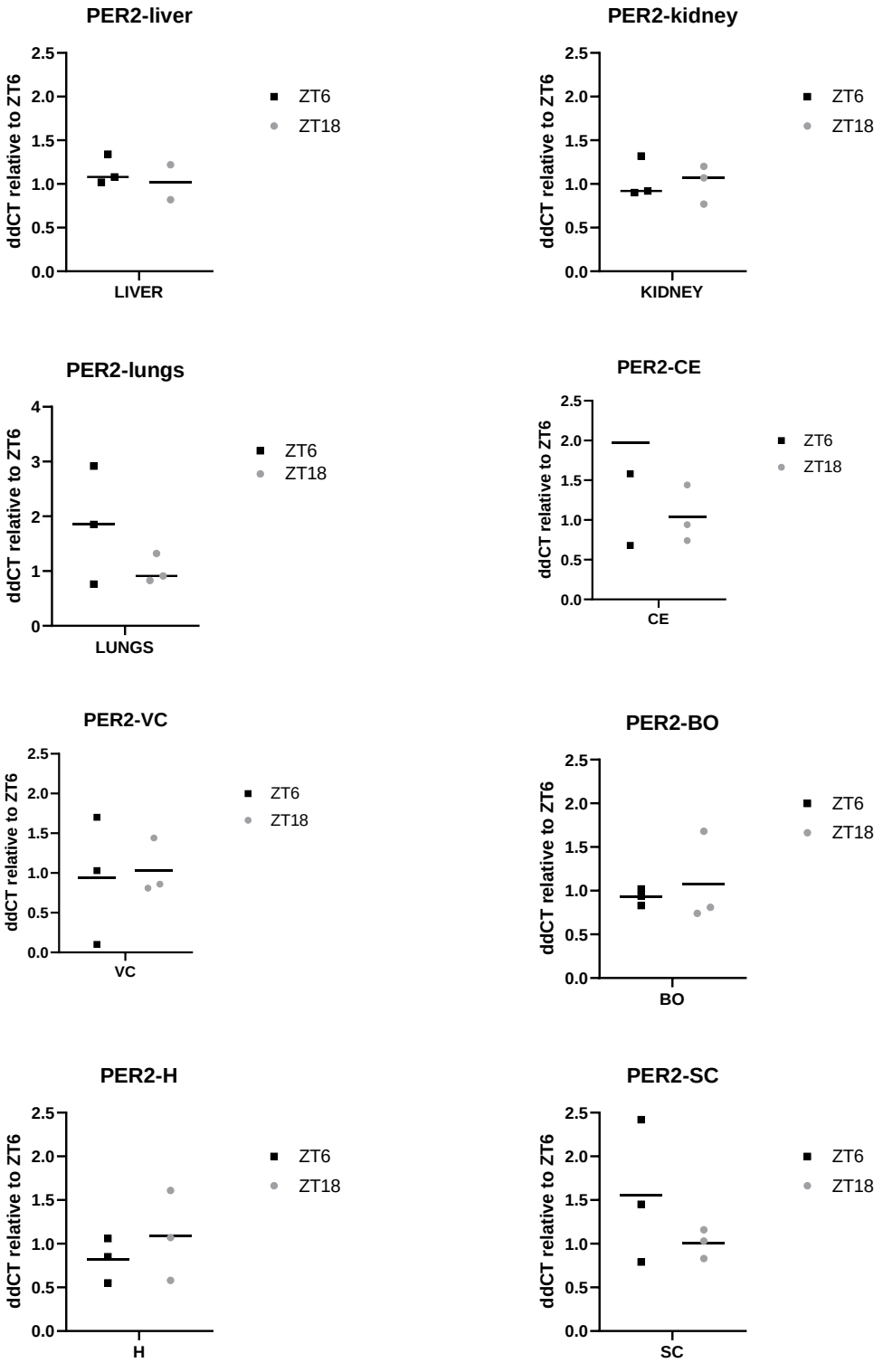

Figure 33 Difference in PER-2 expression between ZT6 and ZT18 across the 8 hooded seal tissues sampled

Appendix

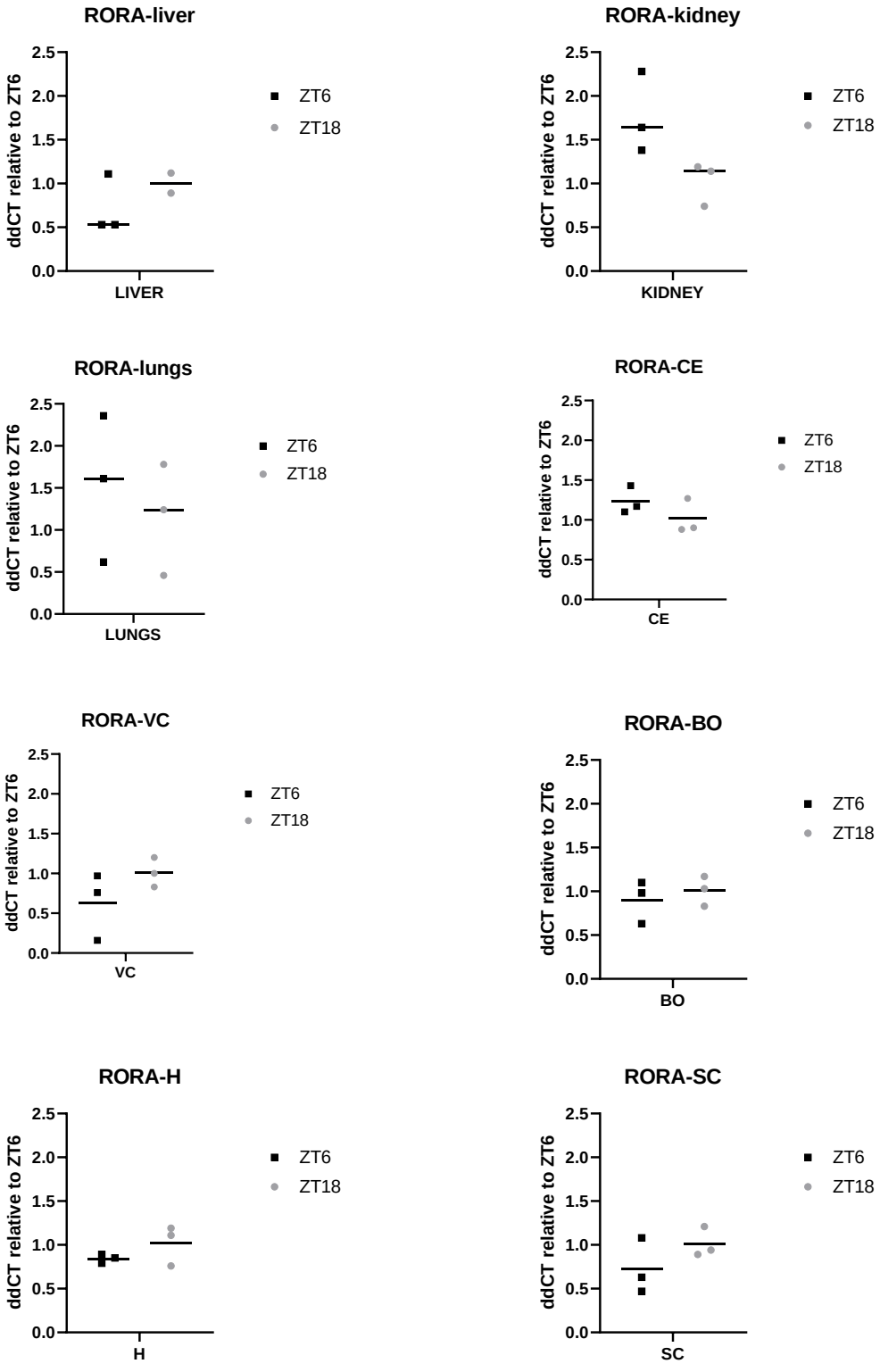

Figure 34 Difference in RORA expression between ZT6 and ZT18 across the 8 hooded seal tissues sampled

Appendix

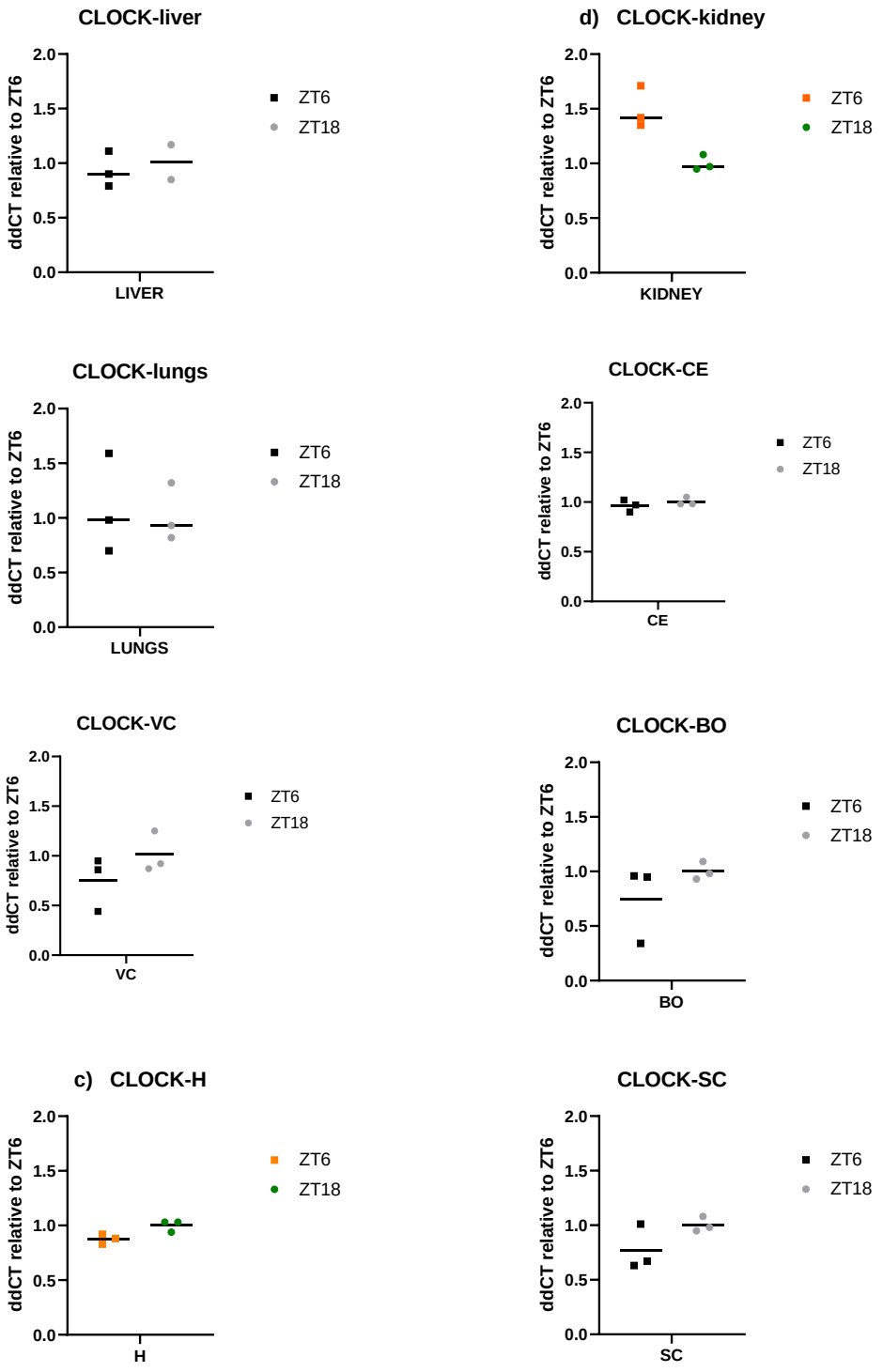

Figure 35 Difference in CLOCK expression between ZT6 and ZT18 across the 8 hooded seal tissues sampled

Appendix

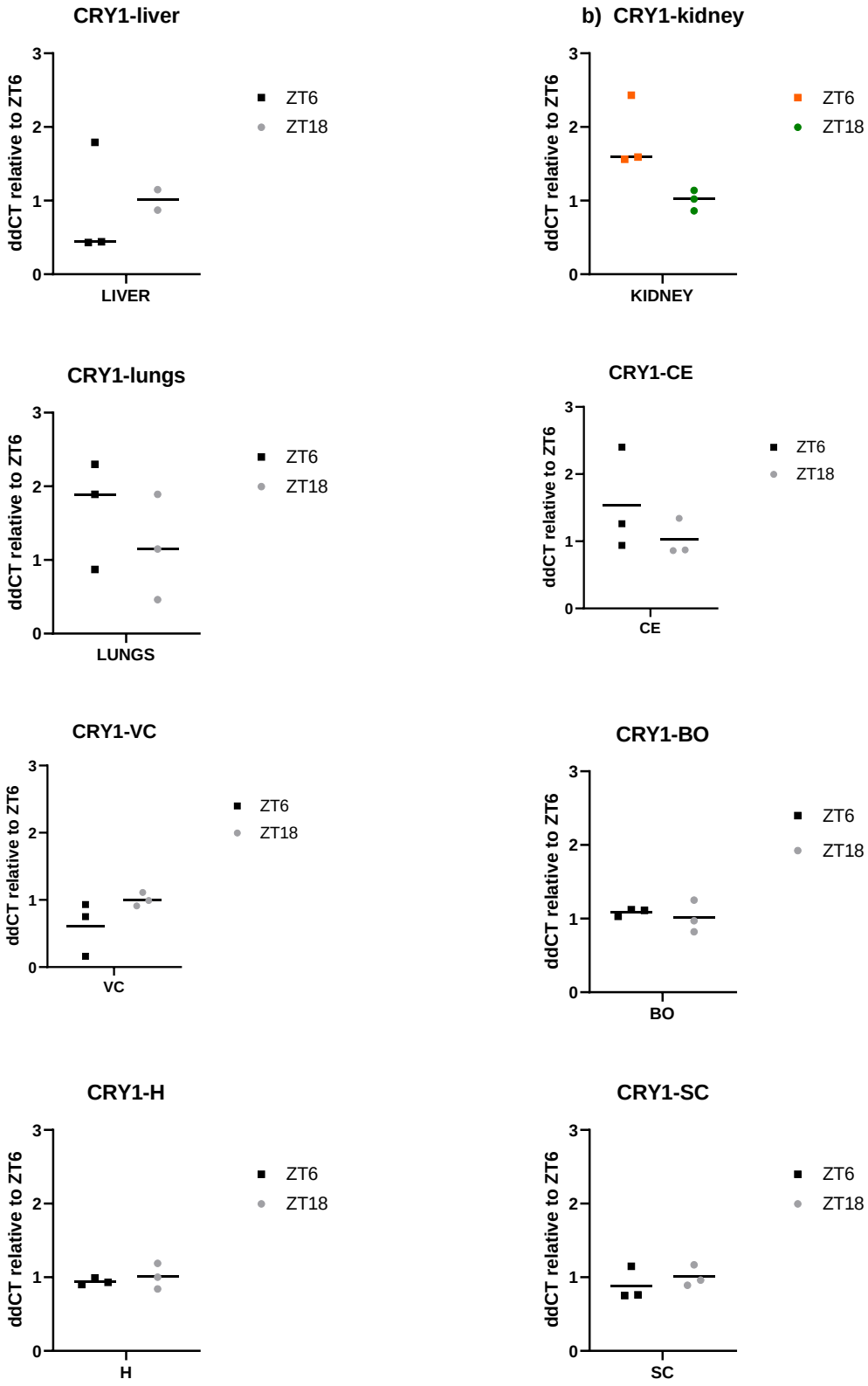

Figure 36 Difference in CRY1 expression between ZT6 and ZT18 across the 8 hooded seal tissues sampled

Appendix

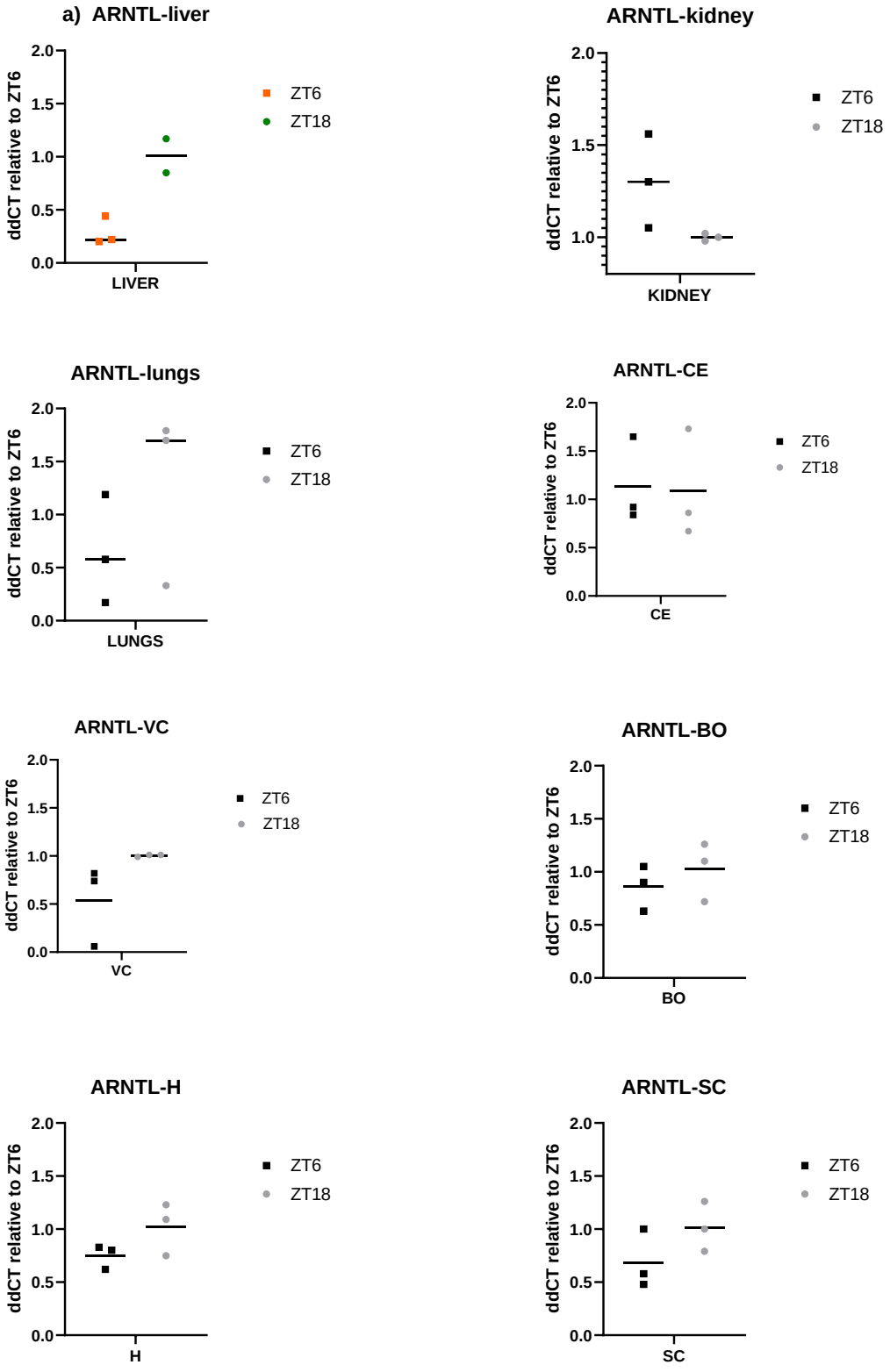

Figure 37 Difference in ARNTL expression between ZT6 and ZT18 across the 8 hooded seal tissues sampled

Appendix

Expression of clock genes under different cell stimulation treatments

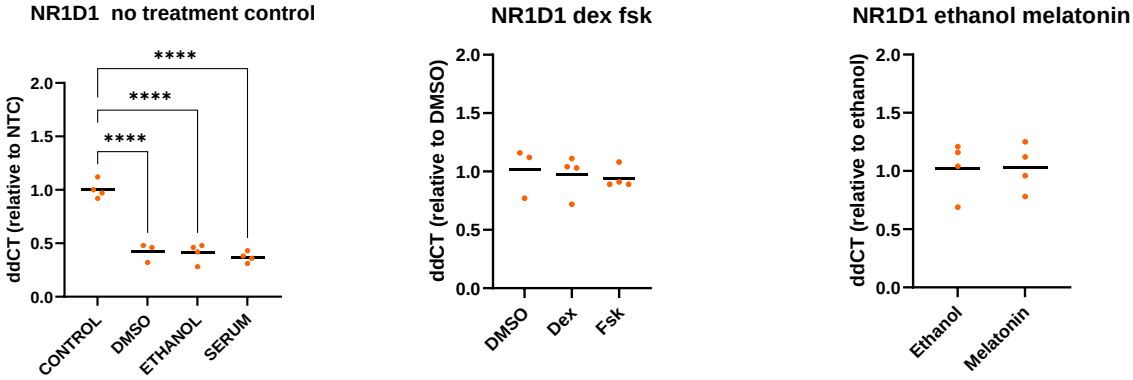

Figure 38 Expression of NR1D1 under different treatments. There is a significant difference between the no treatment control and the other controls $p<0,0001$ and the treatments do not influence the expression of NR1D1.

Appendix

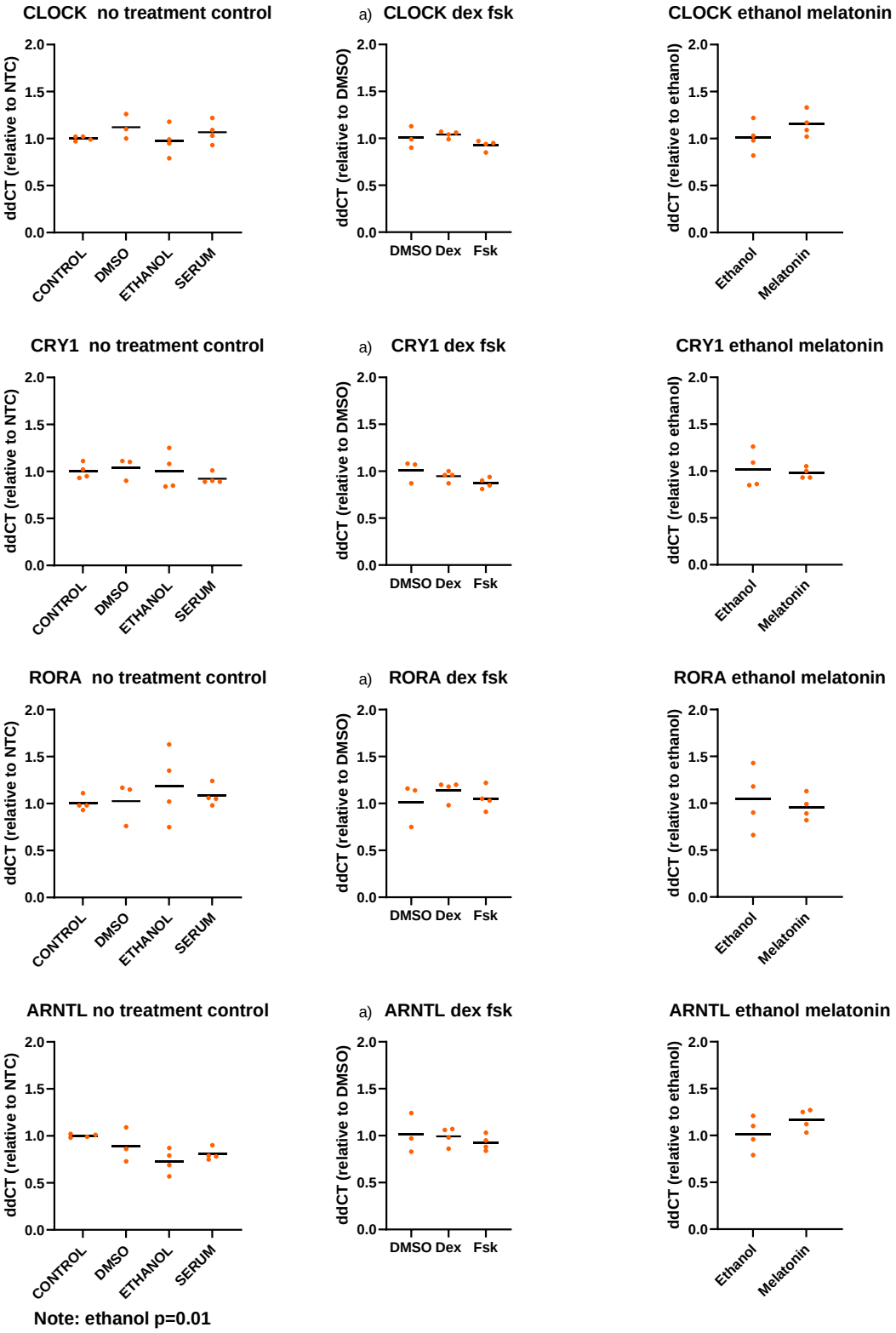

Figure 39 Expression of clock genes under different cell stimulation treatments. There was no significant difference in the expression of CLOCK, CRY1, RORA and ARNTL

Appendix

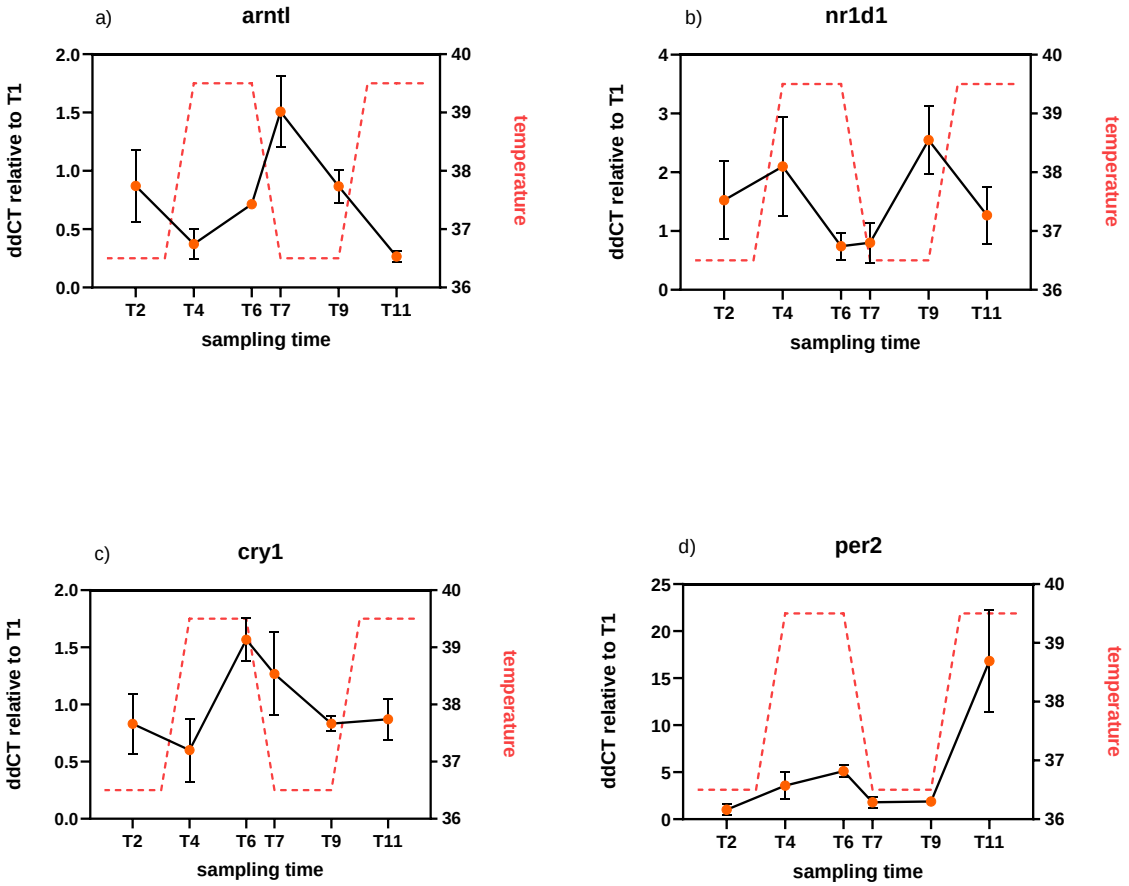

Figure 40 Clock genes significantly oscillating plotted to match the respiration measure experiment

Appendix

Primer design

GENE	SEQUENCE	EFFICIENCY	function	annealing T°C
Ccr_ARNTL_qPCR_F1 Ccr_ARNTL_qPCR_R1	GTGAAGTCTATGGAGTATGTG GTTCTTGTGGTAAATATGCC	98.34%	clock gene	57°C
Ccr_CLOCK_qPCR_F1 Ccr_CLOCK_qPCR_R1	TAAACACAGTCAGTCTCAAG CGTTGGGATCTTTGTTGG	96.32%	clock gene	55°C
Ccr_CRY1_qPCR_F2 Ccr_CRY1_qPCR_R2	CGTTTGGAAAGGCATTTG GGTCTTTCAAAGTTGGCT	96.40%	clock gene	57°C
Ccr_NR1D1_qPCR_F1 Ccr_NR1D1_qPCR_R1	CTCCTGTGTAAAGTGTGC CAGTTCTCGTTCTTCAGAC	98%	clock gene	57°C
Ccr_RORA_qPCR_F2 Ccr_RORA_qPCR_R2	TATTCCTTGCAAGATCTGTG ATTGCTTTGCTGACTTCTC	95.83%	clock gene	57°C
Ccr_RPLP0_qPCR_F2 Ccr_RPLP0_qPCR_R2	TGGAGACTGATTACACCTT CAAACGCAGATGGATCAG	91.39%	clock gene	57°C
Ccr_PER-2_qPCR_F2 Ccr_PER-2_qPCR_R2	CCATAGAAGAGATTGAGAGTG TTGGTCAGAGATGTACAGG	93.84%	clock gene	57°C
Ccr_PPIB_qPCR_F1 Ccr_PPIB_qPCR_R1	CATCTATGGTGAACGCTTC TAACGGTCGTGATAAAGAAC	89.32%	housekeeping gene	57°C
Ccr_TBP_qPCR_F2 Ccr_TBP_qPCR_R2	GAAGAAAGTGAACATCATGG GTAAGGCATCATTGGACTG	92.98%	housekeeping gene	57°C
Ccr_MFN1_qPCR_F1 Ccr_MFN1_qPCR_R1	ACAGGGTTATAGAAACAAGC GATAACAGAACTCTTCCCAC	101,23%	mitochondrial fusion	55°C
Ccr_MFN2_qPCR_F1 Ccr_MFN2_qPCR_R1	AAGTTCTCGATTCACTTCAG GGTGAGTGAACATGTTGAG	101,67%	mitochondrial fusion	55°C
Ccr_OPA1_qPCR_F1 Ccr_OPA1_qPCR_R1	GGAGTTCGATCTTACCAAAG TAACAGTACAGCCTTCTTTC	100,96%	mitochondrial fusion	55°C
Ccr_DNM1L_qPCR_F1 Ccr_DNM1L_qPCR_R1	GATGATCTTCTGACCGAATC ATTATTTGACTGGCTCCTTG	95,30%	mitochondrial fission	55°C
Ccr_NAMPT_qPCR_F1 Ccr_NAMPT_qPCR_R1	TTATGGGTTGCAGTACATTC GGAAATGCTCTCTATACACC	100,21%	NAD+ production	57°C

Table 7 List of the qPCR primers with their sequence, qPCR efficiency and gene function

Appendix

```
ARNTL       GTGAAGTCTATGGAGTATGTGTCTCGGCACGCGATAGACGGGAAGTTTGTTTTTGTAGAC      60
PRODUCT     GTGAAGTCTATGGAGTATGTGTCTCGGCACGCGATAGACGGGAAGTTTGTTTTTGTAGAC      60
            ************************************************************

ARNTL       CAGAGGAGGGCAACAGCTATTTTGGCATATTTACCACAAGAAC        103
PRODUCT     CAGAGG---GCAACAGCTATTTTGGCATATTTACCACAAGAAC        100
            ******   ***********************************

CLOCK       TAAACACAGTCAGTCTCAAGGAAGCCTTGGAAAGGTTTGATCACAGCCCAACACCTTCTG 60
PRODUCT     TAAACACAGTCAGTCTCAAGGAAGCCTTGGAAAGGTTTGATCACAGCCCAACCCCTTCTG 60
            ********************************************************* *******

CLOCK       CTTCCTCCCGGAGTTCAAGAAAATCATCTCACACAGCAGTCTCAGACCCTTCCTCAACAC 120
PRODUCT     CTTCCTCCCGGAGTTCAAGAAAATCATCTCACACAGCAGTCTCAGACCCTTCCTCAACAC 120
            ************************************************************

CLOCK         CAACAAAGATCCCAACG 137
PRODUCT       CAACAAAGATCCCAACG 137
              *****************

CRY1        CGTTTGGAAAGGCATTTGGAAAGAAAAGGCTTGGGTAGCCAACTTTGAAAGACC      54
PRODUCT     CGTTTGGAAAGGCATTTGGAAAG-AAAAGCTTGGGTAGCCAACTTTGAAAGACC      53
            ********************** *** **************************

NR1D1       CTCCTGTGTAAAGTGTGCGGGGACGTGGCCTCGGGCTTCCACTATGGCGTGCATGCCTGT       60
PRODUCT     CTCCTGTGTAAAGTGTGCGGGGACGTGGCCTCGGGCTTCCACTACGGCGTGCATGCCTGT       60
            ****************************************** ***************

NR1D1       GAGGGCTGCAAGGAGGGCTTTTTCCGTCGGAGCATCCAGCAGAACATCCAGTACAAAAGG       120
PRODUCT     GAGGGCTGCAA---GGGCTTTTTCCGTCGGAGCATCCAGCAGAACATCCAGTACAAAAGG       117
            ***********   *******************************************

NR1D1       TGTCTGAAGAACGAGAACTG       140
PRODUCT     TGTCTGAAGAACGAGAACTG       137
            ********************

PER2          CCATAGAAGAGATTGAGAGTGTCACGTCCGAGTTCATTGTGAAGAACGCGGGTATGTTTG     60
PRODUCT 1     CCATAGAAGAGATTGAGAGTGTCACGTCCGAGTTCATTGTGAAGAACGCAGGTATGTTTG     60
PRODUCT 2     CCATAGAAGAGATTGAGAGTGTCACGTCCGAGTTCATTGTGAAGAACGCAGGTATGTTTG     60
              ************************************************ **********

PER2          CGGCCGCCGTGTCCCTGGTCACCGGGAAAATCCTGTACATCTCTGACCAA       110
PRODUCT 1     CGGCCGCCGTGTCCCTGGTCACCGGGAAAATCCTGTACATCTCTGACCAA       110
PRODUCT 2     CGGCCGCCGTGTCCCTGGTCACCGGGAAAATCCTGTACATCTCTGACCAA       110
              ************************************************

PPIB        CATCTATGGTGAACGCTTCCCCGATGAGAACTTCAAGCTGAAACACTACGGGCCTGGCTG       60
PRODUCT     CATCTATGGTGAACGCTTCCCCGATGAGAACTTCAAGCTGAAACACTACGGGCCTGGCTG       60
            ************************************************************

PPIB        GGTGAGCATGGCCAATGCAGGCAAAGACACCAACGGCTCCCAGTTCTTTATCACGACCGT       120
PRODUCT     GGTGAGCATGGCCAACGCAGGCAAGGACACCAATGGCTCCCAGTTCTTTATCACGACCGT       120
            ************** ******** ******** ************************

PPIB        TA 122
PRODUCT     TA 122
            **
```

Appendix

```
RORA        TATTCCTTGCAAGATCTGTGGAGACAAATCATCAGGAATCCATTATGGTGTCATTACATG      60
PRODUCT     TATTCCTTGCAAGATCTGTGGAGACAAATCATCAGGAATCCATTATGGTGTCATTACATG      60
            ************************************************************

RORA        TGAAGGCTGCAAGGAGGGCTTTTTCAGGAGAAGTCAGCAAAGCAAT     106
PRODUCT     TGAAGGCTGCAAGGGCT---TTTTCAGGAGAAGTCAGCAAAGCAAT     103
            *************      *************************


RPLPO       TGGAGACTGATTACACCTTCCCACTTGCTGAAAAGGTAAAAGGTCAAGGCCTTCTTGGCT      60
PRODUCT     TGGAGACTGATTACACCTTCCCACTTGCTGAAA-------AGGTCAAGGCCTTCTTGGCT      53
            *********************************       *******************

RPLPO       GATCCATCTGCGTTTG   76
PRODUCT     GATCCATCTGCGTTTG   69
            ****************


MFN1        ACAGGGTTATAGAAACAAGCTTTCCATCATTGGTGAGGTGCTGTCTCGGAGACATATGAA      60
PRODUCT 1   ACAGGGTTATAGAAACAAGCTTTCCATCATTGGTGAGGTGCTGTCTCGGAGACATATGAA      60
PRODUCT 2   ACAGGGTTATAGAAACAAGCTTTCCATCATTGGTGAGGTGCTGTCTCGGAGACATATGAA      60
            ************************************************************

MFN1        AGTGGCATTTTTTGGCAGGCAGGACAAGCAGTGGGAAGAGTTCTGTTATC       110
PRODUCT 1   AGTGGCATTTTTTGGCAGGAC----AAGCAGTGGGAAGAGTTCTGTTATC       106
PRODUCT 2   AGTGGCATTTTTTGGCAGGAC----AAGCAGTGGGAAGAGTTCTGTTATC       106
            ******************      ************************

MFN2        AAGTTCTCGATTCACTTCAGAGCAAAGCAAAGCTGCTCAGGCAGGAATAAAGCCGGTTGG      60
PRODUCT 1   AAGTTCTCGATTCACTTCAGAGCAAAGCAAAGCTGCTCAGG----AATAAAGCCTGTTGG      56
PRODUCT 2   AAGTTCTCGATTCACTTCAGAGCAAAGCAAAGCTGCTCAGG----AATAAAGCCGGTTGG      56
            ****************************************    ********* *****

OPA1        GGAGTTCGATCTTACCAAAGAGGAGGATCTTGCAGCATTAAGACATGAAATAGAACTCCG      60
PRODUCT 1   GGAGTTCGATCTTACCAAAGAGGAGGATCTTGCAGCATTAAGGCATGAAATAGAACTACG      60
PRODUCT 2   GGAGTTCGATCTTACCAAAGAGGAGGATCTTGCAGCATTAAGGCATGAAATAGAACTACG      60
            ******************************************** ************** **

OPA1        AATGAGGAAAAATGTGAAAGAAGGCTGTACTGTTA      95
PRODUCT 1   AATGAGGAAAAATGTGAAAGAAGGCTGTACTGTTA      95
PRODUCT 2   AATGAGGAAAAATGTGAAAGAAGGCTGTACTGTTA      95
            ***********************************

DNM1L       GATGATCTTCTGACCGAATCTGAGGACATGGCACAGCGCAGGAAGGAAGCAGCGGACATG      60
PRODUCT     GATGATCTTCTGACCGAATCTGAGGACATGGCGCAGCGCAGGAAGGAAGCAGCGGACATG      60
            ******************************** ***************************

DNM1L       CTGAAGGAGGCATTACAAGGAGCCAGTCAAATAAT      95
PRODUCT     CTGAAGGCA---TTACAAGGAGCCAGTCAAATAAT      92
            *******     ************************


NAMPT       TTATGGGTTGCAGTACATTCTTAATAAGTACTTAAAAGGTAAGGTAAAGTAGTGACCAAA      60
PRODUCT 1   TTATGGGTTGCAGTACATTCTTAATAAGTACTTAAAAGG-----TAAAGTAGTGACCAAA      55
PRODUCT 2   TTATGGGTTGCAGTACATTCTTAATAAGTACTTAA------AGGTAAAGTAGTGACCAAA      54
            ***********************************         ****************

NAMPT       GAGAAGATCCAGGAAGCCAAAGAGGTGTATAGAGAGCATTTCC      103
PRODUCT 1   GAGAAGATCCAGGAAGCCAAAGAGGTGTATAGAGAGCATTTCC      98
PRODUCT 2   GAGAAGATCCAGGAAACCAAAGAGGTGTATAGAGAGCATTTCC      97
            *************** ****************************
```

Figure 41 Alignement of the predicted gene primer product (GENE NAME) and the sequence of the product from the qPCR (PRODUCT)

Appendix

in silico prediction				wet lab validation					
gene	clock gene sequence found in dog?	Aligned to weddell genome?	coding region identified?	primer design criteria met	efficient qpcr?	ligation	successful ligation and transformation?	DNA extraxtion	% similarity of PCR product to the weddell genome
MFN1	✔	✔	✔	✔	✔	✔	✔	✔	94.55
MFN2	✔	✔	✔	✔	✔	✔	✔	✔	94.51
OPA1	✔	✔	✔	✔	✔	✔	✔	✔	97.89
NAMPT	✔	✔	✔	✔	✔	✔	✔	✔	93.68
DNM1L	✔	✔	✔	✔	✔	✔	✔	✔	90.29

Table 8 Summary table of the different steps in the identification of the mitochondrial genes in hooded seal and the similarity between the sequenced product and the predicted qPRC target. The laboratory protocols for primer validation were kindly done by Chandra Sekhar Ravuri.

Appendix

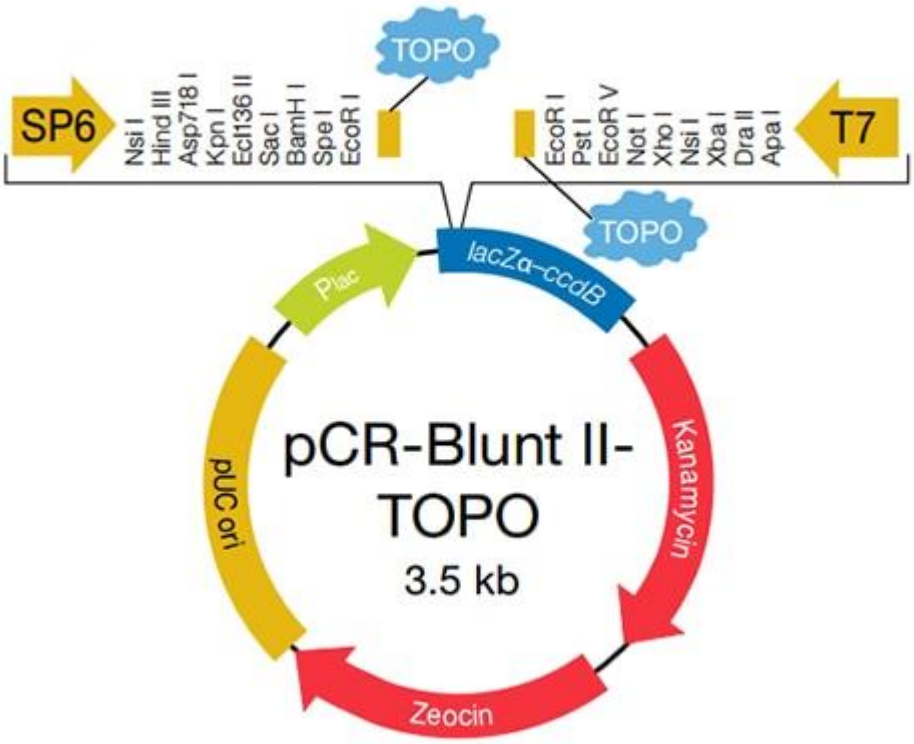

Figure 42 Plasmid Pcr Blunt II-TOPO vector used for sequencing of the primer product (ThermoFisher scientific)

Transfected cells images

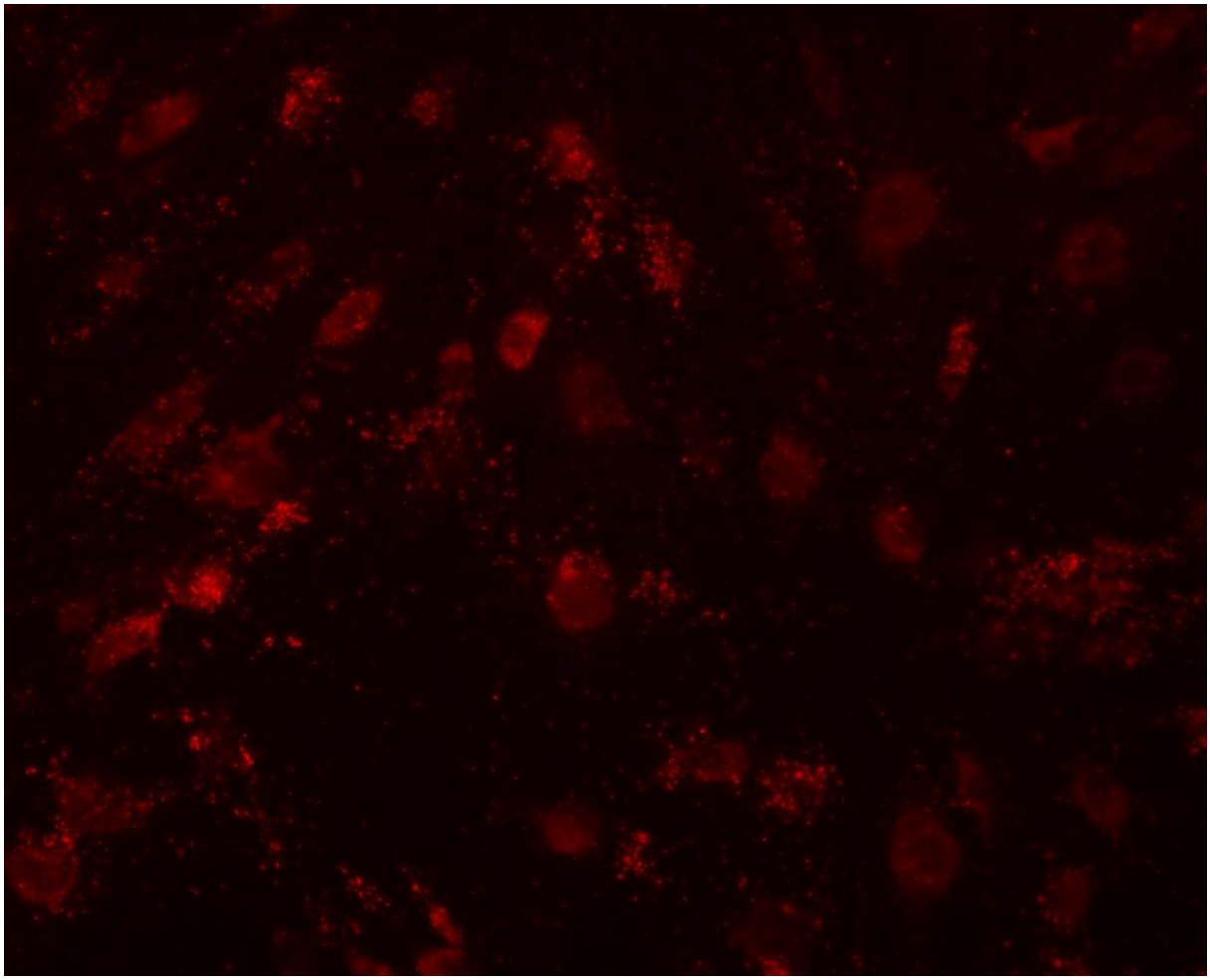

Figure 43 Hooded seal Pia Matter cells successfully transfected with TransIT 2020

Appendix

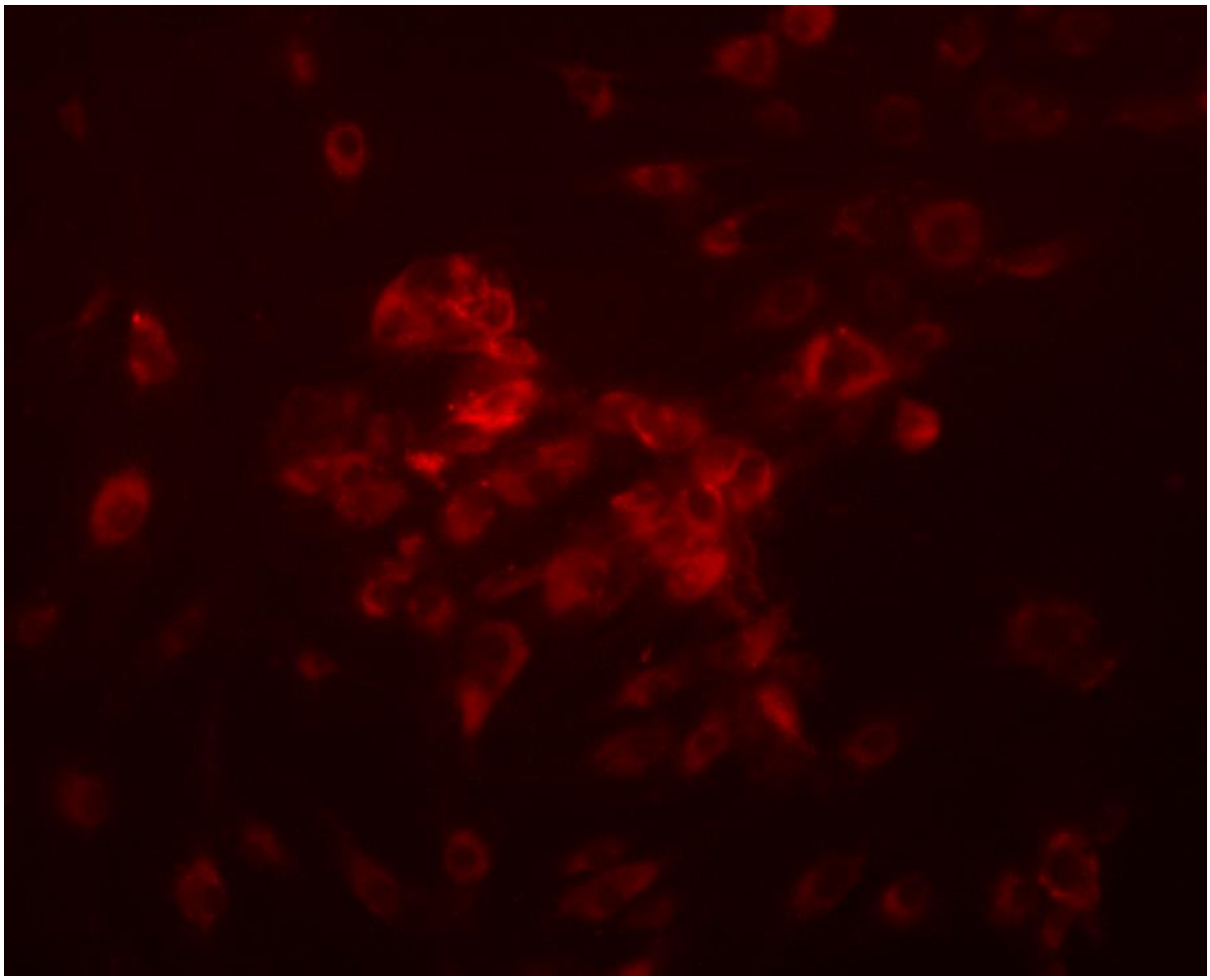

Figure 44 Hooded seal Pia Matter cells successfully transfected with TransIT LT1

Appendix

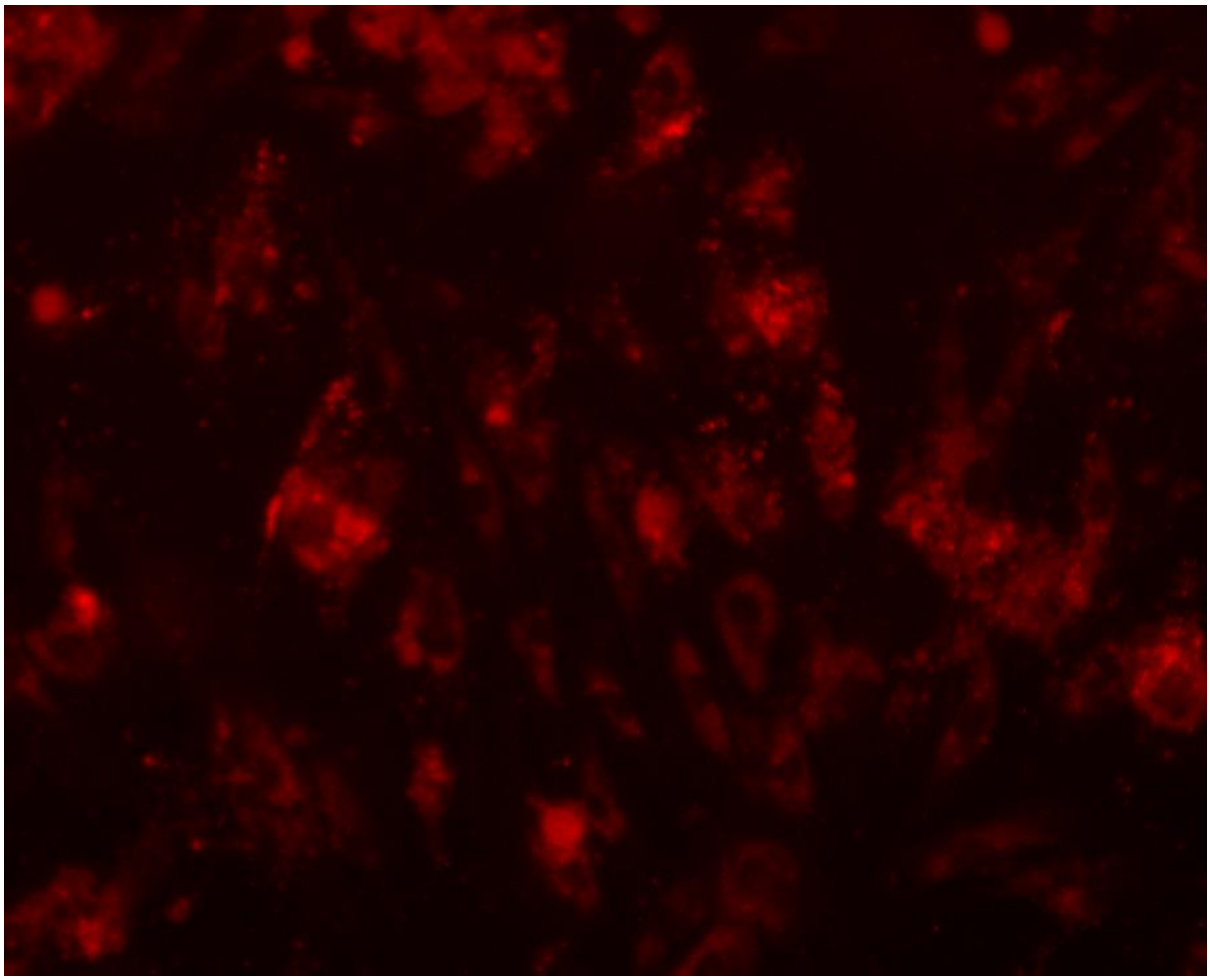

Figure 45 Hooded seal skin firbroblasts cells successfully transfected with TransIT 2020